1/82 | CMCRCZ 11 (1) 1-84 (1982)

ΧΗΜΙΚΑ ΧΡΟΝΙΚΑ

ΝΕΑ ΣΕΙΡΑ

CHIMIKA CHRONIKA

NEW SERIES

AN INTERNATIONAL EDITION OF THE GREEK CHEMISTS ASSOCIATION

CHIMICA CHRONIKA, NEW SERIES Volume 11, No 1 pp 1-84 March (1982)

CHIMIKA CHRONIKA /NEW SERIES
Published by the Greek Chemists' Association
27, Kaningos Street, Athens (147), Greece

Correspondence, submission of papers, subscriptions, renewals and changes of address should be sent to Chimika Chronica, New Series, 27 Kaningos street, Athens, Greece. The Guide to Authors is published in the first issue of each volume, or sent by request. Subscriptions are taken by volume at 500. drachmas for members and 1.000 drachmas for Corporations in Greece and 28U.S. dollars to all other countries except Cyprus, where subscriptions are made on request.

Printed in Greece by FOTOKIMENO E.P.E.

Υπεύθυνος σύμφωνα μέ τό νόμο: Παναγιώτης Ξυθάλης Κάννιγγος 27, Αθήνα (147)

CHIMIKA CHRONIKA, *NEW SERIES*

CONTENTS

March 1982 Volume 11, No 1

Chimika Chronika, New Series, 11, 3-10 (1982)

SPECTROPHOTOMETRIC STUDY OF THE IRON(II) - INDUCED PERBROMATE-IODIDE REACTION. AUTOMATIC REACTION RATE METHOD FOR THE ULTRAMICRODETERMINATION OF IRON

L.A. LAZAROU, E.P. DIAMANDIS & T.P. HADJIIOANNOU
Laboratory of Analytical Chemistry, University of Athens, Athens, Greece.

(Received December 5, 1978; Revised October 21, 1981).

Summary

A kinetic study of the iron(II) -induced perbromate-iodide reaction was carried out spectrophotometrically. Reaction rate constants and activation energies are reported. An automatic reaction rate method is described for the determination of 40-600 ng of iron (1.8×10^{-7}-2.7×10^{-6}M) with relative errors and standard deviations of about 1%.

Key words: Perbromate, iodide, iron, kinetic data.

Introduction

Since the successful preparation of perbromates[1], only a limited amount of work on perbromate chemistry has been published. The earliest studies indicated perbromate to be quite sluggish in its reactions, though not as inert as perchlorate[2]. This inertness of the perbromate ion stands in sharp contrast to its high thermodynamic oxidizing power[3], which is greater than that of any other oxyhalogen that exists in aqueous solution.

The perbromate - iodide reaction is well known and it was used for the detection[4,5] and the iodometric[6] and kinetic[7] determination of perbromate. Iodide reduces perbromate to bromate in alkaline or neutral solutions[6] according to the reaction

$$BrO_4^- + 2H^+ + 3I^- \rightarrow BrO_3^- + I_3^- + H_2O \qquad (1)$$

and to bromide in acidic solutions. The reaction proceeds very slowly in alkaline, neutral or acidic solutions. However, when iron(II) is added, it induces the

oxidation of iodide. Also, iron(III) accelerates the perbromate-iodide reaction, but only if iodide is present in sufficiently high concentrations so as to reduce iron(III) to iron(II) quickly.

In this paper the kinetics of the iron(II) induced perbromate-iodide reaction are studied spectrophotometrically. Also, an automated reaction rate method for the determination of iron is described. The time required for the reaction to produce a fixed amount of triiodide is measured automatically and related directly to the iron concentration. Iron in the 40-600 ng range (1.8×10^{-7}-2.7×10^{-6} M) was determined with relative errors and relative standard deviations of about 1%.

Experimental

Apparatus

A modified Perkin-Elmer 139 single beam spectrophotometer was used[8]. The signal from the photomultiplier output is fed to a logarithmic converter (Pacific Instruments Model 1002), and the signal from the converter is driven to a chart recorder.

The measurement and control system for the automatic determination of iron, assembled from MP-modular units (McKee-Pedersen Instruments, Danville, Calif.), consists of an operational amplifier (MP-1006 C) which was used to make the source impedance negligible, improve the stability and multiply the signal by a factor of ten, and a kinetic time switch (MP-1505) which consists of the following units: A tabletop cabinet, powered (MP-1036 CP), two operational amplifiers (MP-1006 C), a millivolt source (MP-1008 B), a timer-counter (MP-1029), and a plug-in-program for measuring the time (Δt) it takes for the reaction to produce a fixed amount of triiodide. This unit provides the necessary components and interconnections to program the two MP-1006 C amplifiers as comparators. These amplifiers provide switching signals which enable the timer-counter to start and stop when the input signal reaches the appropriate potentials. The toggle switch on the timer-counter should be moved to the "TIME" mode. A parallel connection to the output of the logarithmic converter drives a small portion of the current to the input of the operational amplifier, OA, and the signal is amplified by a factor of ten. The OA output, E_{in}, is driven to the input of the plug-in-program, the lower and upper limits E_I and E_{II} of which are preset externally using the millivolt source. When E_{in} reaches the predetermined value E_I the timer is activated and the time counting starts. When E_{in} reaches the predetermined value E_{II} the timer is inactivated and the time counting stops. Thus, a time interval is determined the reciprocal of which is proportional to the iron concentration. Fig. 1 shows the recording and measurement system. The measurement and control system was adjusted to measure the time required for the recorder pen to cross preselected positions in the chart, corresponding to 0.10 and 0.20 absorbance unit.

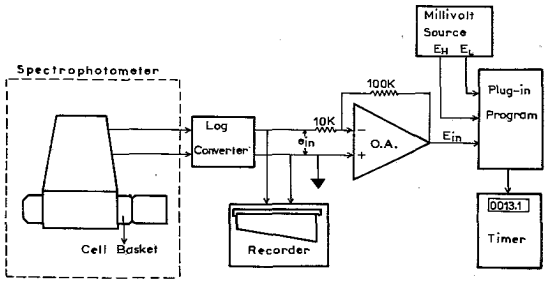

Figure 1. *Schematic diagram of the recording and measurement system.*

Reagents

All solutions were prepared in deionized distilled water from reagent-grade materials, except where otherwise stated.

Stock perbromate solution (0.100 M). Dissolve 1.83 g of potassium perbromate in water and dilute to 100 ml.

Stock iodide solution (1.00 M). Dissolve 16.6 g of potassium iodide (Merck Suprapur) in water and dilute to 100 ml.

Stock iron(II) solution (0.1000 M). Dissolve 39.21 g of $(NH_4)_2Fe(SO_4)_2.6H_2O$ in 50 ml of 2M sulfuric acid (Merck Suprapur) and dilute with water to 1l. Standardize with standard potassium permanganate solution. Prepare more dilute solutions by dilution with 0.0125 M perchloric acid.

Stock iron(III) solution (0.1000 M). Dissolve 40.40 g of $Fe(NO_3)_3.9H_2O$ in 50 ml of 2M sulfuric acid and dilute with water to 1l.

The stock iodide and iron(II) and (III) solutions should be kept in amber bottles. The potassium iodide solution required for each kinetic run was prepared by mixing appropriate amounts of potassium iodide and 1.00 M sodium perchlorate (Merck Suprapur) so as to obtain an ionic strength of 0.125.

During measurements all solutions were thermostated at 25 ± 0.1°C.

Procedure for kinetic studies

Use the hydrogen lamp and set the wavelength at 287.5 nm, where triiodide has an absorption maximum[9]. Into the thermostated quartz cuvette transfer 4.00 ml of the iodide solution, 0.50 ml of 0.125 M perchloric acid solution, 0.50 ml of potassium perbromate solution, and 50 µl of the iron(II) solution. Close the cuvette immediately, start the recorder at once and record the change in absorbance for a few minutes.

Procedure for determination of iron (40-600 ng)

Into the thermostated cuvette transfer 4.00 ml of the standard iron (10, 50, 100, 150 ppb in 0.0125 M $HClO_4$) or sample solution and 0.50 ml of 0.50 M potassium iodide solution. Inject instantaneously 0.50 ml of 2.0×10^{-3} M potassium

perbromate solution and close the cuvette at once. The measurement is completed automatically and the number on the digital readout (time in tenths of a second) is recorded. Press the reset button and empty the cuvette by suction.

Results and Discussion

Kinetics of the iron(II) -induced perbromate-iodide reaction

The reaction was found to be independent of pH in the range 2-7. Using the initial reaction rate method[10] it was found that the reaction rate can be expressed as

$$R = \frac{d[I_2]}{dt} + \frac{d[I_3^-]}{dt} = k_1 [BrO_4^-] [I^-] + k_2 [BrO_4^-] [Fe^{2+}] \qquad (2)$$

where k_1 and k_2 are the reaction rate constants for the uncatalysed and the catalysed reactions, respectively. Given that the reaction $I_2 + I^- \rightleftarrows I_3^-$, $K_f = 720$[9], and that during the measurement period the iodide concentration remains practically constant we have

$$\frac{d[I_2]}{dt} = \frac{1}{K_f[I^-]} \cdot \frac{d[I_3^-]}{dt} \qquad (3)$$

We also have $A = (\varepsilon_{I_3^-}).b[I_3^-] + (\varepsilon_{I_2}).b[I_2]$, or since $(\varepsilon_{I_3^-}) = 4\times10^4\ M^{-1}\ cm^{-1} >> (\varepsilon_{I_2}) = 95$[11],

$$A \simeq (\varepsilon_{I_3^-}).b[I_3^-] \qquad (4)$$

Differentiating equation (4) with respect to time and combining the resulting equation with equations (2) and (3) gives

$$\frac{dA}{dt} = (\varepsilon_{I_3^-}).b \frac{K_f[I^-] [BrO_4^-]}{1 + K_f[I^-]} [\, k_1 [I^-] + k_2 [Fe^{2+}] \,] \qquad (5)$$

Since during the measurement period all concentrations remain practically constant, the absorbance should vary linearly with time. Therefore, under such conditions, dA/dt in equation (5) can be replaced by the term $\Delta A/\Delta t$, which is the actual measured quantity.

Recorded curves for the perbromate-iodide reaction in the presence of iron(II) are shown in Fig. 2. As expected from equation (5), the curves are straight lines.

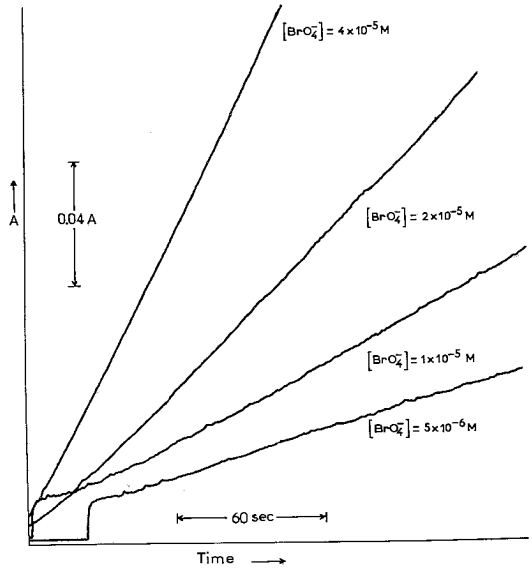

Figure 2. *Recorded curves of absorbance versus time for the iron(II)-induced perbromate-iodide reaction. Initial concentrations: 1.80×10⁻⁶ M iron(II), 0.100 M I^-.[BrO_4^-] is shown on the curves.*

The rate constants k_1 and k_2 were calculated to be (1.6 ± 0.1)×10^{-3} M^{-1} s^{-1} and (240 ± 18) M^{-1} s^{-1} (n=13), respectively. These values were calculated for the following concentration ranges: [I^-] = 10^{-4} -10^{-1} M, [BrO_4^-] = 10^{-5} -5×10^{-3}M, and [Fe^{2+}] = 10^{-7} -5×10^{-6} M.

Effect of temperature

The rates of the perbromate-iodide and the iron(II)-induced perbromate-iodide reactions increase with increasing temperature in the range 19-34°C. From Arrhenius plots of $\ln k_1$ or $\ln k_2$ versus reciprocal of absolute temperature the activation energies were calculated to be (13.7 ± 0.3) kcal mol^{-1} and (8.9 ± 0.2) kcal mol^{-1} (n=4), respectively.

Effect of ionic strength

The rate of the uncatalysed perbromate-iodide reaction increases with increasing ionic strength, whereas the rate of the catalysed reaction decreases with increasing ionic strength indicating that the slow step in the uncatalysed reaction involves ions of the same sign and that the slow step in the catalysed reaction involves ions of the opposite sign[12]. From plots of $\log k_1$ or $\log k_2$ versus $\mu^{1/2}$ (μ=ionic strength), $(k_1)_{\mu=0}$ and $(k_2)_{\mu=0}$ were calculated to be (1.2 ± 0.1)×10^{-3} M^{-1} s^{-1} and (500 ± 28) M^{-1} s^{-1} (n=4), respectively (μ=0.1-1).

Iron(II) acts as an inductor and not as a catalyst, because it was found experimentally that at the end of the reaction the iron(II) is oxidized to iron(III).

Iron(III) accelerates the perbromate-iodide reaction but not as strongly as iron(II) (under controlled conditions, high iodide concentration and low perbromate concentration, iron(III) and iron(II) behave identically). Iron(III) accelerates the perbromate-iodide reaction because of iron(II) produced in the iron(III)-iodide reaction. It was also found that fluoride does not affect the reaction rate. In comparison to perbromate, bromate reacts with iodide in the presence of iron(II), only when present in very high concentrations. Therefore, bromate, which is the product of the perbromate-iodide reaction, does not affect the rate of the iron(II)-induced perbromate-iodide reaction.

Automatic kinetic determination of iron

Equation (5) can be written as

$$[Fe^{2+}] = \frac{1}{\Delta t} \cdot \frac{\Delta A(K_f[I^-] + 1)}{k_2(\varepsilon_{I_3^-})bK_f[I^-][BrO_4^-]} - \frac{k_1}{k_2}[I^-] \qquad (6)$$

If we keep constant the terms $[I^-]$, $[BrO_4^-]$ and ΔA, the curve $[Fe^{2+}] = f(1/\Delta t)$ must be a straight line (working curve) from which iron can be determined. It can be seen from equation (6) that the smaller the iodide concentration the smaller the blank. However, the iodide concentration must be sufficiently high so as to reduce iron(III) to iron(II) quickly, so that total iron can be determined with the proposed method. Straight line working curves (ng of iron vs. $1000/\Delta t$) were determined by least squares fit.

Analysis of aqueous iron(II) and iron(III) solutions of known concentrations gave the results shown in Table 1. The data indicate that iron in the range 40-600 ng (1.8×10^{-7} -2.7×10^{-6} M) can be determined with relative errors of about 1%. The relative standard deviation of the determination of 7.16×10^{-7} M iron(II) solution was 0.5% (n=6).

TABLE 1. *Determination of iron in aqueous solutions*

Iron(II), ng/4ml		Error,	Iron(III), ng/4ml		Error,
Taken	Found[a]	%	Taken	Found[a]	%
40,0	39,7	— 0,8	40,0	40,4	+ 1,0
80,0	79,7	— 0,4	80,0	79,0	— 1,2
160	161	+ 0,6	160	158	— 1,2
240	235	— 2,1	240	235	— 2,1
320	319	— 0,3	320	318	— 0,6
400	402	+ 0,5	400	402	+ 0,5
480	486	+ 1,3	480	477	— 0,6
600	593	— 1,2	600	599	— 0,2
		Mean 0,9			Mean 0,9

[a] Single measurements. Calculated using equation:
ng iron = - 70.7 + 6.90 (1000/Δt).

Interferences

To investigate the effect of various ions that might interfere in the determination of iron, the measurement step was modified as follows: After the addition of an iron standard (40 ppb), 100 μl of water or of the solution of the ion being examined was injected into the cuvette. The following ions did not interfere with the determination even when their concentrations were several thousand times that of the iron: calcium, barium, strontium, magnesium, zinc, aluminum, cobalt(II), chromium(III), cadmium, manganese(II), nickel, chloride, bicarbonate, sulfate, phosphate and bromide. Copper(II) and lead caused a positive relative error of about 5% when their concentrations were 40 and 190 times that of the iron concentration, respectively.

Περίληψη

Φασματοφωτομετρική μελέτη τῆς ὑπό τοῦ σιδήρου(II) προαγομένης ἀντιδράσεως ὑπερβρωμικῶν – ἰωδιούχων. Αὐτόματος κινητική μέθοδος ὑπερμικροπροσδιορισμοῦ σιδήρου

Ἐπιτελεῖται κινητική μελέτη τῆς ὑπό τοῦ σιδήρου(II) προαγομένης ἀντιδράσεως ὑπερβρωμικῶν-ἰωδιούχων. Προσδιορίζονται σταθεραί ταχύτητος ἀντιδράσεως καί ἐνέργειαι ἐνεργοποιήσεως.

Περιγράφεται αὐτόματος κινητική φασματοφωτομετρική μέθοδος διά τόν μικροπροσδιορισμόν τοῦ σιδήρου, βασιζομένη ἐπί τῆς προαγωγικῆς δράσεως τοῦ σιδήρου(II) ἐπί τῆς ἀντιδράσεως ὑπερβρωμικῶν-ἰωδιούχων. Ὁ ἀπαιτούμενος χρόνος διά τόν σχηματισμόν μικρᾶς καθωρισμένης ποσότητος ἰόντων τριιωδίου μετρεῖται αὐτομάτως καί συσχετίζεται ἀπ' εὐθείας πρός τήν συγκέντρωσιν τοῦ σιδήρου. Ἐμελετήθη ἡ ἐπίδρασις τῆς συγκεντρώσεως τῶν ἀντιδραστηρίων, τῆς θερμοκρασίας καί τῆς ἰονικῆς ἰσχύος ἐπί τῆς ταχύτητος ἀντιδράσεως, ὡς καί ἡ παρεμποδιστική δρᾶσις διαφόρων ἰόντων. Ἡ ἀκρίβεια τῶν ἀναλύσεων διά διαλύματα περιέχοντα 40-600 ng σιδήρου ἦτο περίπου 1%, ἡ δέ σχετική τυπική ἀπόκλισις ἦτο μικροτέρα τοῦ 1%.

References and Notes

1. Appelman, E.H.: *J. Am. Chem. Soc.*, **90**, 1900 (1968).
2. Appelman, E.H.: *Inorg. Chem.*, **8**, 223 (1969).
3. Schreiner, F., Osborne D.W., Pocius, A.V. & Appelman, E.H.: *Inorg. Chem.*, **9**, 2320 (1970).
4. Lederer, M. & Sinibaldi M.: *J. Chromatogr.*, **60**, 275 (1971).
5. Ossicini, L. & Balsoni, M.: *J. Chromatogr.*, **79**, 311 (1973).
6. Keil, R.: *Z. Anal. Chem.*, **281**, 123 (1976).
7. Lazarou, L.A., Siskos, P.A., Koupparis, M.A., Hadjiioannou, T.P. & Appelman, E.H.: *Anal. Chim. Acta*, **94**, 475 (1977).

8. Karayannis, M.I. & Kordi, E.V.: *Analyst*, **100**, 168 (1975).
9. Turner, D.H., Flynn G.W., Sutin, N. & Beitz J.V.: *J. Am. Chem. Soc.*, **94**, 1554 (1972).
10. Fleck, G.M.: *Chemical Reactions Mechanisms, (1st edition)*, p. 47, Holt, Rinehart & Winston, New York (1971).
11. Awtrew, A.D. & Connick, R.E.: *J. Am. Chem. Soc.*, **73**, 1812 (1951).
12. Sykes, A.G.: *Kinetics of Inorganic Reactions, (1st edition)*, p. 8.18, Pergamon Press LTD, (1966).

Acknowledgements

The authors thank O. Antonsen of the Eidgenössiches Institut für Reaktovforschung, Wurelingen, Switzerland, for provision of potassium perbromate, and C.E. Efstathiou for stimulating discussions. This research was supported in part by a research grant from the Greek National Institute of Research.

Chimika Chronika, New Series, 11, 11-21 (1982)

"PLATINUM (II) AND PALLADIUM (II) COMPLEXES OF INOSINE, GUANOSINE, XANTHOSINE AND THEIR ACETYL DERIVATIVES"

N. HADJILIADIS, G. PNEUMATIKAKIS & S. PARASKEVAS
University of Ioannina, Laboratory of Inorganic Chemistry Ioannina, Greece.
Laboratory of Inorganic Chemistry, University of Athens, and Laboratory of Organic Chemistry, University of Athens.

(Received May 2, 1980;).

Summary

The reactions of Pd(II) and Pt(II) with purine nucleosides possessing an exocyclic C=0 group at the 6th position, (Ino, Guo, Xao and trino, trguo and trxao) were studied in aqueous solutions. The complexes *cis*-Pd(trino)$_2$Cl$_2$, *cis*-Pd(trguo)$_2$Cl$_2$, *cis*-Pd(trxao)$_2$Cl$_2$, *cis*-Pd(trino -H$^+$)$_2$, *cis*-Pd(trguo -H$^+$)$_2$, *cis*-Pd(trxao -H$^+$)$_2$ and ML (Nucl-H$^+$)Cl, where M is Pd(II), Pt(II), L is Py or Cyd and Nucl is Ino, Guo or Xao were isolated and characterized by elemental analyses, conductivity measurements, molecular weight determinations, ir, ^{1}Hnmr and e.s.r. spectra.

The possiple structures of the complexes based on the above experimental data, are suggested as N(7)0(6) monomeric chelate and/or N(7)0(6) dimeric or polymeric species.

Key words: Complexes, platinum, palladium, inosine guanosine, xanthosine, triacetylinosine triacetylguanosine, triacetylxanthosine, N(7) 0(6) chelates.

Introduction

Antitumour active complexes like *cis*-Pt(NH$_3$)$_2$Cl$_2$ or related compounds, most probably react in a covalent rather than intercalative manner with DNA[1]. The preferred binding site in such reactions has been found to be primarily the N(7) nitrogen atom of the guanine bases of DNA[2-4]. However the interaction of only N(7) of a guanine base with Pt(II) is not believed to be the only attact caused to DNA[2-4] by the platinum drugs[5]. The formation of inter or intra strand cross links[6-9] or of N(7)0(6) chelates[10,11] have been proposed as possible mechanism for the antitumour action of *cis*-Pt(NH$_3$)$_2$Cl$_2$. The proposal for the formation of N(7)0(6)

chelates was mainly based on the fact, that the antitumour drug *cis*-$Pt(NH_3)_2Cl_2$ is able to form one, thereby altering interbase hydrogen bonding, while the inactive *trans*-$Pt(NH_3)_2Cl_2$ is not[11].

On the other hand, the *in vitro* studies of the interactions of metals with nucleosides are interesting, because they may provide models for the mechanism of action of *cis*-$Pt(NH_3)_2Cl_2$ itself reacting with DNA. Many such studies[12,13] have clearly demonstrated the bonding sites and the properties of such reactions and products. In our laboratory[3,14], we have prepared and studied a number of Pt(II) and Pd(II) complexes with nucleosides. On the basis of ir, ^{1}Hnmr spectra, chemical reactions and analysis we provided evidence for the bonding sites and general reactivity, including the possible formation of N(7)0(6) chelates.

In continuation of our studies on such interactions we now present new complexes of Pd(II) and Pt(II) with Inosine=Ino, Guanosine=Guo, Xanthosine=Xao and their acetyl derivatives, triacetylinosine=trino, triacetylguanosine=trguo and triacetylxanthosine=trxao. These bases were chosen because they possess an exocyclic keto oxygen at the 6th position of the purineskeleton and therefore may form N(7)0(6) chelates with metals.

Results and discussion

Based on the lower *trans* effect of Nucl than that of halogens[3,14], we have been able to prepare the complexes *cis*-$Pd(trnucl)_2Cl_2$, where trnucl=triacetylnucleosides, according to the following reactions:

$$K_2PdCl_4 + 2trino \xrightarrow{CH_3CN,H_2O} cis\text{-}Pd(trino)_2Cl_2 + 2KCl \quad (1)$$

$$K_2PdCl_4 + 2trguo \xrightarrow{CH_3CN,H_2O} cis\text{-}Pd(trguo)_2Cl_2 + 2KCl \quad (2)$$

$$K_2PdCl_4 + 2trxao \xrightarrow{0.5N\ HCl} cis\text{-}Pd(trxao)_2Cl_2 + 2KCl \quad (3)$$

The analytical results agree with the assigned formulae (TABLE I).

The keto oxygen of the 6th position is free in these complexes, as it is shown from their ir spectra, since the νC=0 vibration of this group remains unshifted on passing from the ligands to the complexes at about 1700 cm^{-1}. (See Table II). All the complexes and the ligands show also a strong band at about 1750 cm^{-1} in their ir spectra, due to the carbonyl stretchings of the acetyl groups[15]. The complexes also show νPd-Cl vibrations in the region of ca. 330 cm^{-1}. The *cis*-$Pd(trino)_2Cl_2$ has two bands at 331 and 344 cm^{-1}, the *cis*-$Pd(trguo)_2Cl_2$ at 330 and 335 cm^{-1} and the *cis*-$Pd(trxao)_2Cl_2$ at 330 and 337 cm^{-1}, in accordance with the assigned *cis* configurations[16].

The *cis* configuration of the complexes is also confirmed by a Kurnakoff test[17].

TABLE I: *Analytical and physical data of the complexes*

Complex	C%	H%	N%	X_{mol}(c.g.s)X10^{-6}	M.W.	M.P.°C*
cis-Pd(trino-H^+)$_2$	42.91 (43.01)	3.98 (3.80)	11.75 (11.91)	125	918 (893)	270
cis-Pd(trguo-H^+)$_2$	41.55 (41.61	4.13 (3.90)	11.95 (11.53)	137	1750 (923)	280
cis-Pd(trxao -H^+)$_2$	41.22 (41.52)	3.40 (3.67)	11.88 (11.48)	-	1922 (925)	-
cis-Pd(trino)$_2$Cl$_2$	39.87 (39.76)	3.72 (3.52)	11.34 (11.02)	-	-	178
cis-Pd(trguo)$_2$Cl$_2$	38.05 (38.56)	3.81 (3.61)	10.42 (10.68)	-	-	225
cis-Pd(trxao)$_2$Cl$_2$	38.15 (38.48)	3.34 (3.60)	10.73 (10.66)	-	-	-
PdPy(Ino-H^+)Cl	36.59 (36.85)	3.55 (3.27)	21.25 (21.79)	80	378 (488)	205
PdPy(Guo-H^+)Cl	35.54 (35.76)	3.37 (3.97)	21.82 (21.14)	79	478 (503)	210
PdPy(Xao-H^+)Cl	35.65 (35.70)	3.08 (3.57)	21.36 (21.11)	201	251 (504)	230
PdCys(Guo-H^+)Cl	33.82 (34.12)	4.02 (3.74)	15.85 (15.94)	803	505 (668)	200
PdCyd(Ino-H^+)Cl	34.34 (34.91)	3.80 (3.67)	16.61 (16.31)	375	411 (653)	195
PdCyd(Xao-H^+)Cl	33.99 (34.07)	3.89 (3.59)	16.05 (15.92)	20	414 (669)	185
PtPy(Ino-H^+)Cl	30.82 (31.20)	3.00 (2.77)	33.69 (33.81)	352	306 (577)	230
PtPy(Guo-H^+)Cl	30.61 (30.40)	3.07 (2.87)	33.19 (32.96)	116	309 (592)	250
PtCyd(Ino-H^+)Cl	30.25 (30.69)	3.51 (3.23)	26.55 (26.30)			
PtIno(Ino-H^+)Cl	31.07 (31.33)	3.33 (3.00)	26.06 (25.54)	134	376 (766)	230
Pd(Ino-H^+)(Guo-H^+)**	-	-	-	597		
cis-Pd(Ino-H^+)$_2$**	-	-	-	266		
trans-Pd(Ino-H^+)$_2$**	-	-	-	264		
cis-Pd(Guo-H^+)$_2$**	-	-	-	*379*		
trans-Pd(Guo-H^+)**	-	-	-	250		

* The values are referred to decomposition points.

** The analytical results have been given 3c,17

The numbers in parentheses correspond to the calculated values.

TABLE II: *Characteristic ir bands of the complexes.*

Compound	ν C=O acetyls	ν C=O 6th pos.	ν C=O 2nd pos.	ν(C=C,C=N) of the rings	ν NH_2 ν NH	ν Pd-Cl
trino	1748	1706	-	1590, 1550	3133	-
trguo	1750	1706	-	1596, 1537 1486	3452	-
trxao	1750	1705	1705	1599, 1560	3160	-
cis-Pd(trino)$_2$Cl$_2$	1750	1710	-	1592, 1553 1520	-	344, 331
cis-Pd(trguo)$_2$Cl$_2$	1746	1704	-	1590, 1539 1503	3448	335, 330
cis-Pd(trxao)$_2$Cl$_2$	1745	1700	1700	1615, 1562 1498	3140	337, 330
cis-Pd(trino-H^+)$_2$	1749	1640	-	1529, 1496	-	-
cis-Pd(trguo-H^+)$_2$	1748	1622	-	1524, 1494	-	-
cis-Pd(trxao-H^+)$_2$	1740	1625	1690	1562, 1525 1492	-	-
PdPy(Ino-H^+)Cl	-	1630	-	1530, 1495	-	330
PdPy(Guo-H^+)Cl	-	1630	-	1600, 1533	3330	
PdPy(Xao-H^+)Cl	-	1625	1680	1572, 1520	-	330
PtPy(Ino-H^+)Cl	-	1630	-	1610, 1535 1500	-	330
PtPy(Guo-H^+)Cl	-	1630	-	1590, 1530	3330	330
PtIno-H^+)Cl	-	1690,1630	-	1588, 1520	-	330
Ino	-	1690	-	1584, 1510	3291	-
Guo	-	1722	-	1620, 1530	3300	-
Xao	-	1700	1700	1610, 1580	-	-

At pH ca 9 the above *cis* complexes are easily deprotonized and the following possible chelates precipitate:

$$cis\text{-Pd(trino)}_2\text{Cl}_2 \xrightarrow{\text{pH} \sim 9} cis\text{-Pd(trino} - H^+)_2\text{Cl}_2 + 2\text{HCl} \quad (4)$$

$$cis\text{-Pd(trguo)}_2\text{Cl}_2 \xrightarrow{\text{pH} \sim 9} cis\text{-Pd(trguo} - H^+)_2\text{Cl}_2 + 2\text{HCl} \quad (5)$$

$$cis\text{-Pd(trxao)}_2Cl_2 \xrightarrow{pH \sim 9} cis\text{-Pd(trxao -H}^+)_2Cl_2 + 2HCl \qquad (6)$$

The analytical results agree with the formulae (TABLE I). In the ir spectra of these last complexes with v C=0 of the 6th position is shown at ca. 1630 cm^{-1}, while the vC=0 of the acetyl groups are unhifted at about 1750 cm^{-1}.

The *cis*-Pd(trxao -H^+)$_2$ has one more band at ca. 1680 cm^{-1} which is due to the v C=0 of the 2nd position of the base. These shifts strongly indicate once again the existence of Pd-0(6) bonds[3],[14]. Similarly[3],[14], the v Pd-Cl vibrations disappear in the region of 300 cm^{-1}. The ^{1}Hnmr spectra of the initial complexes *cis*-Pd(trnucl)$_2$Cl$_2$ (trnucl = trino, trguo) reveal the N(7) atoms as bonding sites with Pd(II), since the adjacent H(8) protons shift upfield by ca.0.5 ppm[3],[14]. (TABLE III).

This implies this position N(7), as a bonding site also,

TABLE III: *^{1}Hnmr chemical shifts of trino, trguo and their Pd(II) complexes.*

Compound	H_8	H_2	NH_2	H_1	Solvent
trino	8.33	8.03	-	6.13*	$CDCl_3$
				6.20	
cis-Pd($_{trino}$)$_2Cl_2$	8.75	8.23	-	6.20	1N DCl
trguo	7.83	-	6.43	5.93	DMSO-d_6
cis-Pd($_{trguo}$)$_2Cl_2$	8.25**	-	6.66	5.96	DMSO-d_6
	8.20				

* Doublet

** Doublet showing the decomposition of *cis*-Pd(trguo)$_2$Cl$_2$ in DMSO-d_6.

in the possible chelates *cis*-Pd(trnucl)$_2$Cl$_2$ together with the 0(6) position, revealed from their ir spectra.

We have also carried out reactions of the monobase complexes K[PtLCl$_3$][18] and the newly synthesized K[PdLCl$_3$][14], where L is pyridine or cytidine with Ino, Guo and Xao in aqueous solutions in order to obtain similar 1:1 possible chelates. The reactions taking place are as follows:

$$K[MPyCl_3] + Nucl \xrightarrow{pH \sim 7.0 - 7.5} MPy(Nucl\text{-}H^+)Cl + KCl + HCl \qquad (7)$$

$$K[MCydCl_3] + Nucl \xrightarrow{pH \sim 7.0 - 7.5} MCyd(Nucl\text{-}H^+)Cl + KCl + HCl \quad (8)$$

Where M is Pd(II) or Pt(II) and Nucl is Ino, Guo or Xao.

Here again, the *trans* effect of the nucleosides, comparable to pyridine, provide that the first attack of the metal to the N(7) of the nucleosides should be in the *cis* to pyridine or cytidine positions[3,14]. Chu et al[19,20] have reported the lowering of the pK value of the N(1) imino proton of Ino and GMP in the presence of equimolar amounts of the *cis*-$Pt(NH_3)_2Cl_2$ by over 2 and 2.8 log units for the two bases respectively, in aqueous solutions. Such a lowering in the pK value of Ino, after Pt-N(7) coordination, to the value of neutral water (7), should facilitate the ionization of the imino protons and the formation of the N(7)0(6) chelates and/or polymeric compounds[3,14,19,20]. Therefore, the pH of the reactions was kept at ca. 7-7.5 with addition of 0.1 N KOH in order to facilitate the possible chelate formation by removal of the imino N(1) proton, which follows the attack by the metal at the N(7) site. The reactions with Pt(II) were slow and comlete precipitation was obtained in 2-3 days at room temperature, while those with Pd(II) took place almost immediately. The analytical results of the isolated complexes are included in TABLE I.

The ir spectra of the complexes in the region of 1700 cm^{-1}, indicate once again that all the complexes have their 0(6) keto oxygen involved in bonding with the metals[21-24]. The band at ca. 1700 cm^{-1} due to vC=0 of the free bases, Ino, Guo or Xao shifts to about 1625 cm^{-1}. [3](See TABLE II). There is also a weak band at ca. 330 cm^{-1} assigned to v M-Cl. The shift to lower frequencies of the vC=0 band upon ionization of the N(1) imino proton in Ino, Guo, Xao and their acetyl derivatives, indicates the loss of the double bond character of the C=0, in the structure[25,26].

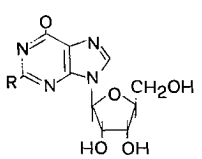

R=H, Inosine
NH_2, Guanosine
OH, Xanthosine

This is possibly more pronounced in the ionic sodium salt of guanosine (shift to 1595 cm^{-1})[24] and less whenever the metal-oxygen bonding is more covalent, as in the case of Pt(II) and Pd(II) for example (shift to 1625 cm^{-1})[3,14]. Certainly, the double bond character of the C=0 is also lowered when the oxygen interacts covalently with a metal without loss of the N(1) imino proton[23]. Oxygen involvement in bonding, following deprotonation of the imino proton, has also been found in the crystal structure of *cis*-diamminoplatinum a-Pyridone blue[27], where both 0^- and N atoms bridge two platinum atoms. Kistenmacher et al[28] have also found an oxygen -Ag(I) interaction in the crystal structure of (Nitrato) (1-methylcytosine) silver (I).

If the 0(6) is involved in bonding with the metals, the analytical results of the above complexes can only be interpreted as follows: either we have monomeric

N(7)0(6) chelates[3],[14], or polymeric structures involving the sites N(7),0(6) or N(7)0(6) and N(1) in a random sequence, like the ones already proposed[3a]. The existence of M-M bonds should also be considered in mixed valence states of the metals[27],[29].

The molecular weight determinations of the complexes performed in DMF or DMSO solutions are summarized in TABLE I. The complex *cis*-Pd(trino $-H^+)_2$ is clearly monomeric in DMF solutions. The complexes *cis*-Pd(trguo $-H^+)_2$ and *cis*-Pd(trxao $-H^+)_2$ give experimental values almost double of the calculated ones in DMSO solutions, as they are not soluble enough in DMF. A higher degree of stacking which occurs for Guo and Xao (free bases)[25],[26] could account for the double of the calculated M.W values found for their complexes. The zero charged complexes ML(Nucl-H^+)Cl dissolve in DMSO by slight heating in the water bath. The found values of the molecular weights are all less than the calculated ones (TABLE I), with the best fit for the complex PdPy(Guo-H^+)Cl.

A partial displacement of the chlorine atoms by DMSO could account for the lower values of the molecular weights found.

$$ML(Nucl\text{-}H^+)Cl + DMSO \rightarrow [ML(Nucl\text{-}H^+)DMSO]Cl \qquad (9)$$

Although a definitive conclusion from the M.W. measurements can hardly be drawn since the experimental values are very approximative, the above results may indicate monomeric complexes rather than polymeric.

The ^{1}Hnmr spectra of the complexes *cis*-Pd(trnucl $-H^+)_2$ showed broad bands, which indicate the presence of paramagnetic species. Indeed, all the complexes with 0(6) involvement in bonding are slightly paramagnetic at room temperature and give values of X_M varying from (+20 to + 800)$\times 10^{-6}$ c.g.s. after the diamagnetic corrections (See TABLE II). The complexes also show distinct e.s.r. signals. In FIG. 1. the e.s.r. spectrum of the complex PdCyd(Guo-H^+)Cl is shown.

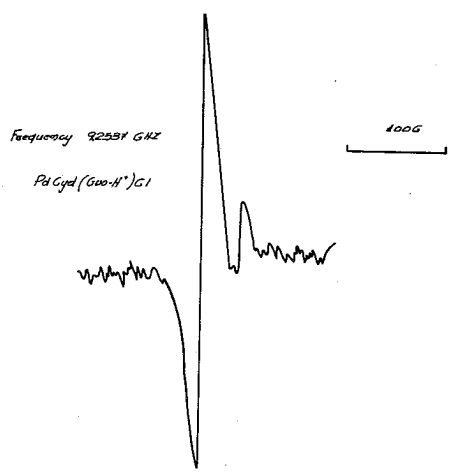

FIG. 1: *E.s.r. spectrum of the complex PdCyd (Guo-H$^+$)Cl in the solid state (powder).*

The existence of strong metal-metal bonds has to be excluded, since this would imply characteristic colours of the complexes, depending on the distance of the metals[29]. The complexes in this study do not have any characteristic color (green, blue or purple) not they possess any characteristic electronic spectrum. There is not distinct absorption maximum in the visible region, except the strong $\pi \rightarrow \pi^*$ transition at about 2650 A° of the ligands shifted to higher wavelenghts in the complexes[30]. It should be noted that the paramagnetism of the complexes is kept in solution. Complexes prepared under nitrogen show again the same small positive X_M values, thus excluding oxydation of the metals by atmospheric oxygen. The magnetic properties of the complexes are not at present well understrood, but they are under investigation.

Therefore, only suggestions concerning the structures of the complexes may be made. Since a strong metal-metal interaction seems not to be present in the complexes, the small values of X_M found, and the narrow esr signals observed, may be due to some impurities or free radicals present.

The molecular weights are also in favor for the N(7)0(6) monomeric chelates, although polymeric structures may also be considered, like:

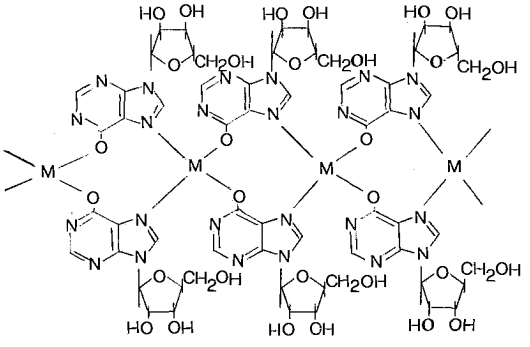

Experimental:

Materials: The nucleosides were purchased from Raylo Chemicals Ltd., and used without further purification. Potassium tetrachloropalladite (II) and potassium tetrachioplatinite (II) were from Fluka A.G. The triacetyl nucleosides were prepared according to the method of Bredereck[31].

Methods: (a) The ir spectra were recorded in a Beckman 2050 model spectrophotometer, in KBr pellets. The positions of the bands are given within $\pm 2cm^{-1}$ (b) The ^{1}Hnmr spectra were recorded in a Varian T60 high resolution spectrometer, in DMSO- d_6 solutions, using TMS as internal reference. (c) UV-Vis spectra were taken with a Carry 17D model spectrophotometer in DMF of DMSO solutions. (d) Magnetic moments were determined by the Gouy method with diamagnetic corrections. (e) Electron spin resonance spectra were recorded by using a Varian Y-4502 spectrometer with 100-Kc field modulation, operating at

9500 Mc. (f) Conductivity measurements were performed using an E 365B conductoscope, Metrohm Ltd, Herisau, Switzerland. (g) The melting points were determined on a Fisher John's apparatus and are uncorrected. (h) The microanalyses were performed in the Laboratories of the National Hellenic Research Foundation (N.H.R.F.) in Athens. (i) The molecular weight determinations were performed in DMF or DMSO solutions, by the Alfered Bernhardt Mikroanalytisches Laboratorium, West Germny. (ia) Pt and Pd were determined by ignition of about 0.1 gr of the samples at 900 C for 30 min. and weighing the residues as pure metals.

Preparation fo the complexes.

The complexes $K[PdPyCl_3]$, $K[PdCydCl_3]$ and $K[PtPyCl_3]$, $K[PtCydCl_3]$ were prepared according to known methods[14 18]

The complexes cis-bis (triacetylinosinato) palladium(II), cis-Pd(trino -H^+)$_2$ and cis-bis (triacetyguanosinato) palladium (II), cis-Pd(trguo -H^+)$_2$.

2mmol of each of the triacetyl nucleosides were dissolved or suspended in 50 ml of acetonitrile. 1 mmol of potassium tetrachlopalladite(II) (0.326 gr) was dissolved in 15ml of distilled water. The two solutions were mixed and stirred for two hours at room temperature until complete dissolution. The pH of the solution was adjusted to about 10, using 0.5N KOH and the precipitate formed, was washed with acetonitrile, hot water, acetone and ether and dried at 60°C under vacuum. Yield 75-80%.

The complexes cis-dichloro-bis (triacetylguanosine) palladium (II), cis-Pd(trguo)$_2$ Cl$_2$ and cis-dichloro-bis(triacetylinosine) palladium(II), cis-Pd(trino)$_2$Cl$_2$.

1mmol of each of the complexes Pd(trguo -H^+)$_2$ and Pd(trino -H^+)$_2$ were suspended in 10 ml of 0.5N HCl and stirred for 15 minutes at room temperature. Then, 15 ml of acetonitrile were added and the stirring was continued until complete dissolution. The solution was then filtered from any undissolved materials and the complexes were precipitated by the addition of excess isopropanol:ether (1:2) (300 ml). It was then filtered, washed with small quantities of isopropanol and ether and dried at 60°C under vacuum. Yield 80%.

The complex cis-dichloro-bis(triacetylxanthosine) palladium(II), cis-Pd(trxao)$_2$Cl$_2$.

2 mmol triacetylxanthosine (0.8180 gr) were dissolved in 50 ml of 0.5N HCl and 1 mmol of potassium tetrachlopalladite (II) (0.3266 gr) was dissolved in 20 ml of 0.5N HCl. The two solutions were mixed and strirred for 2-3 hrs. at room temperature. The precipitate formed was filtered and washed with small quantities of acetone and ether and dried at 60°C under vacuum. Yield 80%.

The complex cis-(triacetylxanthosinato) palladium(II), cis-Pd(trxao -H^+)$_2$.

1 mmol (0.9954 gr) of the complex *cis*-Pd(trxao)$_2$Cl$_2$ was dissolved in 50ml of water and the pH of the solution was kept at about 10 for 5-6 hrs. The precipitate formed in this way was filtered, washed with acetone and ether and dried at 110°C under vacuum. Yield 80%.

General method for the preparation of the Pd(II) chelates, cis-PdL(Nucl-H^+)Cl where L is Py or Cyd and Nucl in Ino, Guo, or Xao.

1 mmol of each of the nucleosides were dissolved or suspended in 50 ml of water and to that, 1 mmol of the complexes $K[PdLCl_3]$ were added in small

portions, by continuous strirring. A yellow precipitate was formed almost immediately and the pH of the solution decreased. The pH was kept constant at ca. 7-7.5, by adding 0.1N KOH and the stirring continued for 2-3 hours at room temperature. It was then filtered, washed with small quantities of acetone and ether and dried under vacuum in the presence of $CaCl_2$ and at 110°C under vacuum. The yield was quantitative. .

*General method for the preparation of Pt(II) chelates, cis-PtL(Nucl-H$^+$)*Cl, where L is Py or Cyd and Nucl is Ino or Guo.

1 mmol of each of the nucleosides was dissolved or suspended in 50 ml of water and to that, 1 mmol of the complexes $K[PtLCl_3]$ were added in small portions. In the case of guanosine the mixture was heated at ca. 40-50°C for 30 to 60 minutes until the solution became clear. It was then left at room temperature for 2-3 days by continuous stirring and by adjusting the pH to ca. 7-7.5 with 0.5N KOH. During this time the precipitates of the chelates were formed and were collected gradually by filtrations.

The precipitates were washed with small quantities of acetone and ether and dried in vacuum at room temperature and 110°C. Yields: 40-50%.

Acknowledgments,: (a) The microanalyses were performed by Dr. Mantzos of the National Hellenic Research Foundation (N.H.R.F.) in Athens. (b) The financial support of the N.H.R.F. is gratefully acknowledged.

Περίληψη

«Σύμπλοκα Pt(II) καί Pd(II) μέ 'Ινοσίνη, Γουανοσίνη, Ξανθοσίνη καί τά ἀκετυλιωμένα παράγωγά τους.

Μελετήθηκαν οἱ ἀντιδράσεις τῶν Pd(II) καί Pt(II) μέ πουρινικούς νουκλεοζῖτες (Ino, Guo, Xao καί trino, trguo, trxao), πού περιέχουν ἐξωκυκλική καρβονυλική ὁμάδα C=0 στήν 6η θέση τοῦ πουρινικοῦ δακτυλίου, σέ ὑδατικά διαλύματα. 'Απομονώθηκαν τά σύμπλοκα: *cis*-$Pd(trino)_2Cl_2$, *cis*-$Pd(trguo)_2Cl_2$, *cis*-$Pd(trxao)_2Cl_2$, *cis*-$Pd(trino\text{-}H^+)_2$, *cis*-$Pd(trguo\text{-}H^+)_2$, *cis*-$Pd(trxao\text{-}H^+)_2$ καί ML (Nucl -H$^+$)Cl, ὅπου τό M εἶναι Pd(II) ἤ Pt(II), τό L εἶναι Py ἤ Cyd καί τό Nucl εἶναι Ino, Guo ἤ Xao καί χαρακτηρίστηκαν μέ στοιχειακές ἀναλύσεις, μετρήσεις μοριακῆς ἀγωγιμότητας καί μοριακῶν βαρῶν καί φάσματα ir, ^{1}Hnmr καί esr. Οἱ δυνατές δομές γιά τά σύμπλοκα αὐτά πού προτείνονται βάσει τῶν πιό πάνω πειραματικῶν δεδομένων, εἶναι: Μονομερῆ N(7)0(6) χηλικά καί/ἤ N(7)0(6) διμερῆ ἤ πολυμερῆ σύμπλοκα.

References

1. Lippard, S.J.: *Acc. Chem. Res.* **11**, 211 (1978).
2. Kong, P.C. & Theophanides, T.: *Inorg. Chem.* **13**, 1167 (1974).
3. (a) Hadjiliadis, N. & Theophanides, T.: *Inorg. Chim. Acta.*, **16**, 77 (1976).
   (b) Pneumatikakis G., Hadjiliadis N., & Theophanides T.: *Inorg. Chim. Acta*, **22**, L_1 (1977).
   (c) Pneumatikakis G., Hadjiliadis N., & Theophanides T.: *Inorg. Chem.*, **17**, 915 (1978).
4. (a) Munchausen L.L. & Rahn R.O.: *Cancer Chemother. Repts.*, **59**, 643 (1975).
   (b) Munchausen L.L. & Rahn R.O.: *Bioch. Biophys. Acta*, **414**, 242 (1975).
5. Rosenberg B.: *J. Clin. Hematol. Oncol.*, **7**, 817 (1977).
6. Roos I.A.G. & Arnold M.C.: *J. Clin. Hematol. Oncol.*, **7**, 374 (1977).
7. Kelman, A.D., Peresie H.J. & Stone P.J.: *J. Clin. Hematol. Oncol.*, **7**, 440 (1977).
8. Roos I.A.G., Thomson A.J., & Mansy S.: *J. Amer. Chem. Soc.*, **96**, 6484 (1974).
9. Gellert R.W. & Bau R.: *J. Amer. Chem. Soc.*, **97**, 7379 (1975).
10. Goodgame D.M.L., Zeeves I., Phillips I.L. & Skapskii A.L.: *Bioch. Biophys. Acta*, **378**, 153 (1975).
11. (a) Millard M.M., Maquet J.P. & Theophanides T.: *Bioch. Biophys. Acta*, **402**, 166 (1975).
    (b) Maquet J.P. & Butour J.L.: *Biochimie*, **60**, 901 (1978).
12. Marzilli L.G.: "*Progress in Inorganic Chemistry*", **23**, 256, (1976) Wiley-Interscience, New York.
13. Harrison R.C. & McAuliffe C.A.: *Inorg. Persp. Biol. Med.*, **1**, 261 (1978).
14. Hadjiliadis N. & Pneumatikakis G.: *J. Chem. Soc.*, Dalton, 1691 (1978).
15. Hadjiliadis N. & Theophanides T.: *Can. J. Spectry.* **16**, 135 (1971).
16. Hartley F.R.: "*The Chemistry of Platinum and Palladium*", John Wiley & Sons, New York (1973).
17. Kurnakoff N.S.: *J. Prakt. Chem.*, **50**, 483 (1894).
18. (a) Kong P.C. & Rochon F.D.: *J. Chem. Soc., Chem. Commun.*, 599 (1975).
    (b) Kong P.C. & Rochon F.D.: *Can. J. Chem.*, **56**, 441 (1978).
19. Chu G.Y.H. & Tobias R.S.: *J. Amer. Chem. Soc.*, **98**, 2641 (1976).
20. Chu G.Y.H., Mansy S., Duncan R.E. & Tobias R.S.: *J. Amer. Chem. Soc.*, **100**, 593 (1978).
21. Ogawa M. & Sakaguchi T.: *Chem. Pharm. Bull.*, **19**, 1650 (1971).
22. Tu A.T. & Heller M.J.: "*Metal ions in biological systems*" **1**, 1 (1974).
23. Dehand J. & Jordanov J.: *J. Chem. Soc., Chem. Commun.*, 598 (1976).
24. Canty A.J. & Tobias R.S.: *Inorg. Chem.* **18**, 413 (1979).
25. Izatt R.M., Christensen J.J. & Rytting J.H.: *Chem. Rev.*, **71**, 439 (1971).
26. Shapiro R.: *Progr. Nucleic Acid Res.*, **73**, 8 (1968).
27. Barton J.K., Rabinowith H.N., Szalda D.J. & Lippard S.J.: *J. Amer. Chem. Soc.*, **99**, 2827 (1977).
28. Kistenmacher T.J., Rossi M. & Marzilli L.G.: *Inorg. Chem.*, **18**, 240 (1979).
29. Krogmann K.: *Angew. Chem. Inter. Ed.*, **8**, 35 (1969).
30. Hadjiliadis N. Kourounakis P. & Theophanides T.: *Inorg. Chim. Acta*, **7**, 226 (1973).
31. Bredereck H.: *Berichte*, **80**, 401 (1947).

Chimika Chronika, New Series, 11, 23-29 (1982)

ΠΑΡΑΣΚΕΥΗ ΚΑΙ ΧΑΡΑΚΤΗΡΙΣΜΟΣ ΣΤΗΡΙΖΟΜΕΝΩΝ ΟΞΕΙΔΙΚΩΝ ΚΑΤΑΛΥΤΩΝ ΚΟΒΑΛΤΙΟΥ, ΥΨΗΛΗΣ ΠΕΡΙΕΚΤΙΚΟΤΗΤΑΣ ΣΕ ΚΟΒΑΛΤΙΟ, ΠΑΝΩ ΣΕ γ-ΑΛΟΥΜΙΝΑ ΤΡΟΠΟΠΟΙΗΜΕΝΗ ΜΕ ΙΟΝΤΑ ΝΑΤΡΙΟΥ.

Α. ΛΥΚΟΥΡΓΙΩΤΗ ΚΑΙ C. DEFOSSÉ

Πανεπιστήμιο Πατρῶν, Ἐργαστήριο Φυσικοχημείας καί Καθολικό Πανεπιστήμιο Louvain (Βέλγιο).

(Received March 31, 1981).

Περίληψη

Στήν ἐργασία αὐτή μελετήθηκε ἡ ἐπίδραση τῶν ἰόντων νατρίου στό καταλυτικό σύστημα Co_3O_4(12%)/γ-Al_2O_3-Na. Βρέθηκε, ὅτι στούς 600°C αὔξηση τοῦ περιεχομένου στό φορέα νατρίου προκαλεῖ ἐλαφρά βελτίωση τῆς διασπορᾶς τῆς ἐνεργοῦ φάσεως στήν ἐπιφάνεια τοῦ ὑποστρώματος.

Σημαντική βελτίωση τῆς διασπορᾶς μέ σύγχρονη μετάπτωση τοῦ Co^{2+} ἀπό τήν ὀκταεδρική στήν τετραεδρική συμμετρία, προκάλεσε ἡ διέγερση τῆς θερμοκρασίας ἀπό τούς 600 στούς 700°C.

Στή θερμοκρασία τῶν 700°C φάνηκε, ὅτι αὔξηση τοῦ περιεχόμενου νατρίου προκαλοῦσε αὔξηση τῆς διασπορᾶς τοῦ Co^{2+} ἐνῶ συγχρόνως παρεμπόδιζε τό σχηματισμό Co^{2+} . [Ὡς Co_t^{2+} συμβολίζεται τό Co^{2+} σέ τετραεδρική συμμετρία].

Γιά τήν ἑρμηνεία τῶν παραπάνω παρατηρήσεων προτάσσεται ἕνας ἁπλός μηχανισμός καί σχολιάζονται οἱ συνέπειες τῶν παραπάνω ἐπιδράσεων στίς καταλυτικές ἰδιότητες τῶν δειγμάτων.

Key words: Catalysis/Cobalt-Catalysts/Cobalt-surface species/γ-Al_2O_3 doped Na^+

Εἰσαγωγή

Ἡ σύνθεση στερεῶν καταλυτῶν μέ ἐλεγχόμενες ἰδιότητες εἶναι ἕνα ἀπό τά πλέον δύσκολα προβλήματα τῆς ἑτερογενοῦς καταλύσεως. Τό πρόβλημα αὐτό γίνεται ὀξύτερο στήν περίπτωση τῶν στηριζόμενων ὀξειδικῶν καταλυτῶν,

ἐξαιτίας τοῦ περιορισμένου ἀριθμοῦ τῶν ὑπαρχόντων φορέων. Ἔτσι, τά τελευταῖα χρόνια ἔχει ἀρχίσει μιά συστηματική προσπάθεια ἐλεγχόμενης τροποποιήσεως κλασσικῶν φορέων, ὅπως ἡ ἀλουμίνα καί ἡ σίλικα (SiO_2). Ἡ τροποποίηση αὐτή ἐπιτυγχάνεται μέ τή μόλυνση τοῦ φορέα μέ διάφορα ἰόντα[1-11]. Οἱ περισσότερες μελέτες, πού ἔχουν γίνει ἕως τώρα, ἀφοροῦν τό σύστημα: Co_3O_4/γ-Al_2O_3-Na. Δηλαδή στηριζόμενους καταλύτες, πού περιέχουν ἑνώσεις τοῦ κοβαλτίου ὡς ἐνεργό φάση καί γ-Al_2O_3 τροποποιημένη μέ ἰόντα νατρίου ὡς φορέα. Οἱ μελέτες αὐτές ἀποσκοποῦσαν στή ρύθμιση τοῦ εἴδους καί τῆς διασπορᾶς τῶν χημικῶν ἑνώσεων, πού συνιστοῦν τήν ἐνεργό φάση. Δηλαδή τῶν παραγόντων ἐκείνων, πού κυρίως προσδιορίζουν τήν καταλυτική δραστικότητα. Ἡ ρύθμιση αὐτή ἐπιτυγχάνονταν μέ τήν κατά βούληση μεταβολή τῶν παραμέτρων τῆς τροποποιήσεως· δηλαδή τῆς συγκεντρώσεως τοῦ τροποποιητῆ καθώς καί τῆς θερμοκρασίας κάτω ἀπό τήν ὁποία αὐτός «εἰσάγεται» στόν ἀτροποποίητο φορέα. Ἡ ἔρευνα ἔχει ἕως τώρα περιορισθεῖ σέ καταλύτες, πού περιέχουν χαμηλή συγκέντρωση ἐνεργοῦ φάσεως (2.8% Co_3O_4) καί πού εἶχαν θερμανθεῖ σέ θερμοκρασίες χαμηλότερες ἀπό 600°C. Οἱ καταλύτες αὐτοί συνιστοῦν πρόδρομες ἐπιφάνειες γιά τή σύνθεση καταλυτῶν ὑδρογονοεπεξεργασίας τοῦ πετρελαίου.

Ὑπάρχουν ὡστόσο πολλές περιπτώσεις, ὅπου ἡ χρησιμοποίηση στηριζόμενων καταλυτῶν κοβαλτίου μέ ὑψηλή συγκέντρωση ἐνεργοῦ φάσεως καί θερμοκρασία πυρώσεως ὑψηλότερη ἀπό 600°C εἶναι τελείως ἀπαραίτητη.

Στήν ἐργασία αὐτή μελετοῦμε τή δυνατότητα ρυθμίσεως τοῦ εἴδους καί τῆς διασπορᾶς τῶν χημικῶν ἑνώσεων πού συνιστοῦν τήν ἐνεργό φάση σέ μιά σειρά καταλυτῶν, πού περιέχουν 12% Co_3O_4 καί πού ἔχουν θερμανθεῖ στούς 700°C. Ἡ ρύθμιση αὐτή ἐπιχειρεῖται μέ τή βοήθεια ἰόντων νατρίου, πού εἰσάγονται στή γ-ἀλουμίνα.

Ἡ φασματοσκοπία διαχύτου ἀνακλάσεως (Diffuse Reflectance Spectroscopy: D.R.S.) καί ἡ ἠλεκτρονική φασματοσκοπία μέ ἀκτίνες X (X-ray Photoelectron Spectroscopy: X.P.S.) χρησιμοποιήθηκαν γιά τόν προσδιορισμό τῆς φύσεως καί τῆς διασπορᾶς τῆς ἐνεργοῦ φάσεως, ἀντίστοιχα.

Πειραματικό μέρος

Ἡ τροποποίηση τῶν φορέων

Ἡ σύνθεση τῶν τροποποιημένων φορέων ἔγινε μέ τή μέθοδο τοῦ ξηροῦ ἐμποτισμοῦ (dry impregnation). Συγκεκριμένα, παρασκευάσθηκαν ὑδατικά διαλύματα $NaNO_3$ διαφόρων συγκεντρώσεων. Σ' αὐτά ἐμβαπτίσθηκε μιά ὁρισμένη ποσότητα γ-ἀλουμίνας (Ho Houdry, εἰδική ἐπιφάνεια: 160m^2/g, ὄγκος πόρων: 0,45cm^3/g). Ὁ ὄγκος τῶν διαλυμάτων πού χρησιμοποιήθηκαν ἦταν πάντοτε ἴσος πρός τό συνολικό ὄγκο τῶν πόρων τῆς γ-ἀλουμίνας.

Ἔπειτα ἀπό ξήρανση 12 ὡρῶν στούς 100°C, τά δείγματα θερμάνθηκαν παρουσία ἀέρος στούς 600°C, γιά 12 ὧρες.

Ἡ παρασκευή τῶν καταλυτῶν

Ἡ ἐναπόθεση τῆς ἐνεργοῦ φάσεως στούς τροποποιημένους φορεῖς ἔγινε ἐπίσης μέ τή μέθοδο τοῦ ξηροῦ ἐμποτισμοῦ. Χρησιμοποιήθηκαν ὑδατικά διαλύματα $Co(NO_3)_2.6H_2O$ (Merk p.a.). Τά δείγματα ξηράνθηκαν στούς 100°C γιά 12h καί κατόπιν θερμάνθηκαν στούς 600 ἤ στούς 700°C γιά 12 ἤ 6 h, ἀντίστοιχα. Ὅλα τά δείγματα περιέχουν κοβάλτιο πού ἀντιστοιχεῖ σέ 12%g Co_3O_4.

Φάσματα Διαχύτου Ἀνακλάσεως

Ἡ λήψη τῶν φασμάτων D.R.S. ἔγινε μέ τή βοήθεια ἑνός φασματοφωτομέτρου Beckman Acta IV, ἐφοδιασμένου μέ ἐξάρτημα D.R.S. σέ θερμοκρασία περιβάλλοντος στήν περιοχή 800-400nm. Δύο κυψελίδες ἀπό quartz χρησιμοποιήθηκαν ὡς ὑποδοχεῖς.

Φάσματα Ἠλεκτρονικῆς Φασματοσκοπίας Ἀκτίνων Χ

Ἔπειτα ἀπό κονιορτοποίηση καί συμπίεση τῶν δειγμάτων κατασκευάσθηκαν «δισκία» διαμέτρου 8mm καί πάχους 1mm. Οἱ μετρήσεις ἔγιναν σέ θερμοκρασία δωματίου χρησιμοποιώντας φασματοφωτόμετρο X.P.S. (Vaccum Generators ESCA 3). Ἡ πειραματική διαδικασία πού ἀκολουθήσαμε ἔχει ἀναφερθεῖ σέ προηγούμενες ἐργασίες[2,9]. Ἡ ἔνταση τῆς γραμμῆς $Co_{2p\ 3/2}$ πού τή συμβολίζουμε ὡς Co_{2p} μετρήθηκε ἀναφορικά μέ τήν ἔνταση τῆς διπλῆς γραμμῆς $Al_{2p\ 3/2,\ 1/2}$ πού τή συμβολίζουμε ὡς Al_{2p}. Σημειώνουμε τό λόγο Co_{2p}/Al_{2p} ὡς R_{Co2p}. Αὐτός εἶναι ἀνάλογος τῆς διασπορᾶς τοῦ κοβαλτίου στήν ἐπιφάνεια τοῦ φορέα[2,9].

Συμβολισμός τῶν δειγμάτων

Τά δείγματα πού παρασκευάσθηκαν, συμβολίζονται ὡς ἑξῆς. Na-X-Y-Co-Z-W. Ὅπου X=%gNa, ἐνῶ τά Y, Z καί W παριστάνουν ἀντίστοιχα τή θερμοκρασία θερμάνσεως (βαθμοί Κελσίου) πρίν καί μετά τήν ἐναπόθεση τοῦ κοβαλτίου καί τή διάρκεια τῆς τελευταίας θερμάνσεως (ὧρες).

Ἀποτελέσματα καί συζήτηση

Ἡ εἰκόνα παριστάνει τά φάσματα D.R.S. τῶν Na-X-600-Co-700-6 καί Na-X-600-Co-600-12 μέ X=0,9, 3,6 καί 5,7.

Ἡ ἑρμηνεία τῶν φασμάτων αὐτῶν στηρίζεται σέ διαγνωστικά κριτήρια πού βρίσκουμε στή βιβλιογραφία[1-11]. Σύμφωνα μέ αὐτά ἕνας ὦμος στά $\simeq$ 750 καί μιά «ἀπορρόφηση» στά $\simeq$ 425nm ὀφείλονται στήν παρουσία Co^{2+} σέ ὀκταεδρική συμμετρία. Συνεπῶς ὑποδηλώνουν τήν παρουσία Co_3O_4. Ἀπό τήν ἄλλη πλευρά ἡ ἐμφάνιση μιᾶς τριπλῆς γύρω στά 600nm ἀποδεικνύει τήν παρουσία Co^{2+} σέ τετραεδρική συμμετρία. Ἡ ὕπαρξη τετραεδρικοῦ κοβαλτίου ἀποδίδεται εἴτε στό σχηματισμό ἐπιταξιακοῦ σπινελίου $CoAl_2O_4$, εἴτε στή διάχυση τῶν ἰόντων Co^{2+} πρός τό ἐσωτερικό τῆς γ-Al_2O_3 καί τήν κατάληψη

τετραεδρικῶν πλεγματικῶν θέσεων. Ἡ συμμετοχή τῆς δεύτερης διεργασίας εἶναι ἀρκετά σημαντική σέ θερμοκρασίες μεγαλύτερες ἀπό 600°C.

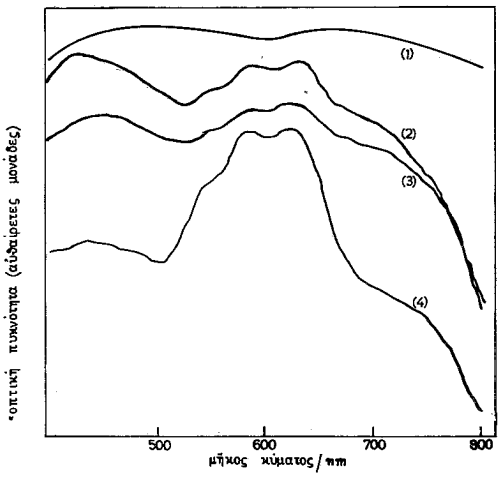

Εἰκόνα: Φάσματα διαχύτου ἀνακλάσεως τῶν καταλυτῶν, πού παρασκευάσθηκαν: (1) Na-X-600-Co-600-12, (X:0,9, 3,6 καί 5,7), (2) Na-5,7-600-Co-700-6, (3) Na-3,6-600-Co-700-6, (4) Na-0,9-600-Co-700-6.

Στόν πίνακα ἀναγράφονται οἱ τιμές R_{Co2p} γιά τά περισσότερα ἀπό τά δείγματα πού παρασκευάσθηκαν. Οἱ τιμές αὐτές ὅπως ἀναφέρθηκε, εἶναι μέτρα τῆς διασπορᾶς τοῦ Co^{2+} στήν ἐπιφάνεια τοῦ φορέα.

ΠΙΝΑΚΑΣ: *Περιλαμβάνει τίς τιμές RCo_{2p} γιά τά διάφορα δείγματα, πού παρασκευάσθηκαν.*

Δεῖγμα	RCo_{2p}
Na-0,9-600-Co-600-12	0,325
Na-3,6-600-Co-600-12	0,376
Na-5,7-600-Co-600-12	0,440
Na-0,9-600-Co-700- 6	0,819
Na-3,6-600-Co-700- 6	——
Na-5,7-600-Co-700- 6	0,970

Τά φάσματα D.R.S. δείχνουν, ὅτι σ' ὅλα τά δείγματα πού θερμάνθηκαν στούς 600°C, καί ἀνεξάρτητα ἀπό τή συγκέντρωση τῶν ἰόντων νατρίου στό φορέα, ἡ ἐπικρατοῦσα φάση εἶναι ἐπιφανειακό καί ἄσχημα διασπαρμένο Co_3O_4. Ἀκόμα, τιμές $R_{\omega 2p}$ δείχνουν, ὅτι αὔξηση τῆς συγκεντρώσεως τῶν ἰόντων νατρίου προκαλεῖ μιά ἐλαφρά βελτίωση (αὔξηση) τῆς διασπορᾶς τοῦ Co_3O_4.

Διέγερση τῆς θερμοκρασίας ἀπό τούς 600 στούς 700°C προκαλεῖ δύο συγχρόνως φαινόμενα: Αὔξηση τῆς διασπορᾶς τοῦ Co^{2+} καί σχηματισμό κοβαλτίου σέ τετραεδρική συμμετρία. Στή θερμοκρασία αὐτή αὔξηση τῆς

συγκεντρώσεως τοῦ νατρίου, αὐξάνει τή διασπορά ἐνῶ ἐμποδίζει τή μετάβαση τοῦ Co^{2+} ἀπό τήν ὀκταεδρική στήν τετραεδρική συμμετρία.

Τά φαινόμενα πού παρατηροῦνται στούς 600°C ἀναμένονται, γιατί βρίσκονται σέ συμφωνία μέ τό γενικό μηχανισμό, πού ἔχουμε προτείνει γιά τή δράση τῶν ἀλκαλίων[2,8]. Ἀντίθετα, τά φαινόμενα, πού παρατηρήθηκαν ἔπειτα ἀπό θέρμανση στούς 700°C δέν ἀναμένονται καί πρέπει νά σχολιασθοῦν.

Ὅπως ἀναφέραμε παραπάνω, αὔξηση τῆς θερμοκρασίας ἀπό τούς 600 στούς 700°C προκαλεῖ δύο φαινόμενα τά ὁποῖα σχηματικά μποροῦν νά παρασταθοῦν ὡς ἑξῆς:

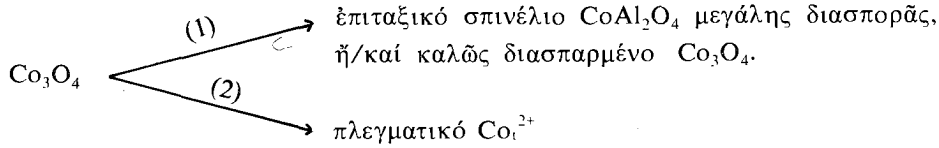

Ἡ διεργασία (1) προκαλεῖ αὔξηση τόσο τῆς διασπορᾶς, ὅσο καί τοῦ τετραεδρικοῦ κοβαλτίου. Ἡ διεργασία (2) προκαλεῖ αὔξηση τοῦ τετραεδρικοῦ Co^{2+} ἀλλά μειώνει τήν ἐπιφανειακή διασπορά. Καί αὐτό γιατί ἡ διάλυση τοῦ Co^{2+} στό πλέγμα τοῦ φορέα μειώνει τή συγκέντρωση τοῦ ἐπιφανειακοῦ Co^{2+}.

Ὁ συνδυασμός τῶν δύο διεργασιῶν μπορεῖ εὔκολα νά ἑρμηνεύσει τή μετάβαση τῶν Co^{2+} ἀπό τήν τετραεδρική στήν ὀκταεδρική συμμετρία, πού παρατηρεῖται μέ τήν αὔξηση τῆς θερμοκρασίας. Ἀπό τήν ἄλλη πλευρά, ἡ παρατηρούμενη αὔξηση τῆς διασπορᾶς δείχνει, ὅτι τό καθαρό ἀποτέλεσμα τῆς ἀνταγωνιστικῆς δράσεως τῶν δύο κλάδων —ἀναφορικά μέ τή διασπορά— εἶναι θετικό.

Ἄς ἑρμηνεύσουμε τώρα τά φαινόμενα, πού προκαλοῦν τά ἰόντα νατρίου στούς 700°C. Αὐτά ἐξηγοῦνται ἄν δεχτοῦμε, ὅτι ἡ αὔξηση τῆς συγκεντρώσεως τῶν ἰόντων Na^+ προκαλεῖ προοδευτικά αὐξανόμενη παρεμπόδιση τῆς διεργασίας (2). Πράγματι, μιά τέτοια ἐπίδραση θά ἐπέφερε σχετική μείωση τοῦ Co_t^{2+} μέ σύγχρονη αὔξηση τῆς διασπορᾶς. Ὁ μηχανισμός μέ τόν ὁποῖο τά ἰόντα Na^+ ἐμποδίζουν τό σχηματισμό πλεγματικοῦ Co_t^{2+} πρέπει νά ἀναζητηθεῖ στήν ἀνταγωνιστική διάχυση τῶν ἰόντων Na^+ μέ τά ἰόντα Co_t^{2+} γιά τήν κατάληψη πλεγματικῶν τετραεδρικῶν θέσεων τῆς γ-ἀλουμίνας. Εἶναι λογικό νά ὑποθέσουμε, ὅτι ἡ πιθανότητα νά καταληφθεῖ μιά τέτοια τετραεδρική θέση ἀπό ἕνα ἰόν Na^+ αὐξάνει μέ τή συγκέντρωσή τους· αὐτό δικαιολογεῖ γιατί ἡ ἔκταση τῆς παρεμποδίσεως αὐξάνει μέ τό περιεχόμενο ποσοστό νατρίου.

Θά πρέπει νά τονίσουμε, ὅτι ἡ συγκεκριμένη ἐπίδραση πού προκάλεσε ἡ αὔξηση τῆς συγκεντρώσεως τῶν ἰόντων Na^+ στή συμμετρία καί στή διασπορά τοῦ Co^{2+} ὀφείλεται στό ὅτι ὁ κλάδος (2) εἶναι ἀρκετά σημαντικός στούς 700°C. Ἀντίθετα, σέ θερμοκρασίες κάτω ἀπό 600°C, καί γιά δείγματα πού περιεῖχαν 2.8% Co_3O_4 ἡ μή σημαντική συμμετοχή τοῦ κλάδου (2) στή συνολική ἐπιφανειακή διεργασία εἶχε ὁδηγήσει σέ αὔξηση τῆς διασπορᾶς, ἐνῶ συγχρόνως εἶχε διευκολύνει τή μετάβαση ἀπό τήν ὀκταεδρική στήν τετραεδρική συμμετρία.

Τέλος, θά πρέπει νά σημειώσουμε, ὅτι καί τά δύο φαινόμενα, πού προκαλοῦν τά ἰόντα νατρίου στούς καταλύτες μέ ὑψηλή συγκέντρωση κοβαλτίου εἶναι

ἀπολύτως εὐνοϊκά ἀπό καταλυτικῆς πλευρᾶς. Πραγματικά εἶναι γνωστό, ὅτι τόσο ἡ αὔξηση τῆς διασπορᾶς ὅσο καί ἡ αὔξηση τοῦ ἐπιφανειακοῦ Co^{2+} βελτιώνουν τίς καταλυτικές ἰδιότητες τῶν στηριζόμενων ὀξειδικῶν καταλυτῶν κοβαλτίου.

Abstract

Preparation and Characterization of high percentage Cobalt Oxide Catalysts supported on γ-Al_2O_3 modified with the sodium ions.

The effects of sodium ions on the Co_3O_4 (12%)/γ-Al_2O_3-Na catalytic system have been studied. It was found that an increase of sodium content causes a slight improvement in the disperesion of Co^{2+} species for the samples heated at 600°C.

A rise of calcination temperature from 600 to 700°C brought about a considerable increase of the cobalt dispersion together with a transition of Co^{2+} from octahedral to tetrahedral coordination symmetry.

At 700°C, it was observed that an increase of sodium content provokes two effects: An increase of the cobalt dispersion and an inhibition of the formation of tetrahedral Co^{2+} .

A mechanism to take into account the above observations has been proposed.

The practical consequences, from the point of view of catalysis, have been mentioned.

Βιβλιογραφία

(1) A. Lycourghiotis, C. Defossé & B. Delmon: *Rev. Chim. Miner* **16**, 473 (1979).
(2) A. Lycourghiotis, C. Defossé, F. Delannay, J. Lemaitre & B. Delmon: *J. Chem. Soc. Faraday-I* **76**, 1677 (1980).
(3) A. Lycourghiotis, C. Defossé, F. Delannay & B. Delmon: *J. Chem. Soc. Faraday-I*, **76**, 2052 (1980).
(4) A. Lycourghiotis, D. Vattis & Ph. Aroni: *Z. Phys. Chem. (N.F.)* **121**, 257 (1980).
(5) A. Lycourghiotis, D. Vattis & Ph. Aroni: *Z. Phys. Chem. (N.F.)* **120**, 211 (1980).
(6) C. Defossé, M. Houalla, A. Lycourghiotis & F. Delannay: 7th International Congress on Catalysis, Tokyo, July 1980 p. 108.
(7) A. Lycourghiotis, D. Vattis, & N.A. Katsanos: *Z. Phys. Chem. (N.F.)* **125**, 239 (1981).
(8) A. Lycourghiotis, D. Vattis, Ph. Aroni & N.A. Katsanos: *Acta Chimika*, in press.
(9) A. Lycourghiotis, C. Defossé & B. Delmon: *Bull. Soc. Chim. Belge* **89**, 929 (1980).
(10) C. Defossé, M. Houalla, A. Lycourghiotis & F. Delannay: *Chinese Symposium on Catalysis*, Taiwan, July 1980.
(11) F. Delannay, C. Defossé, M. Houalla & A. Lycourghiotis: *12th Swedish Symposium on Catalysis, Lund*, October, 11-12, (1979).
(12) A. Lycourghiotis: *React. Kinet. Catal. Lett.*, **17**, 165 (1981).

(13) A. Lycourghiotis, A. Tsiatsios & N.A. Katsanos: *Z. Phys. Chem. (N.F.)* **126**, 95 (1981).
(14) A. Lycourghiotis, A. Tsiatsios & N.A. Katsanos: *Z. Phys. Chem. (N.F.)* **126**, 85 (1981).
(15) M. Houalla & B. Delmon: *C.R. Acad. Sc. Paris, série c*, **289**, 77 (1979).
(16) M. Houalla & B. Delmon: *C.R. Acad. Sc. Paris, série c*, **290**, 301 (1980).
(17) J. Lemaitre & M. Houalla: *C.R. Acad. Sc. Paris, série c*, **291**, 17 (1980).
(18) F. Delannay, M. Houalla, D. Pirotte & B. Delmon: *Surface and interface Analysis* **5**, 172 (1979).

Εὐχαριστίες: Οἱ συγγραφεῖς εὐχαριστοῦν τό Διευθυντή καί τό τεχνικό προσωπικό τῆς ὁμάδας Ἀνοργάνου Φυσικοχημείας καί Καταλύσεως τοῦ Καθολικοῦ Πανεπιστημίου τῆς Louvain γιά τή βοήθεια πού τούς προσέφεραν.

Chimika Chronika, New Series, 11, 31-36 (1982)

^{1}H-NMR -SPEKTROSKOPISCHE UNTERSUCHUNG DER BINDUNGSVERHÄLTNISSE IM DIMETHYLBIS(CYCLOPENTADIENYL)SILAN.

HARTMUT KÖPF UND NIKOLAOS KLOURAS
Institut für Anorganische und Analytische Chemie der Technischen Universität Berlin, D-1000 Berlin 12, Deutschland

(Received April 6, 1981)

Summary

The ^{1}H-NMR spectrum of Me_2SiCp_2 determined at various temperatures is reported and discussed in terms of metallotropic and prototropic rearrangements.

Key words: Dimethylbis(cyclopentadienyl)silan, synthesis, ^{1}H-NMR spectral data, structure.

Einleitung

Von den Cyclopentadienylsilanen ist Me_3SiCp die meist untersuchte Verbindung. Das grosse Interesse für diese Substanz rührt von ihren temperaturabhängigen ^{1}H-NMR-Spektren her, die zur Deutung der Si-Cp-Bindung herangezogen werden[1-3]. Me_2SiCp_2 wurde als erstes Bis(cyclopentadienyl)silan 1953 von K.C. Frisch nach dem Grignardverfahren hergestellt[4,5]:

$$Me_2SiCl_2 + 2\ CpMgBr \rightarrow Me_2SiCp_2 + 2\ MgClBr$$

Eine günstigere Methode (kurze Darstellungszeit und bessere Ausbeuten) zur Synthese von Me_2SiCp_2 stellt sich die Reaktion von Me_2SiCl_2 mit CpLi oder CpNa in Petrolether heraus[7]:

$$Me_2SiCl_2 + 2\ CpNa \rightarrow Me_2SiCp_2 + 2\ NaCl$$

Von der in der Literatur[4-6] nur spärlich charakterisierten Verbindung Me_2SiCp_2 wurde erstmals ein ^{1}H-NMR-Spektrum bei verschiedenen Temperaturen vermessen. In der vorliegenden Arbeit werden die Bindungsverhältnisse im

Dimethylbis(cyclopentadienyl)silan mit Hilfe der ^{1}H-NMR-Spektroskopie untersucht.

Experimenteller Teil

Alle Arbeiten wurden unter strengem Ausschluss von Sauerstoff und Feuchtigkeit durchgeführt. Die verwendeten Glasapparaturen wurden ausgeheizt und mit nachgereinigtem Argon gespült. Die Entfernung von Sauerstoffspuren im Argon erfolgte durch einen ca. 140°C heissen BTS-Katalysator, vorhandene Feuchtigkeit wurde durch Calciumchlorid, Silicagel und Phosphorpentoxid beseitigt. ^{1}H-NMR-Spektren wurden an den Geräten A60 und XL100 der Firma Varian aufgenommen; angegebene Werte sind auf den Standard $SiMe_4$ umgerechnet.

Verwendete Abkürzungen:

R = organischer Rest, Me = CH_3, Cp = C_5H_5 (cyclopentadienyl) M = Metall, E = Element, THF = Tetrahydrofuran, PE = Petrolether, i.V. = im Vakuum.

Darstellung von Cyclopentadienylnatrium

Zu 24,4 g (101,7 mmol) NaH (+20% Paraffinöl) in 450 ml PE und 50 ml THF werden bei 20°C unter mechanischem Rühren 90 ml (109,5 mmol) durch Cracken des Dimeren frisch hergestelltes CpH innerhalb 1 h zugetropft. Nach Zugabe von ca. 20 ml CpH kommt die Reaktion unter Gasentwicklung und Selbsterwärmung in Gang und wird erfordenlichenfalls durch Kühlung mit einem Wasserbad gemässigt. Die anfänglich graue NaH-Suspension wird durch Bildung von CpNa voluminöser und nimmt einen beigen Farbton an. Zur Vervollständigung der Reaktion wird mehrere Stunden weiter gerührt und anschliessend mit einem 40°C heissen Wasserbad nochmals zum Sieden erwärmt. Nach Absetzenlassen des Niederschlags wird die Hauptmenge der überstehenden Lösung abgehebert. Der Rückstand wird auf die gleiche Weise zweimal mit je 200 ml PE gewaschen und im Ölvakuum von Lösungsmittelresten befreit. Dabei wird gegen Ende gelinde erwärmt und der Kolben geschüttelt, bis sich die Krusten von der Wand abgelöst haben und CpNa als feines, leichtbewegliches Pulver vorliegt, das im Schlenkkolben im Dunkeln aufbewahrt wird. Ausbeute: 86 g (96%) bezogen auf das NaH.

Darstellung von Dimethylbis(cyclopentadienyl)silan

24 ml (200 mmol) Me_2SiCl_2 werden bei 20°C unter mechanischem Rühren zu 35,2 g (400 mmol) CpNa in 400 ml PE in einem Guss zugegeben. Die Mischung kommt durch Selbsterwärmung zum Sieden.

Man lässt ohne äussere Wärmezufuhr ca. 45 min unter Rückfluss kochen und noch 2 h bei 20° C weiterrühren. Nach Absetzenlassen des entstandenen Niederschlags wird dieser in einer Umkehrfritte abgetrennt, mit 200 ml PE gewaschen und das gelbe, klare Filtrat i.V. auf ca. 60 ml eingeengt. Man destilliert

das schwach rote Konzentrat über eine Mikrodestille und erhält bei 60-70°C/10 Torr 23 g (61% Ausbeute) Me_2SiCp_2 als wasserklare Flüssigkeit.

Diskussion der Ergebnisse

Me_2SiCp_2 stellt eine hochsiedende Flüssigkeit von eigenartigem, angenehmen Geruch dar, die nach kurzem Stehen an der Luft braun und ölig wird. Unter Schutzgas und bei tiefer Temperatur ist sie für ein paar Tage stabil. Das Vorliegen von Me_2SiCp_2 wird durch Siedepunktsvergleich mit Literaturangaben[4,5], negativen Cl-Test sowie durch das ^{1}H-NMR-Spektrum gesichert.

Rein ionisch gebundene Cp-Ringe zeigen wegen der magnetischen Gleichwertigkeit der fünf Protonen im D_{5h}-symmetrischen C_5H_5-Anion ein einziges Protonenresonanzsignal (z.B. CpNa in THF τ=4,1 ppm). Ebenso fallen beim π-komplexgebundenen Cp-Ring auch bei Koordination an ein Zentralatom mit unsymmetrischer Umgebung wegen der freien Drehbarkeit um die M-C_5H_5-Bindungsachse die Signale der fünf Protonen immer zusammen (z. B. Cp_2TiCl_2 in $CDCl_3$ τ=3,45 ppm). Streng σ-gebundene Cp-Ringe ohne Bindungsfluktuation weisen hingegen in der Struktur (I) (Abb. 1) das komplexe Signalmuster eines AA'BB'X-Problems auf, das aus den Signalgruppen AA'BB' und X im Intensitätsverhältnis 4:1 besteht, so dass diese in den Organoelementcyclopentadienylen erwartete Bindungsweise NMR-spektroskopisch erkannt werden kann.

Die Verhältnisse werden allerdings in Wirklichkeit dadurch kompliziert, dass das Element E am Cp-Ring nicht nur wie in (I) in 5-Stellung, sondern auch in weiteren tautomeren Formen (II) und (III) in 1- bzw. 2-Stellung gebunden sein kann[1,8,9]. Die Signalgruppen ABC und X_2 der hier erwarteten $ABCX_2$-Systeme haben hier die relative Intensität 3:2.

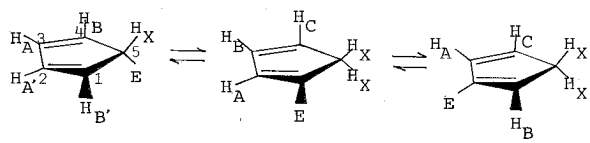

(I) (II) (III)

Abb. 1. *Tautomeriemöglichkeiten bei C_5H_5-Systemen.*

Für das Me_2SiCp_2 sind sogar maximal 6 Tautomere (IV)-(IX) denkbar:

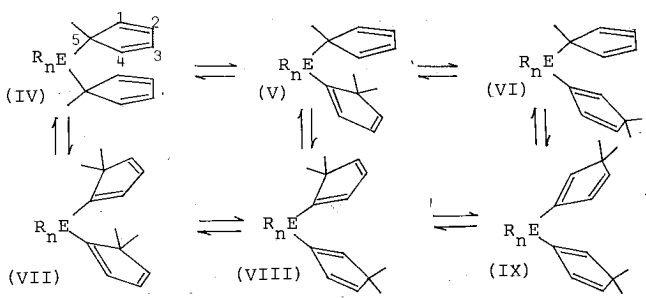

Abb. 2. *Denkbare Tautomere bei Organoelementbis(cyclopentadienylen).*

Als Intensitätsverhältnis der Signale von gesättigten und ungesättigten Protonen erwartet man für (IV) 2:8, für (V) und (VI) 3:7 und für (VII), (VIII) und (IX) 4:6.

Zuweilen wird jedoch auch für σ-gebundene Cp-Ringe bei 20°C ein Koaleszenzphänomen und bei erhöhter Temperatur ein einziges scharfes Signal für sämtliche Ringprotonen beobachtet[1-3,9]. Dieses Phänomen, das nur beim Tautomeren (I) auftritt, wird durch eine 1,2-Verschiebung von E am Cp-Ring nach Abb. 3 erklärt (Valenztautomerie, Metallotropie), deren Geschwindigkeit mit der Temperatur stärker zunimmt als die Umlagerung der Tautomeren (I)-(III) ineinander (Prototropie).

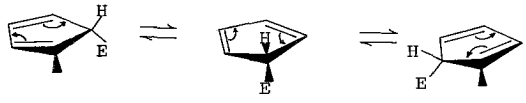

(X) (XI) (XII)

Abb. 3. *Schematische Darstellung der Valenztautomerie (Silikotropie) bei C_5H_5E-Systemen.*

Abb. 4 bringt das ^{1}H-NMR-Spektrum von Me_2SiCp_2 bei 20°C (ohne Lösungsmittel, 60 MHz), das verglichen mit dem entsprechenden von Me_3SiCp[1] grundsätzlich die gleichen Signale zeigt. Auffallend ist das Mehrliniensignal der Methylgruppen auch im frisch destillierten Produkt, was auf die unterschiedliche, chemischen Verschiebungen der Methylgruppen in den verschiedenen Tautomeren (IV)-(IX) zurückzuführen ist. Theoretisch würde man, entsprechend dem Vorliegen von sechs denkbaren Prototropen Formen, sechs Linien für die Methylgruppen erwarten, die im Falle eines 1:1 Mengenverhältnisses gleicher Intensität sein müssten. In Wirklichkeit treten zwei fast gleich intensive Signale (a und b) auf und 4 kleinere rechts und links der Hauptsignale. Dies bedeutet, dass im Gleichgewicht (Abb. 2) zwei Tautomere bevorzugt gebildet werden. Eine Zuordnung dieser Linien zu den einzelnen Isomeren ist, aus den gleichen Gründen wie beim CH_2Cp_2[8], schwierig wenn nicht unmöglich. Jedoch kann man in Analogie zu Me_3SiCp[1] annehmen, dass der intensivste Methyl-Peak (a) (Abb. 4) dem Tautomeren (IV)

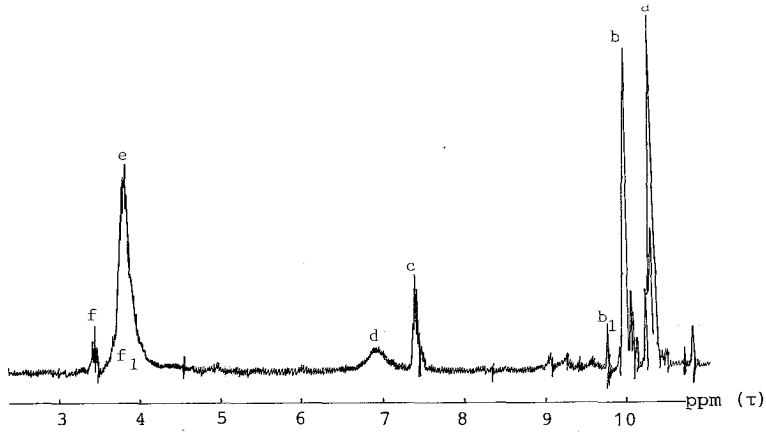

Abb. 4. ^{1}H-NMR-Spektrum von Me_2SiCp_2.

gehört, während für das zweitgrösste Methylsignal (b) das Isomere (V) am wahrscheinlichsten ist.

Bei Temperaturerhöhung treten ähnliche Phänomene auf wie im Falle des Me_3SiCp[1] (Abb. 5). Ein Teil des Signalmusters e und das breite Signal d verschieben sich zu ihrem Schwerpunkt hin und bilden dort bei 110°C das Signal e+d. Mit zunehmender Koaleszenz des temperaturabhängigen Teils des Signals e kommt dadurch ein kleineres, temperaturstabiles Signal f_1 mit ausgeprägter Feinstruktur zum Vorschein (ab 70°C). Es ist also anzunehmen, dass das-den ungesättigten CH-Gruppen der in 5-Stellung substituierten metallotropen Ringe in den Tautomeren (IV) (hauptsächlich), (V) und (VI) zugeordnete - Multiplett e das entsprechende Signal f_1 der 1- bzw. 2-substituierten Ringe in den Tautomeren (V)-(IX) überdeckt. Dàs triplettartige Signal f, das bei diesen Messungen fast unverändert bleibt, ist auch den olefinischen CH-Protonen der 1-bzw. 2-substituierten Ringe in (V)-(IX) zuzuordnen. Das Signal c bleibt, wie zu erwarten, grundsätzlich unverändert (lediglich seine Struktur wird etwas feiner). Bei den Methylsignalen verändert sich die Intensität, so dass bei 110°C die Signale b_1, b_2,..... fast gleich gross wie a werden, was für eine Verschiebung im Gleichgewicht (Abb. 2) nach rechts spricht.

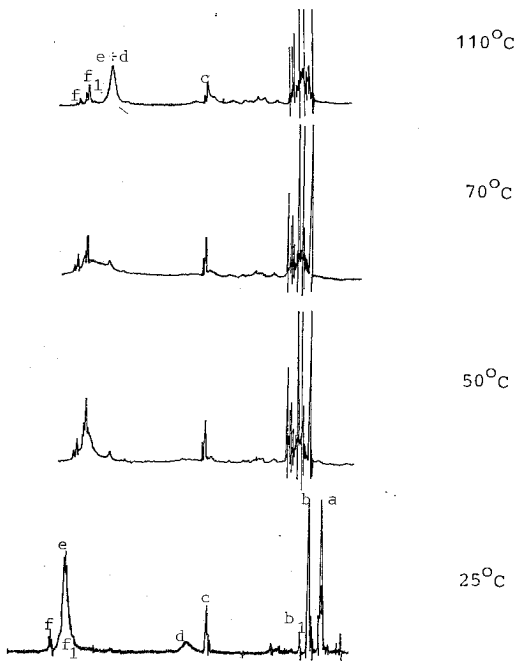

Abb. 5. *^{1}H-NMR-Spektren von Me_2SiCp_2 bei verschiedenen Temperaturen.*

Zusammenfassend kann man feststellen, dass auch für das Dimethylbis(cyclopentadienyl)silan sowohl Silicotropie, als auch Prototropie gleichzeitig stattfinden. Die Silicotropie führt durch die Wanderung der Si-C-Bindung zu Molekülen (X)-(XII), die untereinander identisch sind; sie zeigt sich durch das reversibel temperaturabhängige ^{1}H-NMR-Spektrum an. Die Prototropie (Abb. 1) verläuft nicht rasch genug, um reversibel temperaturabhängige NMR-Ergebnisse zu

verursachen. Folglich werden die einzelnen Resonanzsignale von Me_2SiCp_2 wie in Tab. 1 zugeordnet.

TABELLE 1. *Zuordnung der ^{1}H-NMR-Signale von Me_2SiCp_2.*

Peak	$\tau_{(ppm)}$	Zuordnung	Tautomere (s. Abb. 2)
a	10,01	Me_2Si	(IV)
b	9,68	»	(V)
b_1, b_2,...	9,47, 9,75	»	(VI)-(IX)
c	7,10	gesättigte CH	1-bzw. 2-C_5H_5(V)-(IX)
d	6,65	»	5-C_5H_5 (IV) und (V), (VI)
e	3,53	ungesättig. CH	» » » »
f_1	3,53	»	
f	3,17	»	1-bzw. 2-C_5H_5 (V)-(IX)

Περίληψη

^{1}H-NMR Φασματοσκοπική ἔρευνα τῶν σχέσεων δεσμοῦ στό διμεθυλοδι(κυκλοπενταδιενυλο)σιλάνιο.

Σ' αὐτή τήν ἐργασία ἐρευνῶνται μέ τή βοήθεια φασμάτων πυρηνικοῦ μαγνητικοῦ συντονισμοῦ, ληφθέντων σέ διαφορετικές θερμοκρασίες οἱ σχέσεις τοῦ δεσμοῦ Si-Cp στήν ἕνωση Me_2SiCp_2. Γιά τήν ἑρμηνεία τῶν φασμάτων αὐτῶν προτείνονται δύο μηχανισμοί:

α) ἡ μεταλλοτροπία (εἰκ. 3), ἡ ὁποία λόγω τῆς συνεχοῦς μεταθέσεως τοῦ δεσμοῦ Si-C ὁδηγεῖ σέ ταυτόσημα μόρια καί β) ἡ πρωτοτροπία (εἰκ. 1), ἡ ὁποία λαμβάνει χώρα ταυτόχρονα μέ τή μεταλλοτροπία ἀλλά μέ μικρότερη ἀπό αὐτή ταχύτητα μέ ἀποτέλεσμα νά μή παρέχει κατά τρόπο ἀντιστρεπτό φάσματα ^{1}H-NMR ἐξαρτώμενα ἀπό τή θερμοκρασία ὅπως ἡ μεταλλοτροπία.

Literatur

1. E. Abel, M. Dunster, A. Waters.: *J. Organometal. Chem.* **49**, 287 (1973).
2. A. Davison, P. Rakita.: *Inorg. Chem.* **9**, 289 (1970).
3. H. Fritz, C. Kreiter.: *J. Organometal. Chem.* **4**, 313 (1965).
4. K. Frisch.: *J. Am. Chem. Soc.* **75**, 6050 (1953).
5. R. Martin.: U.S. Patent 2, 667, 501 (1954); *Chem. Abstr.* **49**, 2493 (1955).
6. H. Köpf, W. Kahl.: *J. Organometall. Chem.* **64**, C37 (1974).
7. N. Klouras Dissertation.: *Techn. Univ. Berlin* (1977).
8. H. Schalteger, M. Neuenschwander, D. Meuche.: *Helv. Chim. Acta* **48**, 955 (1965).
9. Yu. Ustynyuk, A. Kisin, A. Zenkin.: *J. Organometal. Chem.* **37**, 101 (1972).

Chimika Chronika, New Series, 11, 37-50 (1982)

COMPOUNDS OF COMPLEX HALO AND PSEUDOHALO ACIDS OF THE GROUP IIB METALS, PART IV VIBRATIONAL SPECTRA OF SOME PYRIDINETRIHALOGENO-,TRI-IODO- AND TETRAIDOMETALLATE ANIONS

S.P. PERLEPES, T.F. ZAFIROPOULOS, M.E. KANELLAKI, J.K. KOUINIS AND A.G. GALINOS
Department of Inorganic Chemistry, University of Patras (Greece).

(Received May 28, 1981).

Summary

The Far-IR spectra (350-50 cm^{-1}) of some complexes of the types $[Py_2H]$ $[ZnX_3Py]$, $[Py_2H]$ $[CdI_3Py]$, $[An_2H]_2[CdI_4]$, $[Qu_2H]$ $[HgI_3]$ (X = Cl, Br, I, Py = pyridine, An = aniline, Qu = quinoline) have been recorded in the solid state at room temperature. Structure-spectra correlations have been found for the complexes. The spectra of the pyridine complexes show that pyridinetrihalogenometallate (II) anions possess C_{3v} symmetry.

An associated anionic structure is present in $HHgI_3.2Qu$, while in the tetraiodocadmate (II) the cadmium atom is tetrahedrally coordinated to the iodine. The relationship of the numbers of ν(MX) and ν(ML) vibrations and their frequencies to the stereochemistries of the complex anions is outlined. The spectroscopic results of the pyridine compounds, particularly in the 3μ region are compatible with, and lend support to, outer spheres comprising $(N\text{-}H\text{---}N)^+$ groups.

Key words: Far-IR Spectra, Pyridinetrihalogenozincate (II), Pyridinetri-iodocadmate (II), Tetraiodocadmate (II), Tri-iodomercurate (II).

Abbreviations

X = Cl, Br, I
Py = pyridine
An = aniline
Qu = Quinoline
B = pyridine, aniline, quinoline etc
M= metal atom of Group IIB
L= neutral ligand
R= Me, Et or Bu^n

Introduction

During the last few years our department's interest was centered on the compounds of the simple and mixed haloacids of the Group IIB metals with Lewis organic bases [1-9] (a representative selection of references is given).

Preparative work, vibrational spectroscopy, electronic spectroscopy, powder methods and conductometric measurements have established the existence of these complexes. With the aid of these techniques, we have shown that, in the solid state, the compounds of the simple complex haloacids of the metal ions of the Group IIB have inner spheres of the forms $[MX_3]^-$, $[MX_3B]^-$, $[MX_4]^{2-}$ and $[MX_4B_2]^{2-}$, where X = halogen and B = pyridine, aniline, quinoline etc. As outer spheres appear the cations of the types BH^+ or $(BHB)^+$.

However, several problems still remain and there are some aspects in our previous work which are not wholly satisfactory:

a) Because of difficulties in obtaining samples suitable for single-crystal X-ray diffraction, definite structural data on these systems are not common.

b) The completely filled d-sublevel precludes deduction of coordination geometry by study of visible spectra or magnetic properties.

c) So far we have accepted the view that the aforementioned complex anions are monomers. Polymeric structures, however, cannot be ruled out, since anionic complexes of Cd(II) and Hg(II), having in addition to others, halogens as ligands, show a notable and much varied structural behavior [10-16].

d) Apart from relatively minor (but in some respects still quite worrying) variations in wavenumbers observed for corresponding bands by different authors, there are some instances of great discrepancy, *viz* the ν(CdN) assignments [8,9,17-21].

e) There appears to be a dependence of ν(MN) on coordination geometry [19], which requires substantiation.

f) The data on the $[HgI_3]^-$ complexes cast doubt on some of the ν(HgI) assignments [1]. There are evidences for monomeric or iodine-bridged associated anions depending on the cation [14].

g) Nearly all our previous IR studies were restricted to the spectral range above 250 cm^{-1}, whereas diagnostic information is to be found in the 250-100 cm^{-1} region.

In order to help clarify some of these points, particularly c,d and f, we have undertaken a detailed Far-IR investigation of the complexes $HZnX_3.3Py$, $HCdI_3.3Py$, $H_2CdI_4.4An$ and $HHgI_3.2Qu$, which may be regarded as the "model systems" for the $[MX_3]^-$, $[MX_3B]^-$ and $[MX_4]^{2-}$ series. Low-frequency vibrational spectroscopy is the most amenable technique for determining their skeletal structures.

The majority of L-M-X complexes give rise to three types of characteristic vibrations, namely, the internal modes of the ligand, metal-ligand and metal-halogen vibrations. The degree of interaction of these modes will vary from compound to compound, but separation into these groups is a reasonable generalization. In the majority of these complexes, the metal-halogen vibration gives rise to the most intense features of the spectrum. The number of M-X peaks

and their position in the spectrum will be dependent on a variety of factors, such as oxidation state, coordination number and mass of the central metal, stoichiometry, terminal or bridging bonding and stereochemistry [22-24]; with charged complex species, there may also be a dependence of ν(MX) on the counterion [22]. The ν(MN) modes in many inorganic systems may not involve pure stretching motions, because of the possibility of coupling stretching vibrations with bending vibrations, and also with other stretching modes of the same symmetry. Metal-halogen bending modes occur below 200 cm^{-1} in the main (often below 100 cm^{-1}) and are thus less likely to be of value to the inorganic chemist than stretching modes, partly because of the difficulty in distinguishing them from lattice vibrations.

In this paper we also include a spectroscopic study of the $[Py_2H]^+$ group, since compounds with $(N\text{-}H\text{---}N)^+$ bonding have attracted the attention of investigators recently [25].

Experimental

All the Zn(II) and Cd(II) complexes studied in the present work have been described previously and were prepared similarly [4, 8]. The preparation of the new compound $HHgI_3.2Qu$ (brown crystalline solid, decomposition range 65-75° C, yield 70%) was analogous to that of the corresponding pyridine [5] and aniline [1] complexes.

Analysis [%] for $HHgI_3.2Qu$

Calcd H^+ 0.12 Hg 23.86 I 45.29 Qu 30.73,
Found H^+ 0.13 Hg 24.15 I 45.01 Qu 29.97.
For ca. 10^{-3} M solutions at 25° C:
Λ_M (C_2H_5OH) = 42 and Λ_M (CH_3NO_2) = 97 S cm^2 mol^{-1}.

Far-IR spectra were recorded as Nujol mulls supported between polyethylene sheets in Perkin Elmer-Hitachi FIS-3 and Polytec FIR 30 spectrophotometers, at room temperature. The instruments and procedures for the other physicochemical measurements have been described in detail [7, 8].

Results, Assignments and Discussion

The study of the analytical data, stability tests, IR spectra (4000-250 cm^{-1}), UV spectra, X-ray powder spectra and conductometric data [4, 8] brings forth strong indications that, in the solid state, the complexes in question may be represented by the formulae $[Py_2H]^+$ $[ZnX_3Py]^-$, $[Py_2H]^+$ $[CdI_3Py]^-$, $[An_2H]_2^{2+}$ $[CdI_4]^{2-}$ and $[Qu_2H]^+$ $[HgI_3]^-$.

Pyridinetrihalogenozincate(II), pyridinetri-iodocadmate(II) and tetraiodocadmate(II) ions

Two general classes of monomeric tetrahedral Zn(II) and Cd(II) compounds

are known. The first class includes the truly tetrahedral ones, $[MX_4]^{2-}$, where all four ligands are the same. The second general class embraces those which may be called pseudotetrahedral. The latter have four ligands at about or, perhaps by chance, exactly at the apices of a tetrahedron surrounding the M(II) ion, but two or more different kinds of ligands are present. Of the three cases involvning 2 kinds of ligands which are in prineipal possible, *viz.*, $[LMX_3]^-$, $[L_2MX_2]$ and $[L_3MX]^+$, where L is a neutral ligand and X an anion, only the second has previously well been realized.

Pseudotetrahedral complexes A $[ZnX_3L]$ have been prepared and studied by Far-IR spectroscopy [26, 27] where L is pyridine, α-picoline, triphenyl phosphine and A tetraethylammonium, N-alkylpyridinium, but have not previously been reported for cadmium.

The vibrational representation of an $[MX_3L]^-$ anion [28] is $\Gamma_v = 3A_1 + 3E$ and these ions should give rise to six IR-active skeletal vibrations [26]. Assuming that the ligand acts as a point mass, the three A_1 modes are designated as $\nu_s(MX_3)$, $\nu_s(ML)$ and the symmetric deformation, while the three E modes are $\nu_d(MX_3)$, $\delta_d(MX_3)$ [XMX scissors] and ω_d [wagging of L perpendicular to the MX_3 axis] (s = symmetric, d = degenerate). The C_2 axis of pyridine cannot, however, be reconciled with the C_3 axis of the MX_3 group and, therefore, deviations from the predicted spectra are to be expected [26]. In addition, since all the complexes were examined in the solid state, interaction may give rise to additional splittings.

The Far-IR spectra of salts of composition $[Py_2H]$ $[MX_3Py]$ as solids are reported in Table I. Features at < 350 cm^{-1} are listed, since it was clear that fundamentals of pyridine occurred above this wavenumber. Assignments have been made by noting: (i) the positions of internal modes of pyridine, (ii) bands principally dependent on the halogen, (iii) the variation in band position with changing metal in the $[MI_3Py]^-$ ions, and (iv) the reports of references 11, 15, 19, 20, 24, 26, 27 and 29. The most characteristic feature of the Far-IR spectra of Zn(II) complexes is the appearance of two high-wavenumber bands which are at lower wavenumbers for the bromide and iodide than for the corresponding chloride by amounts given by ν(bromide) / ν (chloride) $\simeq$ 0.76 and ν(iodide) / ν (chloride) = 0.65. These ratios are comparable to those found [23, 30] for other tetrahedral complexes of Zn(II) and imply that the origin of the bands is in vibrations involving stretching motion of the halide groups. For the Zn(II) complexes the metal-halogen stretching frequencies are observed to occur about 25 cm^{-1} lower than those of the corresponding diligand complex $ZnX_2.2Py$ [23, 29, 31, 32] and are in turn about 30 cm^{-1} higher than the metal-halide asymmetric stretch [30, 33, 34] in the complex halide ion $[ZnX_4]^{2-}$ (Table III). The ν(ZnX) and ν(CdI) modes are also much higher than would be expected for M-X-M bridging frequencies [15, 26]. It is clear that the positions of metal-halide stretching frequencies distinguish between a complex $[Py_2H]$ $[MX_3Py]$ and an equimolar mixture of $MX_2.2Py$ and $[Py_2H]_2$ $[MX_4]$. The ν(ZnN) bands are not significantly shifted when chlorine is replaced by bromine in the complexes, so in these cases there is little coupling with the ν(ZnX) modes. Three bands, at 213, 199 and 192 cm^{-1}, are observed in the expected region of $\nu_s(ZnN)$ in the spectrum of $[ZnCl_3Py]^-$, instead of the predicted singlet; we suggest

Table I. Far-IR[a] assignments (350-50 cm^{-1}) for pyridinetrihalogenometallate salts.

Assignment		$[Py_2H]$ $[ZnX_3Py]$			$[Py_2H]$ $[CdI_3Py]$
A_1	E	X = Cl	X = Br	X = I	
	$\nu_d(MX_3)$	306 s	230 s	199 s	165 m
$\nu_s(MX_3)$		285 s	219 m	185[c] sbr	157 m
$\nu_s(MN)$		213 m, 199 m, 192 m	196 m, 177 w	194[d] m, 174 m	143 m, 108 m
sym.def.		151 m	114 m	86 m	75 m
	$\delta_d(MX_3)$	126 m, 117 sh	98 s, 91 w	78 s	66 w
	ω_d	93 w, 82 w	b	53 w	55 s
Other bands		101 sh, 59 m	120 w, 57 w	60 wbr	187 m, 97 m, 88 m

[a]Data obtained at room temperature. [b]Not observed owing to ghost peak. [c]May be Zn-N.
[d]May be Zn-I. s = strong, m = medium, w = weak, br = broad, sh = shoulder.

Table III. Comparison of ν(MX) IR assignments (cm^{-1}) for C_{2v}, C_{3v} and T_d complexes of Zn(II) and Cd(II).

Complex	Structure	ν(MX)[a]	Reference	Limit of study [cm^{-1}]
$ZnCl_2 \cdot 2Py$	Tetrahedral[b]	329, 296	[23]	200
		327, 295[c]	[29]	50
$[Et_4N][ZnCl_3Py]$	Pseudotetrahedral[d]	310,292,283	[26]	40
$[Py_2H][ZnCl_3Py]$	Pseudotetrahedral[d]	306, 285	e	50
$[Et_4N]_2[ZnCl_4]$	Tetrahedral[f]	277	[34]	70
		271	[33]	190
		281,273	[30]	200
$ZnBr_2 \cdot 2Py$	Tetrahedral[g]	254, 220[h]	[23]	200
		260, 254	[32]	50
$[Et_4N][ZnBr_3Py]$	Pseudotetrahedral[d]	236,226,213[h]	[26]	40
$[Py_2H][ZnBr_3Py]$	Pseudotetrahedral[d]	230, 219	e	50
$[Et_4N]_2[ZnBr_4]$	Tetrahedral[f]	207	[34]	70
		207,20.	[30]	200
$ZnI_2 \cdot 2Py$	Tetrahedral[g]	220[h]	[23]	200
		210	[32]	50
$[py \cdot pr][ZnI_3Py]$	Pseudotetrahedral[d]	204,190[h]	[27]	40
$[Py_2H][ZnI_3Py]$	Pseudotetrahedral[d]	199,185[h]	e	50
$[n\text{-}Pr_4N]_2[ZnI_4]$	Tetrahedral[f]	165	[34]	70
$CdI_2 \cdot 2Py$	Tetrahedral[d]	146,137	[21]	20
$CdI_2 \cdot 2An$	Tetrahedral[b]	155, 140	[21]	20
$[Py_2H][CdI_3Py]$	Pseudotetrahedral[d]	165,157	e	50
$[Et_4N]_2[CdI_4]$	Tetrahedral[d]	145	[11]	40
		141	[15]	50
$[An_2H]_2[CdI_4]$	Tetrahedral[d]	149,135	e	50

[a]All values refer to data obtained at room temperature. [b]The structures of these complexes have been determined by X-ray studies: $ZnCl_2 \cdot 2Py$ [40] and $CdI_2 \cdot 2An$ [41]. [c]Assignments have been made by multiple isotopic labelling. [d]Structure deduced from Far-IR spectral analysis. [e]Present work. [f]A considerable number of salts of tetrahedral tetrahalogenozincates has been examined by X-rays; see [34] and references cited therein. [g]Structure deduced from ν(MX) positions. [h]May be ν(MN). py·pr = N-n-propylpyridinium.

that this is due to Fermi resonance between $2\omega_4$ and/or $2\delta_4$ ($ZnCl_3$). It is recognised that these assignments place ν (CdN) as low as 108 cm^{-1} but, as Goldstein and Hughes [20] pointed out, this is fully compatible with the relatively high values for ν(CdI). For $[ZnI_3Py]^-$ the ν(ZnI) come close to the ν(ZnN) modes and the interpretation of the region around 190 cm^{-1} is not clear. It is interesting that the highest ν(MN) frequency in a $[MX_3Py]^-$ ion is always lower than the highest ν(MN) frequency in a corresponding $MX_2.2Py$ (C_{2v}) complex [20, 21, 23, 26, 31, 32]. This has been observed previously in other species, for example O_2SF_2 and FSO_3^-, where S-F frequencies show a similar relationship [26]. Up to three other bands are found in the spectra, which do not correlate readily through the series. These bands are likely to comprise δ(NMX) and δ(MX) modes, although those at lower wavenumbers may involve lattice modes.

In all the $[MX_3Py]^-$ complexes examined the Far-IR spectra clearly support formulation as C_{3v} pseudotetrahedral anions; these species are intermediate in type between $MX_2.2Py$ complexes and $[MX_4]^{2-}$ ions. On the basis that local C_{3v} symmetry is operative for the $[MX_3Py]^-$ species, the anions are assumed to be sufficiently separated by the large $[Py_2H]^+$ ions that intermolecular coupling of vibrational motions can be ignored.

IR and Raman spectra of solid ditetra-alkylammonium tetraiodocadmates $[R_4N]_2[CdI_4]$ (R = Me, Et or Bu^n) have been interpreted on the basis of tetrahedral $[CdI_4]^{2-}$ ions [11]. Goggin and his co-workers [15] observed that in some of the solid-state spectra of $[CdX_4]^{2-}$ there is evidence of splitting of degenerate vibrations and environmentally induced IR activity of the symmetric breathing mode.

The low-frequency tetraiodocadmate spectrum showed similarity with the spectra of similar compounds in the solid state [11, 15] and the observed frequencies have therefore been assigned on the same basis, namely that the tetrahedral $[CdI_4]^{2-}$ ion (point - group T_d) is present (Table II). The normal vibrations may be represented by $\Gamma_{vib}(T_d) = A_1 + E + 2T_2$, with the A_1, E and T_2 symmetry species being Raman-active, while only the T_2 modes (one stretching and one bending) are IR-active.

The absorption present at 203 cm^{-1} requires some additional discussion. An internal mode of aniline is expected in the spectral region under study, namely, a substituent-sensitive mode of the aromatic ring [19], found in the Raman spectrum of the free ligand at 233 cm^{-1} [35]. Whereas this band has been assigned [29] at 205 and 225 cm^{-1} in the spectrum of $ZnCl_2.2An$, described as γ (ring), it is not apparent in the spectra of $M(NCS)_2.2An$ species (M = Co, Ni, Cu, Zn) [36], nor (at least above 200 cm^{-1}) in the spectra of other halide complexes [21, 37-39]. The band at 203 cm^{-1} is clearly too high in wavenumber to be ν(CdI). We tentatively assign this band to an aniline mode. The alternative of assigning the same feature to a combination band cannot be ruled out. It might have been expected that the T_2 vibration would be split in the crystal from either or both of two possible sources.

First, any deviations from perfectly tetrahedral symmetry remove the triple degeneracy; and secondly, the next nearest (and other) neighbour interactions in the crystal which, together with the primary coordination sphere, decide the site symmetry of the ion will again cause removal of the degeneracy in all but very

Table II. Assignments[a] of IR frequencies (350-50 cm^{-1}) observed for solid $[An_2H]_2[CdI_4]$ on the assumption of tetrahedral symmetry.

γ(ring)[b]	ν_3^c (T_2)	ν_4^d (T_2)	Other bands[e]
203 s	149 m 135 s	75 m	122 wbr 90 w 52[f] m

[a]Data obtained at room temperature. [b]May be a combination band (149 + 52). [c]Stretching mode. [d]Bending mode. [e]Lattice vibrations are expected to occur <50 cm^{-1} [15]. [f]See text. s = strong, m = medium, w = weak, br = broad.

special crystallographic cases. The medium band at 52 cm^{-1} may be assigned to the $\nu_4(E)$ bending frequency, activated by site symmetry, or alternatively to a lattice mode. If the 52 cm^{-1} band were the ν_2 frequency, we should expect [34] to observe also the $\nu_1(A_1)$ stretching vibration, as well as a splitting of the two vibrations of T_2 species; the second is observed.

The tri-iodomercurate(II) ion

The characteristic coordination numbers and stereochemical arrangements of the divalent mercury ion are two-coordinate linear and four-coordinate tetrahedral. In addition to these, octahedral and five-coordination are also known. Coordination number three is rather rare for mercury (II); it is known in some systems, but the species are anionic.

The $[HgI_3]^-$ ion has been known for a long time [42-48]. In the only tri-iodomercurate(II) whose crystal structure has been determined, $[SMe_3]$ $[HgI_3]$, approximately trigonal planar anions are loosely linked by long iodine contacts to give a trigonal - bipyramidal environment for each mercury atom [49]. Hooper and James studied the vibrational spectra of crystalline tri-iodomercurate(II) salts and reported bridging modes $\nu(HgI)_b$ [10]. Goldstein and Barr [14] carried out a systematic study of the Far-IR and Raman spectra, in the solid state, of the salts of the type $A[HgI_3]$ ($A = SMe_3$, Me_4N, Et_4N, $n\text{-}Bu_4N$). They proved that the weak iodine bridging, found in the crystal structure of $[SMe_3]$ $[HgI_3]$ can be disregarded in qualitative interpretation of the vibrational data; they interpreted the spectrum of $[Me_4N]$ $[HgI_3]$ in terms of monomeric anionic structure, while the spectra of the remaining two were indicative of strongly iodine-bridged anions. In a previous paper [1], we have carried out a Far-IR study of the pyridine and aniline compounds of the acid $HHgI_3$, in the solid state. We are extending this study to the quinoline compound, with the purpose of verifying whether in this complex exist monomeric anionic units $[HgI_3]^-$ or iodine-bridged associated anions.

There are two possible monomeric structures for the $[HgI_3]^-$ ion. This ion can be described in terms of the C_{3v} (pyramidal) or D_{3h} (planar) point groups. The selection rules for a planar XY_3 species of D_{3h} point group symmetry are $A_1' + A_2'' + 2E'$ [50]. The symmetrical stretching mode (A_1') is Raman-active but IR-inactive; the XY_3 out-of-plane deformation mode A_2'' is Raman-forbidden but IR-active. The two E′ modes, $\nu_{asym}(XY)$ and δ (YXY), are Raman- and IR-active. The selection rules for a pyramidal XY_3 species of C_{3v} point group symmetry are $2A_1 + 2E$ [50]. The four fundamentals are each allowed both in the Raman and IR.

All the observed bands in the region 200-20 cm^{-1} are given in Table IV. The appearance of $\nu(HgI)_b$ bands convinces us that the spectrum seems incompatible with a planar or pyramidal $[HgI_3]^-$ skeleton, but it can be explained on the basis of iodine-bridged anions, while the complex still contain terminal Hg-I bonds. The band centered on 91 cm^{-1} is very broad and may well be a result in part of some type of bridging stretch. The bands at 101 and 91 cm^{-1}, assigned as $\nu(HgI)_b$, are clearly of complex origin, but their wavenumbers warrant such description rather than as translatory lattice modes [14]. The considerable complexity of the Far-IR spectrum may well indicate that the bridging interactions are largely ionic in nature [10]. It is probable that the spectrum can be assigned on the basis of a C_{3v} unit in which the bridging interaction appears to be important. The spectrum of the present salt shows four bands in the region appropriate to HgI stretching (the high-frequency bands may be reasonably [1, 10, 14] assigned to asymmetric and symmetric terminal stretching vibrations). The same applies to the corresponding

Table IV. Far-IR[a] assignments (200-50 cm^{-1}) for $[Qu_2H][HgI_3]$ in the solid state.

$\nu_{asym}(HgI)_t$	$\nu_{sym}(HgI)_t$	$\nu(HgI)_b$	$\delta(IHgI)$	Other
151 m	130 s	101 m 91 mbr	63m 54 m	184w 110m 83w 51sh

[a]Data obtained at room temperature. s = strong, m = medium, w = weak, br = broad, sh = shoulder.

aniline complex [1]. This number of stretching vibrations is, of course, much greater than that to be expected for a $[HgI_3]^-$ ion of any shape, but is in accordance with predictions for a D_{2h} dimeric anion $[Hg_2I_6]^{2-}$ which, based on tetrahedral

geometry around the metal should show four IR-active ($B_{1u} + B_{2u} + 2B_{3u}$) stretching modes [15]. On this basis the bands at 151, 130, 101 and 91 cm^{-1} in the Far-IR spectrum of $[Qu_2H]$ $[HgI_3]$ are attributed to the B_{2u}, B_{3u}, B_{1u} (bridge) and B_{3u} (bridge) respectively. The possibility of our $[(HgI_3)_x]^{x-}$ systems being mixtures can be ruled out on the grounds that they do not systematically show bands at the same wavenumbers as the other vibrations of $[HgI_4]^{2-}$ [10, 51] and $HgI_2.2L$ [52, 53]. The Far-IR study of $[Qu_2H]$ $[HgI_3]$, just described, ascertains the conclusion that the trihalogenomercurate (II) salts with large cations acquire associated structures [14].

The $[PyHPy]^+$ ion

Compounds with $(N\text{-}H\text{---}N)^+$ bonding have attracted the attention of inorganic chemists comparatively recently. Following the work of Wood and co-workers [54], in which various salts with $(BHB)^+$ cations were considered, where B is a heterocyclic amine, the number of analogous reports is rising continuously. The range of appearance of the $(N\text{-}H\text{---}N)^+$ vibrations for these substances has been examined spectroscopically as a function of the anion and solvent, the nature of the amine and the temperature (see [25] and literature cited therein).

Most of the investigations were carried out in solutions and only recently have there been reports [55, 56] of the isolation of such compounds in the solid phase. Usually, all the compounds studied are substances [BHB]X, where X^- is an acidic residue. However, investigations of compounds with amine complexes including a metal have been published [25, 57, 58]. One of us [4] had proposed, many years ago, the existence of cations $[PyHPy]^+$ in the outer sphere of complex compounds and this view was established by a series of subsequent publications [5, 7, 8, 17, 18]. The NH stretching vibrations were of the greatest interest for finding the nature of the hydrogen bonding in B-H---B systems. Published views on the width of ν(NH) and its structure are not unanimous. The symmetric cations $[BHB]^+$, where B is pyridine or a substituted pyridine, show a doublet for ν_s(NHN) at ca. 2000 and 2500 cm^{-1}, which is thought to arise from a double minimum-low-barrier potential well [54]. A remarkable view for this problem is that the reason for the band being a doublet in hydrogen-bridged complexes could be the Fermi resonance of the NH stretch with the overtones or with the intramolecular vibrations of the amines [59].

Our results are summarized as follows:

a) In the spectra of the pyridine complexes appears a broad, of medium intensity band, at ca. 2800 cm^{-1}, which we attribute to ν_s(NHN); the doublet structure was not observed.

The shoulders and weak side bands, which vary from complex to complex, can be accounted for as interactions with internal mode combinations. The singlet nature of ν_s(NHN) here perhaps indicates a single minimum.

b) The spectra do include weak bands of the NH vibrations in the region 3220-3100 cm^{-1}, characteristic of PyH^+. The presence of NH peaks of very low intensity above 3100 cm^{-1} suggests that there are some non-associated PyH^+ groups in these complex salts. In the recently determined crystal structure of the complex $[HPy]_2$ $[Fe_2Cl_6O].Py$ [57], there is just one short intermolecular contact, *viz.* N....N 2.747

Å, which represents a strong hydrogen bond between PyH^+ and Py; this complex shows an NH stretching vibration as a moderately strong, slightly broad band at 3235 cm^{-1}. It is, therefore, surprising that the ν(NH) in the above complex is so little affected by hydrogen bonding to the pyridine nitrogen, particularly since the structural data suggest a strong interaction.

c) In our systems there is a broad band of medium intensity at 525 cm^{-1}, which is due to the $[PyHPy]^+$ group [25].

d) We did not observe a well defined Far-IR band at ca. 135 cm^{-1}. Wood and co-workers [54] reported that this inter-molecular mode ν_σ is characteristic of $[PyHPy]^+$ groups; the ν_σ band in $[PyHPy]^+ X^-$ systems decreases only slightly in frequency on deuteriation, exhibits no doublet structure and the frequency and profile are independent of counter-ion.

Final Conclusions

This work has highlighted some of the problems which arise when seeking to make Far-IR spectral assignments for compounds of simple complex haloacids of the Group IIB metal ions and has illustrated the types of considerations which need to be made in solving such problems. It is apparent that the Far-IR spectra of the $[ZnX_3Py]^-$ and $[CdI_3Py]^-$ ions support their monomeric existence in the solid state as the discrete C_{3v} pseudotetrahedral species indicated by their formulae. The spectrum of $[CdI_4]^{2-}$ can be satisfactorily understood in terms of a tetrahedral structure. For $[HgI_3]^-$, treatment based on D_{2h} dimeric structure leads to acceptable assignments; it is emphasized that to distinguish between a dimeric and a polymeric geometry, very careful analysis of the spectra is needed and we believe that the availability of Raman data is important. For the above structural types, more bands are found than are predicted for the simple models normally adopted. It is clearly desirable to obtain solution spectra in order to be certain that lattice vibrations and other solid state effects are not responsible for any of the absorption bands or for their shapes and frequencies; unfortunately, the compounds have a negligible solubility in solvents appropriate for IR spectra. If the structures of the complexes were exactly known it might be possible to account for this increased complexity of the spectra in terms of factor-group splitting but in the absence of any structural information this possibility cannot be further discussed. Our investigations also show that the formation and release in the solid phase of compounds containing complex $[Py_2H]^+$ groupings is not limited to simple salts of pyridine, but includes cation-anion complexes of metals. However, from the above study it is concluded that the location of the proton in $[B_2H]^+$ systems is still open to question.

Περίληψη

Ἐνώσεις τῶν Συμπλόκων Ἀλογονο- καί Ψευδοαλογονο- Ὀξέων τῶν Μετάλλων τῆς Ὁμάδος ΙΙΒ, Μέρος IV Φάσματα Δονήσεως μερικῶν Πυριδινοτριαλογονο-, Τριϊωδο καί Τετραιωδο Μεταλλοανιόντων.

Ἐλήφθησαν τά φάσματα τῶν συμπλόκων τῶν τύπων $[Py_2H]$ $[ZnX_3Py]$, $[PyH]$ $[CdI_3Py]$, $[An_2H]_2$ $[CdI_4]$, $[Qu_2H]$ $[HgI_3]$ (X = Cl, Br, I, Py = πυριδίνη, An = ἀνιλίνη, Qu = κινολίνη), εἰς τήν ἄπω ὑπέρυθρον περιοχήν (350-50 cm^{-1}), ἐν στερεᾶ καταστάσει καί εἰς τήν θερμοκρασίαν δωματίου. Συσχετισμοί δομῆς-φάσματος ἔχουν ἐδραιωθεῖ διά τά ἐν λόγω σύμπλοκα. Τά φάσματα τῶν πυριδινικῶν συμπλόκων δεικνύουν, ὅτι τά πυριδινοτριαλογονο-μεταλλικά (II) ἀνιόντα ἔχουν C_{3v} συμμετρίαν.

Μία συνεζευγμένη ἀνιοντική δομή ὑφίσταται εἰς τήν ἕνωσιν $HHgI_3.2Qu$, ἐνῶ τό ἀνιόν $[CdI_4]^{2-}$ ἔχει τετραεδρικήν δομήν. Ἡ σχέσις τῶν ἀριθμῶν τῶν δονήσεων ν(MX) καί ν(ML) καί τῶν συχνοτήτων αὐτῶν πρός τάς στερεοχημείας τῶν συμπλόκων ἀνιόντων περιγράφεται, ἐν συντομία.

Τά φασματοσκοπικά ἀποτελέσματα τῶν πυριδινικῶν ἑνώσεων, εἰδικῶς εἰς τήν περιοχήν 3μ, ἐναρμονίζονται μέ τήν ὕπαρξιν ἐξωτερικῶν σφαιρῶν ἐξ ὁμάδων $(N\text{-}H\text{---}N)^+$.

Bibliography

1. Perlepes S.P., Zafiropoulos Th.F., Kouinis J.K., & Galinos A.G.: *Z. Naturforsch.* **35b**, 1244 (1980). (Part III of this series).
2. Galinos A.G.: *Angew. Chem.* **69**, 507 (1957).
3. Galinos A.G.: *J. Am. Chem. Soc.* **82**, 3032 (1960).
4. Galinos A.G.: *J. Inorg. Nucl. Chem.* **19**, 69 (1961).
5. Galinos A.G., & Perlepes S.P.: *Z. Naturforsch.* **32b**, 850 (1977).
6. Galinos A.G., & Perlepes S.P.: *Bull. Soc. Chim. Fr.* 1-46, (1979).
7. Galinos A.G., Kouinis J.K., Ioannou P.V., Zafiropoulos Th. F. & Perlepes S.P.: *Z. Naturforsch.* **34b**, 1101 (1979).
8. Galinos A.G., Perlepes S.P. & Kouinis J.K.: *Monatsh. Chem.* **111**, 829 (1980).
9. Perlepes S.P., Zafiropoulos Th. F., Kouinis J.K., Galinos A.G.: *Z. Naturforsch.* **35b**, 1241 (1980).
10. Hooper M.A. & James D.W.: *Aust. J. Chem.* **24**, 1331 (1971).
11. Ross S.D., Siddigi I.W. & Tyrrell H.J.V.: *J. Chem. Soc. Dalton Trans.* 1611 (1972).
12. Barr R.M. & Goldstein M.: *J. Chem. Soc. Dalton Trans.* 1180 (1974).
13. Contreras J.G. & Tuck D.G.: *Can. J. Chem.* **53**, 3487 (1975).
14. Barr R.M., & Goldstein M.: *J. Chem. Soc. Dalton Trans.* 1593 (1976).
15. Goggin P.L., Goodfellow R.J. & Kessler K.: *J. Chem. Soc. Dalton Trans.* 1914 (1977).
16. Albinati A., Meille S.V., Cariati F., Marcotrigiano G., Menabue L. & Pellacani G.C.: *Inorg. Chim. Acta* **38**, 221 (1980).
17. Galinos A.G., Tsangaris J.M., Perlepes S.P., & Zafiropoulos Th. F.: *Proceedings of Academy of Athens* **55**, 234 (1980).
18. Zafiropoulos Th. F., Perlepes S.P., Kouinis J.K., & Galinos A.G.: *Acta Chim. Acad. Sci. Hung.* **109**, 93 (1982).

19. Goldstein M., & Hughes R.J.: *Inorg. Chim. Acta* **40**, 229 (1980).
20. Goldstein M., & Hughes R.J.: *Inorg. Chim. Acta* **37**, 71 (1979).
21. Goldstein M., & Unsworth W.D.: *J. Mol. Structure* **14**, 451 (1972).
22. Clark R.J.H.: *Spectrochim. Acta* **21**, 955 (1965).
23. Clark R.J.H., & Williams C.S.: *Inorg. Chem.* **4**, 350 (1965).
24. Nuttall R.H.: *Talanta* **15**, 157 (1968).
25. Kobets L.V., Khod'ko N.N., Kopashova I.M., & Umreiko D.S.: *Russ. J. Inorg. Chem.* **25**, 729 (1980).
26. Bradbury J., Forest K.P., Nuttall R.H., & Sharp D.W.A.: *Spectrochim. Acta, Part A* **23**, 2701 (1967).
27. Brown D.H., Forest K.P., Nuttall, R.H., & Sharp D.W.A.: *J. Chem. Soc. A* 2146 (1968).
28. Drake J.E., Hencher J.L., Khasrou L.N. Tuck D.G., & Victoriano L.: *Inorg. Chem.* **19**, 34 (1980).
29. Hutton A.T., Thornton D.A.: *Spectrochim. Acta, Part A* **34**, 645 (1978).
30. Clark R.J.H. & Dunn T.M.: *J. Chem. Soc.* 1198 (1963).
31. Frank C.W., & Rogers L.B.: *Inorg. Chem.* **5**, 615 (1966).
32. Postmus C., Ferraro J.R., & Wozniak W.: *Inorg. Chem.* **6**, 2030 (1967).
33. Adams D.M., Chatt J., Davidson J.M., & Gerratt J.: *J. Chem. Soc.* 2189 (1963).
34. Sabatini A. & Sacconi L.: *J. Am. Chem. Soc.* **86**, 17 (1964).
35. Evans J.C.: *Spectrochim. Acta* **16**, 428 (1960).
36. Engelter C. & Thornton D.A.: *J. Mol. Structure* **33**, 119 (1976).
37. Ahuja I.S., Brown D.H., Nuttall R.H., & Sharp D.W.A.: *J. Inorg. Nucl. Chem.* **27**, 1105 (1965).
38. Ahuja I.S., Brown D.H., Nuttall R.H., & Sharp D.W.A.: *J. Inorg. Nucl. Chem.* **27**, 1625 (1965).
39. Key D.L., Larkworthy L.F., & Salmon J.E.: *J. Chem. Soc. A* 2583 (1971).
40. Poraî-Koshits, M.A., Atovmyan L.O., & Tishchenko G.N.: *Zh. Strukt. Khim.* **1**, 337 (1960).
41. Ablov A.V., & Malinovskii T.I.: *Doklady Akad. Nauk. SSSR* **132**, 336 (1960).
42. Rây P.C. & Adhikary N.: *J. Indian Chem. Soc.* **7**, 297 (1930).
43. Bluhm M.M., Bodo G., Dintzis H.M., & Kendrew J.C.: *Proc. Roy. Soc. A* **246**, 369 (1958).
44. Griffiths T.R., & Symons M.C.R.: *Trans. Faraday Soc.* **56**, 1752 (1960).
45. Deacon G.B. & West B.O.: *J. Chem. Soc.* 3929 (1961).
46. Deacon G.B. & West B.O.: *J. Inorg. Nucl. Chem.* **24**, 169 (1962).
47. Buckingham A., & Gasser R.P.H.: *J. Chem. Soc. A* 1964 (1967).
48. Fenn R.H., Oldham J.W.H., & Phillips D.C.: *Nature (London)* **198**, 381 (1963).
49. Fenn R.H.: *Acta Crystallogr.* **20**, 20 (1966).
50. Wait S.C. & Janz G.J.: *Quart. Rev. Chem. Soc.* **17**, 225 (1963).
51. Deacon G.B., Green J.H.S., & Kynaston W.: *Aust. J. Chem.* **19**, 1603 (1966).
52. Marcotrigiano.: *Z. Anorg. Allg. Chem.* **417**, 75 (1975).
53. Bell, N.A., Dee T.D., Goggin P.L., Goldstein M., Goodfellow R.J., Jones T., Kessler K., McEwan D.M., & Nowell I.W.: *J. Chem. Research (S)* 2, (1981).
54. Clements R., Dean R.L., Singh T.R., & Wood J.L.: *Chem. Commun.* 1125 (1971).
55. Glowiak T., Sobczyk L., & Grech E.: *Chem. Phys. Lett.* **34**, 292 (1975).
56. Minshall P.C. & Sheldrick G.M.: *Acta Crystallogr. Part B* **34**, 1378 (1978).
57. Drew M.G.B., McKee V., & Nelson S.M.: *J.Chem. Soc. Dalton Trans* 80, (1978).
58. Brencic J.V., Ceh B., & Segedin B.: *J. Inorg. Nucl. Chem.* **42**, 1409 (1980).
59. Dean R.L., Masri F.N., & Wood J.L.: *Spectrochim. Acta, Part A* **31**, 79 (1975).

Chimika Chronika, New Series, 11, 51-58 (1982)

NONIDEAL FLOW AND ITS APPLICATION TO FLOTATION

K.A. MATIS
Laboratory of General and Inorganic Chemical Technology, University of Thessaloniki

(Received July 1, 1981).

Summary

The efficiency of a flotation unit is expected to be a function of the residence time distribution, so an investigation of the hydrodynamics was undertaken. The stimulus-response technique was used in this experimentation. The tracer input signal was an electrolyte and had the form of a step function. Assuming that the flow regime was composed of various flow types, a theoretical mixed model was applied, and the experimental data were fitted accordingly.

Key words: Plug, backmix flow, by-pass, deadwater, tracer, model, operation, flotation.

Introduction

When a fluid flows through a vessel in plug flow or backmix flow then predictions of performance of the vessel, as a reactor, can be found in a straightforward manner. However, when flow deviates from either of these two ideal patterns, performance predictions cannot be made simply. In the latter case one approach is to represent the real vessel by a flow model, determine the parameters of this model and then, predict the performance of the real vessel from the model.

The stimulus-response technique has been used for exploring the flow characteristics of vessels, providing sufficient information for performance predictions when linear processes (such as first order reactions) are taking place. The stimulus is a tracer input into the fluid entering the vessel, whereas the response is a time record of the tracer leaving the vessel. Any material that can be detected and which does not disturb the flow pattern in the vessel can be used as tracer, and also, any type of input signal may be used. Although usually, only two stimuli are considered, the perfect step and the perfect pulse input, since they are simplest to treat.

The dispersion model has been extensively applied, and is well reviewed by Weir and Fan (1). However, it is not suitable in our case. Besides that, the tanks - in - series model is the other one - parameter model widely used. In this the actual reactor is simulated by n ideal stirred tanks in series. The total volume of the tanks is the same as the volume of the actual reactor. Thus for a given flow rate the total mean residence time is also the same. The mean residence time per tank is $\bar{t}$ /n.

The objective is to find the value of n, for which the response curve of the model would best fit the response curve for the actual reactor. To do this the relation between $(C/C_o)_{step}$ and n should be developed. Buffham and Gibilaro (2) have shown how the model can be used with non integer (but positive) values of n.

The efficiency of many processes and operations is largely a function of the hydrodynamic characteristics of the system in which they operate. The measurement and analysis of the detention time distribution of a fluid and of the flow regime in a system is usually of great importance, in evaluating the systems performance. The hydrodynamics theory has been applied in sedimentation basin design (3), (4), and also to froth flotation machines (5).

Degner (6) in his studies of dispersed-air flotation distinguished four hydraulic regions. Only a portion of the flotation vessel volume was said to be utilised in the actual gas flotation process. This is represented by the volume contained within one of the four regions, in which the effective density and size of the contaminating species is modified via attachment to a gas bubble, to achieve rapid gravity separation from the remaining liquid. It is evident that Stokes law consideration for this region is only one of several hydrodynamic design factors, which influence the flotation design.

If the average size of the bubble is reduced signigicantly, in general, the required total ingested air flow will be accordingly reduced, because of the more favourable surface: volume ratio of the smaller size bubble. However, the production of ultra-fine gas bubbles in the mixing zone, is not the dominant dispersed-air flotation cell design requirement. Rather, a balance between total air flow, mixing region shear turbulence, surface and flotation zone quiescence, liquid droplet reemulsification (if applied), and gas bubble size is sought for the final design.

Experimental Part

The present study was conducted after extensive experiments on the application of electrolytic flotation in effluent treatment (7), (8). So, the fundamental variables of the process, such as current density, retention time, effluent concentration, percentage removal, etc., had been established in advance.

The flotation tank was 1 m tall and had an internal diameter of 146 mm. A pair of horizontal stainless-steel electrodes was flanged on, while a weir was constructed and fitted at the top, for the froth layer to be passed over it.A copper tube, with 12.7 mm internal diameter, closed at the end and with small openings on the top side only, was diametrically entering into the tank, 0.17 m from the edge; there was also a bottom drain (with the same diameter) in the centre of the base under the

electrodes cell. These two were used respectively as inlet and/or outlet, according with the mode of operation. Near the inlet and outlet of the tank were sampling points.

The current density during the tests in continuous flow was at 100 A/m^2 and the voltage dropped from 40 V initially to 4 V at the end of the process, due to the acid. The flow rate was kept steady at 5 mm^3/ms, while the vessel volume was 16.7×10^6 mm^3. Both countercurrent and coccurrent operations were studied; the two modes of continuous flow are represented in Figure 1.

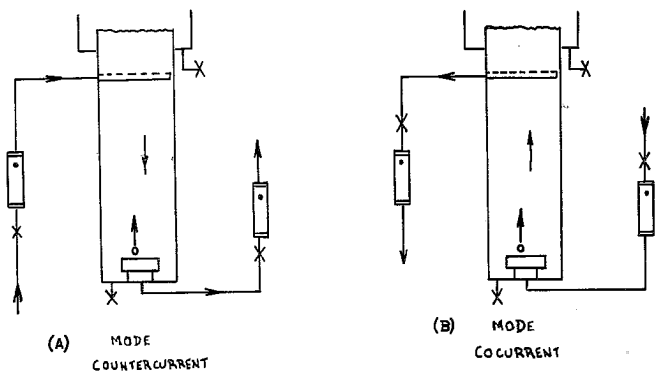

Fig. 1. *Modes of continuous flow operation.*

The hydrogen produced by electrolysis was found to be 173 mm^3/s for the current density of 100 A/m^2, with the oxygen volume half that of hydrogen. Assuming - and this assumption has been certified - that the bubbles have a spherical shape with a diameter of approximately 0.05 mm, the number of bubbles evolved was around 4×10^6/s, at the above current intensity. The bubbles measurements in electrolytic flotation was the subject of another group of experiments (7c).

At first a dye was selected as tracer and tried; however, observations at that stage were made only by flow visualization, as it was realized that the tracer (Congo red) was affected by electrolysis, having its optical density changed with time, which prevented the analysis. Then, a sulphuric solution was used in a unit step input. In this case, acidimetry was the method of analysis.

The effluent was an oil-water sludge sample, taken from a refinery's interceptor; this was treated successfully by electrolytic flotation, while it was only mixed by dispersed-air flotation, as the bubbles were insufficiently fine. Preparatory tests showed that when the sample was allowed to come to rest in a beaker, three layers were apparent: a bottom layer of solids, an oily layer at the surface and a stable one in the middle containing a mixture of oil, suspended solids and an aqueous solution. This middle layer was the problem for treatment. A representative batch test (at 100 A/m^2 and 15 V) gave after 1.8 ks a BOD_5 removal of the order of 96%, as the final was around 15 ppm.

Results and Discussion

The tanks-in-series model was applied at first to this study. This is represented as Figure 2. The equation was given by Smith (9) as:

$$F_\Theta = 1 - e^{-\eta\theta} \left[1 + \eta\theta + \frac{1}{2!}(\eta\theta)^2 + ... + \frac{1}{(\eta-1)!}(\eta\theta)^{n-1} \right]$$

Where the symbols are described in the nomenclature.

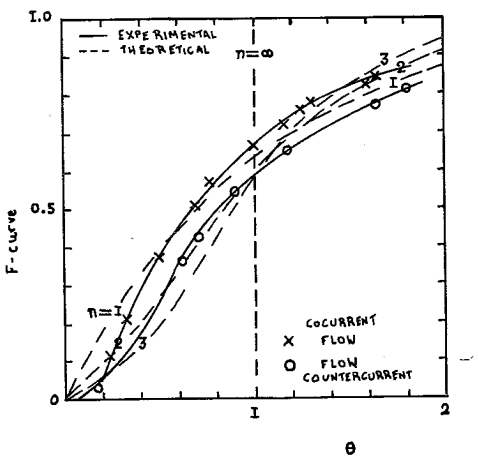

Fig. 2. *Studying the flow regime by the tanks-in-series model.*

The model was solved for the small values of n, which are shown in the figure together with the experimental results. From the comparison a conclusion can be drawn, which certifies a previous guess, that the process is nearer to a continuous stirred tank reactor than to a tubular one. This is why the dispersion model has not been tried.

When one-parameter models are unable to account satisfactorily for deviations from the ideals, or cannot give enough information, then more complicated models are attempted (10). These usually consider the real reactor to consist of different regions (plug, dispersed plug, backmix, deadwater) interconnected in different ways (bypass, recycle, or crossflow). A number of multiparameter models (called mixed models) were described by Levenspiel (11), in order to represent the flow of fluids through vessels.

Generally, the number of parameters used in a model is an indication of its flexibility in fitting a wide variety of situations and in addition, suggests to some extent the complexity of the accompanying mathematics. The parameters of the model should have physical meaning and be predicted by independent methods.

The mixed model that was applied on the experimental results is shown in Figure 3 (after Reference 11), with its corresponding characteristic response curves. The data were drawn in a semi-logarithmic paper shown in Figure 4, as an I-curve

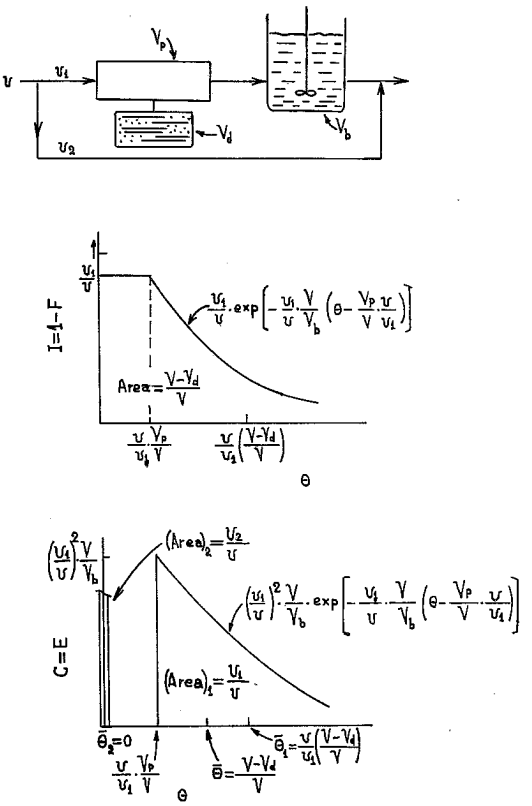

Fig. 3. *Multiparameter flow model (after Levenspiel).*

against θ. The problem is to find the relative volumes of the various regions, and the various types of flow, such that the response curves of the model closely match the response curves for the real vessel.

The existence of deadwater regions can be found by the area under the I-curve. A cut-off point should be selected, and as a reasonable one, the point $\theta = 2$ was proposed (11b). When the area of the age distribution function was measured, it was found a V_d of 1% for countercurrent flow, and 13% for cocurrent flow. Although this gives a preliminary idea for the two modes of operation, it was believed that there was an inaccuracy, perhaps in the selection of the cut-off point, in view of the results that will be given in the following.

The magnitude of short-circuiting can be estimated from the rapid initial drop in the I-curve. It is believed that by-pass flow, in our case, is nil, i.e. $v_2 = 0$ and $v = v_1$. This is apparent from the graph. Further, rough analysis of the flotation tank showed that approxiamtely 8% of the volume lay under the electrodes, and around 17% was between the entering pipe and the top (Fig. 1).

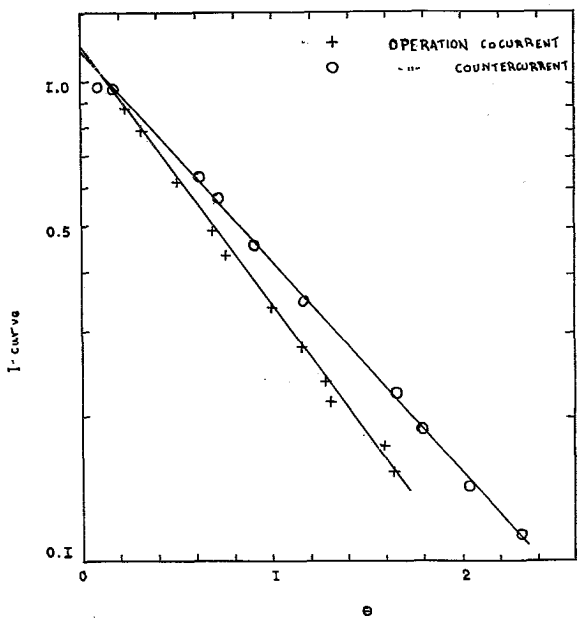

Fig. 4. *Internal age distribution function of effluent.*

The equation of the line in Figure 4, according to the model (Fig. 3, I-curve), if rearranged becomes:

$$\ln (1-F_\theta) = - \frac{1}{(1-p)(1-d)} .\theta + \frac{p}{1-p}$$

where the factor (1-d) stands for the effective volume included in θ (see also the nomenclature). The solution gave that the plug flow fraction of the effective part p = 12.3% and d $\simeq$ 0 for countercurrent flow, and for cocurrent p = 12.5% and d = 6.7% (where d is the dead space fraction of the tank volume). In fact, the value of d in the countercurrent operation was negative, but this has no physical meaning and was attributted rather to an experimental error, although the experiments were repeated.

Dollfus and Burgaud (12) discussed the mode of operation in an electrolytic flotation plant. Elsewhere (13), the counterflow circulation of the liquid was found to give a high efficiency "filtration" effect.

From previous experiments (7), (8), it was found that for a paint system, which actually was a solid/liquid separation, cocurrent operation was preferable, while countercurrent operation was better for oily effluents (liquid/liquid separation).

Concluding Remarks

It can be concluded from our experience that disadvantage of the cocurrent mode is that the floating solids could be carried out in the exit, which would decrease the removal. Advantage of the process, however, is that the feed comes first in contact with the electrodes; the importance of the electrochemical effect is noted.

On the other hand, disadvantage of the countercurrent flow, at least for the present flotation tank design, is that, for a solid/liquid application, suspended solid particles can pass to the outlet while settling. In contrast, particulate matter and bubbles have a better possibility of contact between them, and this is one of the advantages of this operation, together with a quiescent exit. So, the mode followed should be a matter of optimization of the specific application.

Concluding it can be said that an investigation of hydrodynamics was undertaken, as the efficiency is expected to be a function of the residence time distribution. The stimulus-response technique was used in this experimentation. The tracer input signal was an electrolyte and had the form of a step function. Assuming that the flow regime was composed of various flow types, a theoretical multiparameter model was applied, and the experimental data were fitted accordingly. The advantages of the different modes of operation have been also discussed. It was found that the plug flow region during electroflotation was about the same for both the modes of operation, while the difference, as might be expected, was in the mixed and deadwater regions; there was more backmix flow in the countercurrent flow, and in the cocurrent operation deadwater region appeared.

Nomenclature (Units in SI).

C-curve	dimensionless output to a pulse input	-
C_o	concentration at t = 0	$mol.m^{-3}$
C_t	concentration at t = t	»
d	dead space fraction of tank volume	-
(1-d)	effective fraction of tank volume	-
E-curve	exit age distribution function	s^{-1}
F-curve	output corresponding to 0 to 1 step input (measured as C_t/C_o)	-
I-curve	internal age distribution function (I = 1-F)	-
n	number of ideal stirred tanks in series	-
p	plug flow fraction of the effective part	-
(1-p)	perfect mixing fraction of the effective part	-
t	time	s
$\bar{t}$	mean residence time	s
v	volumetric flow rate of incoming fluid	m^3s^{-1}
v_1	flow rate of fluid passing through the vessel	»
v_2	flow rate of fluid by-passing the vessel	»
V	volume of the flotation tank	m^3
V_b	volume of backmix flow fraction	»
V_d	volume of dead space fraction	»

V_p	volume of plug flow fraction
θ	dimensionless time unit ($\theta = t/\bar{t}$)
$\bar{\theta}_c$	mean of C-curve

Περίληψη

Ἡ Μή – Ἰδανική Ροή καί ἡ Ἐφαρμογή της στήν Ἐπίπλευση

Ἡ παραδοχή τῆς ἰδανικῆς ροῆς στή μελέτη τῶν χημικῶν ἀντιδραστήρων, δηλαδή τῆς πλήρους ἀνάδευσης γιά δοχεῖα μέ ἀνάδευση ἤ τῆς ἐμβολικῆς ροῆς στούς αὐλωτούς ἀντιδραστῆρες, δέν εἶναι ἀρκετή γιά τήν περιγραφή τῆς ὑδροδυναμικῆς ἑνός ρευστοῦ καί κατ' ἐπέκταση γιά τήν πρόβλεψη τῆς λειτουργίας ἑνός ἀντιδραστήρα. Ἔτσι, ὅταν ἡ ροή ἀποκλίνει ἀπό τίς δυό ἰδανικές καταστάσεις, οἱ προβλέψεις γιά τή λειτουργία γίνονται πιό δύσκολα. Ἕνας τρόπος ἐργασίας εἶναι νά παρασταθεῖ ὁ πραγματικός ἀντιδραστήρας μέ ἕνα πρότυπο ροῆς, πού τοῦ ταιριάζει, μετά νά ὑπολογισθοῦν οἱ παράμετροι αὐτοῦ τοῦ μοντέλου καί νά προβλεφθεῖ ἡ λειτουργία καί ἡ ἀπόδοση τοῦ πραγματικοῦ ἀντιδραστήρα ἀπό τό θεωρητικό πρότυπο.

Τό πρότυπο πού ἐφαρμόσθηκε εἶχε πολλές παραμέτρους καί ἡ πειραματική διεργασία ἔγινε μέ τή χρήση κατάλληλου ἰχνηθέτη κατά τή διάρκεια τῆς ἐπίπλευσης. Ἀπό τή μελέτη συνεπάγεται ὅτι δέν ὑπῆρχε ἐναλλακτική δίοδος, ἐνῶ κατά τήν παράλληλη ροή ἐμφανίσθηκαν στάσιμες περιοχές. Ἡ ἐπικρατοῦσα κατάσταση ἦταν κύρια τῆς πλήρους ἀνάδευσης. Προσοχή χρειαζόταν στήν κατακάθιση αἰωρούμενης ὕλης, συνήθως σάν ἀποτέλεσμα στροβιλώδους ροῆς γύρω ἀπό τήν εἴσοδο. Αὐτός εἶναι ἕνα ἀνταγωνιστικός παράγοντας ὅταν τά σωματίδια εἶναι βαρύτερα τοῦ νεροῦ. Τά πλεονεκτήματα τῶν διαφόρων τρόπων λειτουργίας συζητήθηκαν.

References

1. Wen, C.Y. & Fan, L.T.: *Models for Flow Systems and Chemical Reactors Vol.* 3, p. 113, Marcel Dekker, N. York (1975).
2. Buffham, B.A. & Gibilaro, L.C.: *AIChE J.* **14**, 805 (1968).
3. Camp, T.R.: *Sewage & Ind. Wastes* **25**, 1, 1 (1953).
4. Rebhun, M. & Argaman, Y.: *J. San. Eng. Div., Proc. ASCE, Oct.*, 37 (1965).
5. Jowett, A.: *Brit. Chem. Eng.* **6**, 254 (1961).
6. Degner, V.R.: *Water-1975, AIChE Symp. Series*, p. 257 (1976).
7. (a) Matis, K.A.: *Water Pollut. Control* 136 (1980).
   (b) *Τεχν. Χρον. - Ἐπιστ. Ἔκδ. (Τομέας Χημ. Μηχ.)* **4**, 19 (1979).
   (c) *Chim. Chron. - New Ser.*, **1**, 71 (1980).
8. Backhurst, J.R. & Matis, K.A.: *J. Chem. Tech. & Biotech.*, **31**, July, 431 (1981).
9. Smith, J.M.: *Chemical Engineering Kinetics*, p. 258 McGraw-Hill, N. York (1970).
10. Cholette, A. & Cloutier, L.: *Can. J. Chem. Eng.*, June, 105 (1959).
11. (a) Levenspiel, O.: *Chemical Reaction Engineering*, p. 253 Wiley, N. York (1972).
    (b) *Can. J. Chem. Eng., Aug.*, 135 (1962).
12. Dollfus, J. & Burgaud, J.L.: *La Houille Blanche* **4**, 411 (1967).
13. PD Process Eng.: "*Water and wastewater clarification*", Technical Paper.

Chimika Chronika, New Series, 11, 59-72 (1982)

ADSORPTION OF VINYLCHLORIDE MONOMER ONTO SELECTED PLASTICIZED POLYVINYLCHLORIDE RESINS: STUDY OF THERMODYNAMIC PARAMETERS BY GAS CHROMATOGRAPHY.

M.G. KONTOMINAS AND E. VOUDOURIS.
Department of Food Chemistry University of Ioannina, Ioannina, Greece.

(Received November 30, 1981).

Summary

The adsorption of Vinylchloride monomer (VCM) onto selected plasticized polyvinylchloride (PVC) resins, has been studied using Gas Chromatography.

Thermodynamic parameters such as partial molar enthalpy of mixing, partial molar entropy of mixing, partial molar free energy and partial molar excess free energy of mixing were derived from retention data.

The concentration dependent specific retention volume of vinylchloride as well as the negative values determined for the above thermodynamic parameters support the "active site" hypothesis.

It is shown that the high binding energy of "active sites" for VCM is the limiting factor, providing an "essentially zero" migration of the monomer into a food cantacting phase when its residue in the polymeric matrix is finite but very low (< 1 ppm).

Key words: Adsorption, Vinyl chloride, Polyvinyl-chloride, Migration.

Introduction

Polyvinylchloride (PVC) is being used both in flexible forms (films) and rigid forms (bottles) in food packaging applications. Its use has raised serious questions, in recent years concerning the possibility of migration of the monomer (VCM) from the polymer into a contacting food phase[1,2,3,4,5]. Preliminary experiments[6,7,8] on rats have shown carcinogenicity of vinyl chloride via inhalation.

The toxicity of vinylchloride via inhalation in humans has also been reported to the National Institute of Occupational Safety and Health of the U.S.[9].

Finally the migration of vinylchloride from rigid PVC forms into alchohol, n-

pentane and distilled water has been reported in the literature[10].

Potential migration of VCM into a food contacting phase is controlled by the following two factors:

1. The concentration of VCM in the polymer, as a residue of the polymerization process.
2. The chemical affinity of the monomer with the specific food phase in contact with the polymer.

The concentration of residual monomer in the polymer can be related to the nature of the polymer (film, rigid plastic) as well as to polymer composition (% plasticizer, type of stabilizer etc).

The migration of a low molecular weight compound from a polymer to a contacting phase can be considered at equilibrium as a function of polymer-migrant interaction. Thus the equilibrium distribution of the migrant will be determined by the thermodynamics of the interaction while the rate of attaining equilibrium will be measured by diffusion.

Previous studies[11,12] on the subject of VCM migration, in which unplasticized PVC resin was used, showed a non-linear relation-ship between concentration of VCM in the polymer and the activity coefficient of the PVC/VCM interaction in favor of the polymer.

These studies resulted in the development of the "active site" hypothesis, which states that certain regions (active sites) within the polymer network seem to show a higher affinity for monomer molecules, than others do.

In this paper the thermodynamic parameters of the PVC/VCM interaction are studied, namely free energy, entropy and enthalpy of sorption using gas chromatography, with the purpose to obtain valuable information on the nature of the above interaction as well as to test the "active site" hypothesis.

Theory

Inverse phase chromatography

Inverse phase gas chromatography (IPGC) has been successfully used in recent years, for both sorption isotherms and the determination of thermodynamic parameters, as a means of interaction evaluation of different polymer/probe molecule systems.

In IPGC, the polymer powder is the stationary phase of the GC column and the probe molecule (monomer) is injected as a gas into the column. The monomer partitions between the stationary and mobile phase (carrier gas) and it is possible from chromatographic data to calculate the major thermodynamic parameters of such interaction.

Calculation of Thermodynamic parameters from gas Chromatographic Data

The Clasius-Clapeyron expression of V^0g[13] is given by equation (1)

$$\frac{d\ (\ln V^0 g)}{dT} = \frac{\Delta H_s}{RT^2} \qquad (1)$$

where V^0g = specific retention volume, or the apparent retention volume (V_R) corrected for all oprerational variables, dependent only on the thermodynamic variables of the system.

ΔH_s: partial molar heat of solution of vapor in the column stat. phase.

The specific retention volume, V^0g, is defined by equation (2)

$$V^0g = \frac{J\dot{V}\ (t_r - t_f)}{W_s} \times \frac{273}{T} \qquad (2)$$

Where: J= compressibility factor, which accounts for the pressure drop along the column

$\dot{V}$= flow rate of carrier gas (ml/sec)

t_r= time from solute injection to elution (sec)

t_f= retention time of unsorbed indicator (air)

W_s= weight of st. phase (gr).

The partial molar enthalpy and entropy are related to the column capacity coefficient (k) by equation (3).

$$\ln k = \ln f + \left(\frac{\Delta H}{RT}\right) - \left(-\frac{\Delta S}{R}\right)^{14} \qquad (3)$$

Where: ΔH= partial molar enthalpy of the solute when transferring from the st. phase to the mobile phase.

(Apparently $\Delta H_s = -\Delta H$) (4)

ΔS= partial molar entropy of the solute when transferring from the st. phase to the mobile phase.

f= ratio of vol. of st. phase to the mobile phase

k= column capacity coefficient = $\frac{V^0g}{Vo}$

Vo= dead vol. of the column associated with 1gr of st. phase.

The partial molar entropy of solution of vapor solute in the column stationary phase is $\Delta S_s = -\Delta S$.(5) Equations (3), (4), (5) provide:

$$\Delta S_s = R(\ln k - \ln f) + \frac{\Delta H_s}{T} \qquad (6)$$

Equations (1) and (6) provide the ΔH_s and ΔS_s values necessary to calculate the change in Gibb's free energy (ΔG_s) of the solute/solvent interation by use of equation (7)

$$\Delta G_s = \Delta H_s - T\Delta S_s \qquad (7)$$

A negative sign for ΔG_s, will indicate that the interaction takes place spontaneously, while the sign of ΔH_s will indicate whether there are attractive of repulsive forces between the solute and solvent molecules. The sign of ΔS_s will show whether of not the solute/solvent interaction leads to a more ordered system (binding of monomer on specific sites).

If we define an "excess" free energy of mixing (ΔG_{ss}) for a real solution in comparison with an ideal solution then:

$$\Delta G_{ss} = \Delta Gs - \Delta G_i \qquad (8)$$

Where: ΔG_s= partial molar free energy of mixing of solute/solvent in real solution
ΔG_i= partial molar free energy of mixing of solute/solvent in ideal solution

Equation (8) can be written in terms of the activity coefficient (γ) of the interaction:

$$\Delta G_{ss} = RT\ln\gamma \qquad (9)$$

Values for γ greater than 1 are indicative of repulsive forces between solute and solvent (positive deviation from Raoult's Law).

Values for γ lower than 1 are indicative of attractive forces between solute and solvent.

Equations (1), (6), (7), (8) and (9) were used to calculate the thermodynamic parameters of the PVC/VCM interaction.

Experimental Procedures

Three different columns were used in all IPGC experiments. Each column was packed with one of the following three PVC powdered resins: TYPE I, DRY BLEND 6200 and DRY BLEND 7200 containing 15%, 25% and 33% plasticizer respectively. All resins were supplied by Borden Chem. Co., N. Andover Mass, U.S.A. The PVC resins were sieved, so that particle sizes between 100-150 Mesh were used for column preparation. The aluminum columns of 6′ × 1/4′′ O.D. were weighed before and after the packing procedure to determine the amount of powdered resin used in each column.

A series of gas VCM in nitrogen standard samples were prepared by direct injection of known volumes of high purity (99.99%) VCM into 60ml serum vials (Wheaton vials, Fisher Sci. Co.) which were previously flushed with pure nitrogen.

All retention data were obtained on a Hewlett Packard 5750 Gas Chromatograph equipped with a dual flame ionization detector. Nitrogen was used as the carrier gas and the flow rate was measured using a soap bubble flow meter.

The pressure drop along the column was measured with a mercury manometer at the injection port (P_{outlet} = 1atm). The detector was calibrated prior to all experiments with a 10% SE-30 column coated on ABS 90/100 Mesh.

The temperatures selected, for the different columns used, were the following:

a) TYPE I RESIN 30°C, 40°C, 55°C
b) DRY BLEND 6200 RESIN 30°C, 40°C, 55°C
c) DRY BLEND 7200 » 30°C, 40°C, 55°C

Operating conditions of the G.C. were the following:

T_{det} = 200°C
T_{inj} = 30°C
Carrier gas: N_2, 60ml/min

All three columns were insulated from the detector by a 3'' column packed

TABLE I. Specific rentention volume (V^0g) as a function of concentration of VCM injected, into column TYPE I at temperatures: a) 30°C b) 40°C c) 55°C.

a) 30°C

V^0g (ml/g)	$(VCM)_{PVC}$ (ppb W/W)
2.6	6.0
2.3	12.0
2.1	25.0
2.0	48.5
1.9	74.0
1.9	120.0

b) 40°C

V^0g (ml/g)	$(VCM)_{PVC}$ (ppb W/W)
2.3	6.0
2.1	12.0
1.9	25.0
1.8	48.5
1.8	74.0
1.8	120.0

c) 55°C

V^0g (ml/g)	$(VCM)_{PVC}$ (ppb W/W)
2.0	6.0
1.9	12.0
1.8	25.0
1.7	48.5
1.7	74.0
1.7	120.0

with glasswool, which was connected between the column and the detector inlet.

Retention times were determined to ± 0.1 sec. The retention time of air was taken to be that of an undsorbed component.

Results

Retention Data

Values for the specific retention volume (V^0g) in ml/g as a function of VCM concentration in PVC % (W/W) injected at three different temperatures in each of the three columns, are shown in Tables I-III and Figures 1-3.

TABLE II. Specific rentention volume (V^0g) as a function of concentration of VCM injected into column DRY BLEND 6200 at temperatures: a) 30°C b) 40°C c) 55°C.

a) 30°C

V^0g (ml/g)	$(VCM)_{PVC}$ (ppb W/W)
6.0	6.0
5.7	12.0
5.3	25.0
5.0	50.0
4.8	75.0
4.8	120.0

b) 40°C

V^0g (ml/g)	$(VCM)_{PVC}$ (ppb W/W)
5.0	6.0
4.8	12.0
4.6	25.0
4.5	50.0
4.4	75.0
4.4	120.0

c) 55°C

V^0g (ml/g)	$(VCM)_{PVC}$ (ppb W/W)
3.9	6.0
3.8	12.0
3.7	25.0
3.6	50.0
3.6	75.0
3.6	120.0

TABLE III. Specific rentention volume (V^0g) as a function of concentration of VCM injected, into column DRY BLEND 7200 at temperatures: a) 30°C b) 40°C c) 55°C.

a) 30°C

V^0g (ml/g)	$(VCM)_{PVC}$ (ppb W/W)
10.0	7.0
9.5	13.0
9.3	27.0
9.0	55.0
8.8	82.0
8.8	130.0

b) 40°C

V^0g (ml/g)	$(VCM)_{PVC}$ (ppb W/W)
8.0	7.0
7.7	13.0
7.5	27.0
7.4	55.0
7.4	82.0
7.4	130.0

c) 55°C

V^0g (ml/g)	$(VCM)_{PVC}$ (ppb W/W)
6.1	7.0
6.0	13.0
5.9	27.0
5.8	55.0
5.8	82.0
5.8	130.0

Family regression analysis of this data provided the general formula $Y=a+b\ln x$ to fit the plots for all PVC columns used.

In Figures 1-3 the intersept a in each plot was taken as the specific retention volume at infinite dilution ($V^0g\ \infty$). These values are shown in Table IV.

The effect of temperature on the specific retention volume (V^0g) at a) infinite dilution b) lowest VCM concentration c) highest VCM concentration in shown in Tables V-VII and Figures 4-6.

Thermodynamic Parameters

Values for partial molar enthalpy (ΔH_s) partial, molar entropy (ΔS_s) and partial molar free energy (ΔG_s) corresponding to the dissolution of VCM in the

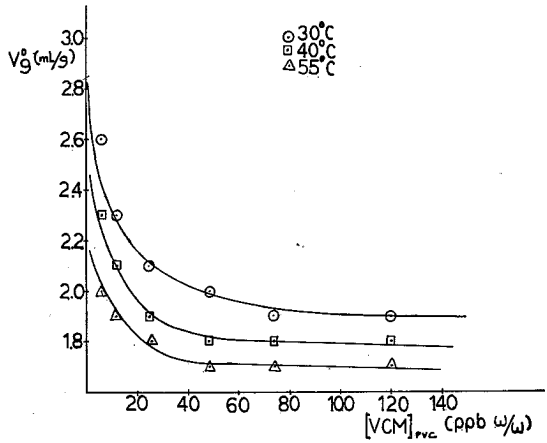

Figure 1. *Specific rentention volume (V^0g) as a function of concentration of VCM injected, into column TYPE I at temperatures: a) 30°C b) 40°C c) 55°C.*

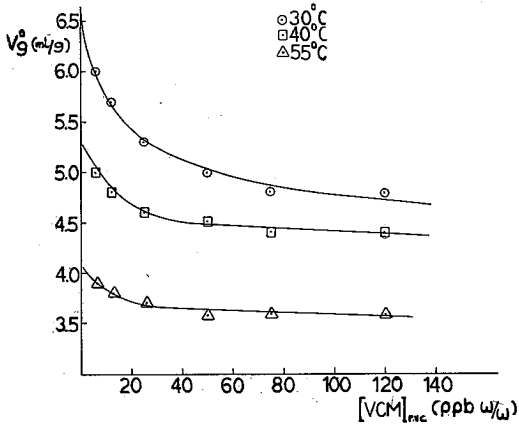

Figure 2. *Specific rentention volume (V^0g) as a function of concentration of VCM injected, into column DRY BLEND 6200 at temperatures: a) 30°C b) 40°C c) 55°C.*

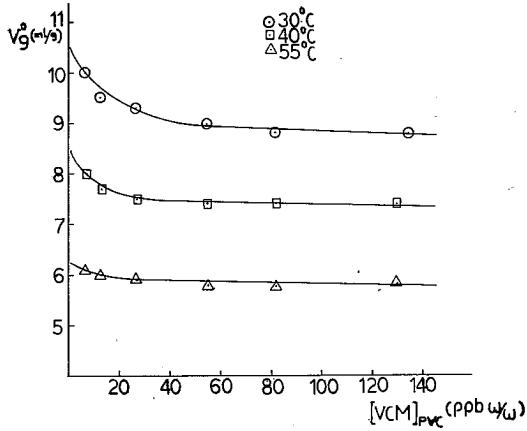

Figure 3. *Specific rentention volume (V^0g) as a function of concentration of VCM injected, into column DRY BLEND 7200 at temperatures: a) 30°C b) 40°C c) 55°C.*

TABLE IV. Specific rentention volume at infinite dilution ($V^0g\ \infty$) for resins TYPE I, DRY BLEND 6200 AND DRY BLEND 7200 at temperatures: a) 30°C b) 40°C c) 55°C.

a)resin TYPE I

$V^0g\infty$ (ml/g)	T(°C)
2.95	30
2.60	40
2.20	55

b)resin "DRY BLEND" 6200

$V^0g\infty$ (ml/g)	T(°C)
6.60	30
5.30	40
4.10	55

c)resin "DRY BLEND" 7200

$V^0g\infty$ (ml/g)	T(°C)
10.6	30
8.50	40
6.25	55

TABLE V. In V^0g as a function of reciprical temperature at a) infinite dilution b) 6ppb c) 120 ppb for column with resin TYPE I.

a) infinite dilution

In V^0g	$1/T\ (K^{-1})$
1.081	3.30×10^{-3}
0.955	3.19×10^{-3}
0.788	3.05×10^{-3}

b) 6ppb

In V^0g	$1/T\ (K^{-1})$
0.955	3.30×10^{-3}
0.833	3.19×10^{-3}
0.693	3.05×10^{-3}

c) 120ppb

In V^0g	$1/T\ (K^{-1})$
0.642	3.30×10^{-3}
0.587	3.19×10^{-3}
0.531	3.05×10^{-3}

TABLE VI. In V^0g as a function of reciprocal temperature at a) infinite dilution b) 6ppb c) 120 ppb for column with resin DRY BLEND 6200.

a) infinite dilution

In V^0g	$1/T\ (K^{-1})$
1.887	3.30×10^{-3}
1.668	3.19×10^{-3}
1.411	3.05×10^{-3}

b) 6ppb

In V^0g	$1/T\ (K^{-1})$
1.792	3.30×10^{-3}
1.609	3.19×10^{-3}
1.361	3.05×10^{-3}

c) 120ppb

In V^0g	$1/T\ (K^{-1})$
1.569	3.30×10^{-3}
1.482	3.19×10^{-3}
1.281	3.05×10^{-3}

TABLE VII. In V^0g as a function of reciprocal temperature at a) infinite dilution b) 7ppb c) 130 ppb for column with resin DRY BLEND 7200.

a) infinite dilution

In V^0g	$1/T\ (K^{-1})$
2.361	3.30×10^{-3}
2.140	3.19×10^{-3}
1.832	3.05×10^{-3}

b) 7ppb

In V^0g	$1/T\ (K^{-1})$
2.302	3.30×10^{-3}
2.079	3.19×10^{-3}
1.808	3.05×10^{-3}

c) 130ppb

In V^0g	$1/T\ (K^{-1})$
2.174	3.30×10^{-3}
2.001	3.19×10^{-3}
1.758	3.05×10^{-3}

PVC columns (solvent/solute interaction), are shown in Table VIII. Changes in excess molar free energy (ΔG_{xs}) and activity coefficient values, corresponding to the dissolusion of VCM in the PVC columns are shown in Table IX.

Discussion

Results shown in Tables I-III and Figures 1-3 indicate that for all three of the PVC resins used, the specific retention volume is concentration dependent al all temperatures below Tg=81° C increasing exponentially at very low VCM concentrations.

This means that the lower the residual amount of VCM is in the resin, the better it is bound by the polymer. These results support the "active site" hypothesis which states that certain irregularities or "active sites" exist with in the polymer network that tend to thermodynamically bind the monomer, thus reducing its possibility for migration in to food.

For a given resin and concentration of VCM the specific retention volume increases with the decrease of temperature. Thus ambient temperature favors the retention of the monomer by the polymer.

Another very interesting point is that the amount of plasticizer seems to influence the specific retention volume significantly. The higher the degree of plasticization of the resin, the longer the VCM is retended, or the better VCM is bound with in the polymer matrix. This is in accordance with previous results[11].

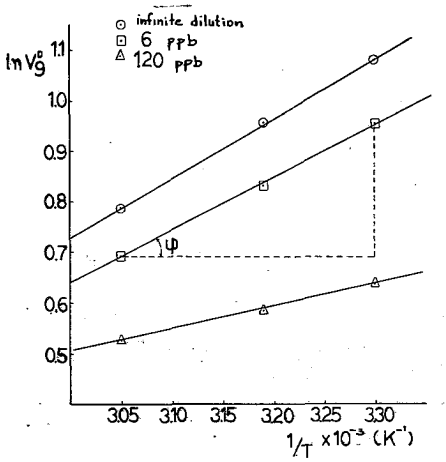

Figure 4. *In V^0g as a function of reciprocal temperature at a) infinite dilution b) 6ppb c) 120 ppb for resin TYPE I.*

The relation of the specific retention volume at infinite dilution, at 6ppb and 120 ppb with temperature (Tables IV-VII, Figures 4-7) is of the Arrhenius type and the slope of each curve ($\frac{\Delta H}{R}$) shows the contribution of enthalpy change on the change of Gibb's free energy (ΔG_s) for the PVC/VCM interaction.

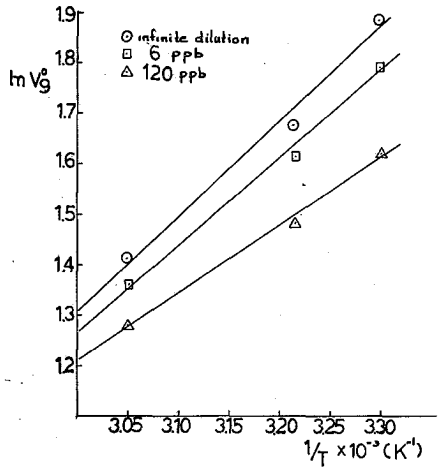

Figure 5. *In V°g as a function of reciprocal temperature at a) infinite dilution b) 6ppb c) 120 ppb for resin DRY BLEND 6200.*

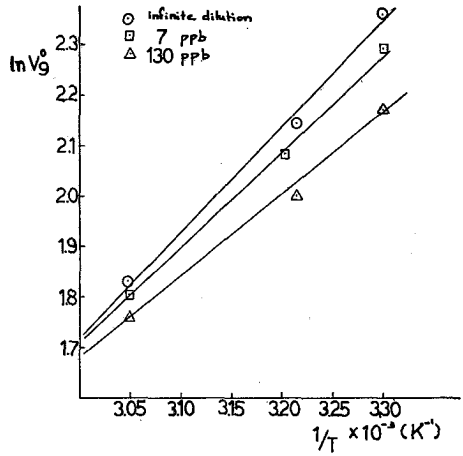

Figure 6. *In V°g as a function of reciprocal temperature at a) infinite dilution b) 7ppb c) 130 ppb for resin DRY BLEND 7200.*

TABLE VIII. Change in partial molar enthalpy (ΔH_s) partial, molar Entropy (ΔS_s), and partial free energy (ΔG_s) for dissolution of VCM in the three PVC resins at 30°C.

PVC RESIN	ΔH_s(Kcal/mol)	ΔS_s(cal/mol)	ΔG_s (Kcal/mol)
TYPE I	-2.08	-4.81	-0.624
DRY BLEND 6200	-3.42	-7.81	-1.05
DRY BLEND 7200	-3.92	-8.19	-1.44

Values of thermodynamic parameters shown in Tables VIII and IX are indicative of the exothermic character of the VCM/PVC interaction ($\Delta H < 0$) and the binding of the monomer on specific sites with in the polymer network ($\Delta G_s < 0$).

Results shown in Tables I-III and Figures 1-3 indicate that for all three of the PVC resins used, the specific retention volume is concentration dependent at all temperatures below Tg=81^0 C increasing exponentally at very low VCM concentrations.

TABLE IX. Change in excess molar free energy (ΔG_{xs}) and activity coefficient for dissolution of VCM in the three PVC resins at 30^{0}C.

PVC RESIN	ΔG_{xs}(Kcal/mol)	γ(activity coeff)
TYPE I	-4.71	3.97 X 10^{-4}
DRY BLEND 6200	-5.14	1.96 X 10^{-4}
DRY BLEND 7200	-5.52	1.04 X 10^{-4}

which is indicative of strong attractive forces between VCM, PVC molecules.

The major significance of these results is that the VCM binding energy on to PVC, exhibits a non-liner inverse relation with VCM concentration. Thus at low concentrations (< 1ppm) of residual VCM in the packaging material, the high thermodynamic free energy required for desorption is the limiting factor which provides an "essentially zero" migration of VCM to a contacting food phase.

Results are in general accordance with previous work conducted with similar systems using classical partition[15].

Περίληψη

Προσρόφηση τοῦ μονομεροῦς βινυλοχλωριδίου ἀπό πλαστικοποιημένες ρητίνες πολυβινυλοχλωριδίου: Μελέτη τῶν θερμοδυναμικῶν παραμέτρων μέ τήν Ἀέρια Χρωματογραφία.

Σ' αὐτή τήν ἐργασία, μελετήθηκε ἡ προσρόφηση τοῦ μονομεροῦς βινυλοχλωριδίου (VCM) σέ σειρά ἀπό πλαστικοποιημένες ρητίνες πολυβινυλοχλωριδίου (PVC). Ἡ μελέτη ἔγινε μέ τήν Ἀέριο Χρωματογραφία. Θερμοδυναμικές παράμετροι ὅπως ἡ ἐνθαλπία, ἡ ἐντροπία καί ἡ ἐλεύθερη ἐνέργεια προσροφήσεως ὑπολογίστηκαν μέ βάση τά χρωματογραφικά μεγέθη τοῦ χρόνου καί ὄγκου κατακράτησης. Ἡ ἐξάρτιση τοῦ εἰδικοῦ ὄγκου κατακράτησης τοῦ μονομεροῦς ἀπό τή συγκέντρωση καθώς καί οἱ ἀρνητικές τιμές πού βρέθηκαν γιά τίς παραπάνω θερμοδυναμικές παραμέτρους, στηρίζουν τήν ὑπόθεση τῶν ἐνεργῶν κέντρων (active site hypothesis).

Ὑποστηρίζεται πώς ἡ ὑψηλή ἐνέργεια δέσμευσης τῶν «ἐνεργῶν κέντρων» γιά τό μονομερές βινυλοχλωρίδιο εἶναι ὁ περιοριστικός παράγων πού παρέχει «οὐσιαστικά μηδενική» μετανάστευση τοῦ μονομεροῦς ἀπό τό πλαστικό συσκευασίας στό τρόφιμο, ὅταν ἡ συγκέντρωσή του στό τελευταῖο εἶναι πεπερασμένη ἀλλά πολύ χαμηλή (< 1ppm).

Bibliography

1. Daniels G.A. & Proctor D.E.: *VCM extraction from PVC bottles Modern Packaging April*, 45 (1975).
2. Figge K.: *Food Cosmet. Toxicol.*, **10**, 815 (1972).
3. Gilbert S.G.: *J. Food. Sci.* **41**, 955 (1976).
4. Χατζηχριστίδη Ν., Κωμαΐτη Μ. & Βουδούρη Ε.: *Χημικά Χρονικά (Γεν. έκδ.)*, **42**, 26 (1976).
5. Σαγρέδος Α.Ν., & Συν.: *Chimica Chronica, New Ser.*, **8**, 9 (1979).
6. Hefner R.E., Watanabe, P.G., & Gehring P.J.: *Ann. N.Y. Acad. Sci.*, **246**, 135 (1975).
7. Maltoni C. & Lefemine G.: *Env. Res.*, **7**, 387 (1974).
8. Maltoni C. & Lefemine G.: *Ann. N.Y. Acad. Sci.*, **246**, 195 (1975a).
9. Federal Register.: *Enviromental Protection Agency*. **40**, No 248: 59532 Dec. 24 (1975α).
10. Federal Register.: *U.S. Dept of Health, Education and Welfare, Food and Drug Administration* **40**, No 171: 45029 Sept. 3 (1975b).
11. Kashtock M.E.: *Interaction of Vinylchloride with Polynylchloride. A comparison of Classical sorption and sorption by Gas-Solid chromatography Ph.D. Thesis Rutgers University*, New Brunswick N.J., U.S.A. (1977).
12. Morano J.R., Giacin J.G. & Gilbert S.G.:"*The Vinylchloride Problem as related to Food Packaging - Analytical and Migration Considerations.* Presented at June 1975 meeting, Institute of Food Technologists.
13. Kiselev A.V. & Yashin Y.J.: *Gas Adsorption Chromatography*, p. 105 Plenum Press, New York (1969).
14. Knox J.H. & Vasvari G.: *J. Chromat.* **83**, 181 (1973).
15. Kontominas M.G. & Gilbert S.G.: *Adsorption - desorption phenomena in PVC/VCM/Food solvents by classical partition: Thermodynamic Aspects.* Presented at the IFT Convention st. Louis Mo. June (1979).

Chimika Chronika, New Series, 11, 73-84 (1982)

SYNTHESIS AND STUDY OF SOME SYMMETRICALLY DIAMINO-SUBSTITUTED GLYOXIMES, FUROXANS AND FURAZANS.

D.N. NICOLAIDES, K.E. LITINAS and I. NAIDOU
Laboratory of Organic Chemistry, University of Thessaloniki, Thessaloniki, Greece.

(Received December 11, 1981).

Summary

The synthesis of some symmetrically N,N′-substituted diaminoglyoximes, their stereochemical study by ^{1}H-NMR spectroscopy and their oxidation and dehydration to the corresponding furoxans and furazans respectively, as well as the deoxygenation of some of the prepared furoxans to furazans are reported.

Key words: Diaminoglyoximes, diaminofuroxans, diaminofurazans, stereochemical study.

Introduction

Symmetrically substituted diaminoglyoximes are known since 1893 when Holleman[1] described the preparation of bis-anilino-glyoxime from furoxan and aniline. Several compounds of this type are known today prepared from dichloroglyoxime[2] or its diacetate[3,4] or dicyano-di-N-oxide[5,6] and ammonia or primary and secondary mono-amines. On the other hand reactions of dicyano-di-N-oxide with 1,2-diamines resulted in a similar way to the formation of 2,3-bis-hydroxyiminopiperazine and 2,3-bis-hydroxyimino-1,2,3,4-tetrahydroquinoxalines[7,8]. Although the diamino-glyoximes prepared from primary amines can exist in several tautomeric forms, it has been suggested that they adopt the dioximino-structure[6,9]. Like other α-dioximes[10] some diamino-glyoximes have been converted to the corresponding diamino-furazans[2,9] while some of those, fully substituted, were oxidized with potassium ferricyanide to the corresponding furoxans[4]. There are indications that the amphi- forms of the dioximes undergo these reactions most readily and it may be that other dioximes which yield furazans and furoxans do so by a preliminary rearrangement[4,10].

Table I. Diamino-glyoximes 4(d,e,f), Furoxans 6(a-f) and Furazans 7(a,d,f).

Compound	Yield [%] (Method)	m.p. [°C] (Lit. m.p.)	Recrystal. solvent	Molecular Formula	Calculated/Found %C	%H	%N	IR ν [cm^{-1}]
4d	46 (A)	119-121	Methanol	$C_{28}H_{26}N_4O_2$	74.64	5.82	12.44	3200, 3040, 1643, 1615,
	80 (B)			(450.5)	74.99	5.87	11.98	1595, 1000, 977, 938[a]
4e	15 (A)	168-170	Chloroform/	$C_{16}H_{30}N_4O_2$	61.90	9.74	18.05	3300, 1645, 1610, 990,
			Petr. Ether	(310.4)	61.85	9.76	18.00	960[a]
4f	48 (A)	181-182	Chloroform/	$C_{10}H_{18}N_4O_4$	46.50	7.02	21.69	3260, 1645, 1615, 985,
	54 (B)	(181-183)[4]	Petr. Ether	(258.3)	46.54	7.08	21.71	960[a]
6a	55	121-123	Ether	$C_{16}H_{16}N_4O_2$	64.85	5.44	18.91	1604, 1588, 1550, 1493,
				(296.3)	64.82	5.46	18.40	1452, 1418, 1372[b]
6b	48	93-94	Ether/Petr.	$C_{18}H_{20}N_4O_2$	66.65	6.22	17.27	1604, 1589, 1548, 1495,
			Ether	(324.4)	66.48	6.27	17.09	1486, 1444,1380[b]
6c	64	56-58	Petr. Ether	$C_{20}H_{24}N_4O_2$	68.16	6.86	15.90	1608, 1590, 1547, 1493,
				(352.4)	68.35	7.00	16.01	1483, 1450, 1379[b]
6d	60	112-114	Chloroform/	$C_{28}H_{24}N_4O_2$	74.98	5.39	12.49	1603, 1588, 1547, 1537,
			Petr. Ether	(448.5)	74.98	5.44	12.55	1495, 1484, 1452, 1440, 1380[b]
6e	75	oil	----------	$C_{16}H_{28}N_4O_2$	62.30	9.15	18.17	1630, 1582, 1548, 1482,
				(308.4)	62.32	9.08	17.99	1450, 1416, 1360, 1347[b]
6f	85	141-142	Ether/Petr.	$C_{10}H_{16}N_4O_4$	46.87	6.29	21.87	1608, 1591, 1547, 1537,
		(143)[4]	Ether	(256.3)	47.04	6.37	22.07	1479, 1452, 1372[b]
7a	14 (A)	137-139	Chloroform/	$C_{16}H_{16}N_4O$	68.55	5.75	19.99	1602, 1590, 1568, 1540,
	70 (B)		Petr. Ether	(280.3)	68.36	5.90	19.80	1500, 1455, 1404, 1380[b]
7d	42 (A)	99-100	Petr. Ether	$C_{28}H_{24}N_4O$	77.75	5.59	12.96	1600, 1589, 1568, 1528,
	85 (B)			(432.5)	77.70	5.54	12.73	1496, 1455, 1370[b]
7f	18 (A)	151-153	Chloroform/	$C_{10}H_{16}N_4O_3$	49.99	6.71	23.32	15.75, 1545, 1530, 1510,
	58 (B)		Petr. Ether	(240.3)	49.52	6.61	23.30	1451, 1380[b]

a: in Nujol b: in Chloroform

Table II. ^{1}H-NMR spectra of compounds 4(a-f), 6(a-f), 7(a,c,d,f),

Compound	δ[ppm]
4a	2.50 (s, 6H, N-CH_3), 6.65-7.58 (m, 10H, C_6H_5)[a]; 11.43 (s, 2H, N-OH)[b].
4b	0.90 (t, 6H, CH_3, J=7 Hz), 2.70 (q, 4H, CH_2 , J=7 Hz), 6.50-7.40 (m, 10H, C_6H_5)[a]; 11.27 (s, 2H, N-OH)[b].
4c	0.90 (t, CH_2-CH_3, J[c]=7Hz), 2.30 (s, C_6H_4-CH_3), 2.73[c] (q, -CH_2-CH_3, J[c]=7 Hz), 6.40-7.33[c] (m, arom.)[a]; 0.88 (t, 6H, CH_2-CH_3, J=7 Hz), 2.25 (s, 6H, -C_6H_4-CH_3) 2.77 (q, 4H, -CH_2-CH_3, J=7 Hz), 6.33-7.30 (m, 8H, arom.), 11.20 (s, 2H, N-OH)[b].
4d	4.17 (s, 4H, C_6H_5-CH_2-), 6.37-7.50 (m, 20H, arom.), 11.28 (s, 2H, N-OH)[b].
4e	1.17-2.00 (m, 22H), 2.70 (s, 6H, N-CH_3)[a]; 8.87 (s, 2H, N-OH)[b].
4f	2.92-3.42 (m, 8H, -CH_2-N-CH_2-), 3.50-3.97 (m, 8H, -CH_2-O-CH_2-)[a]; 10.22 (s, 2H, N-OH)[b].
6a	2.77 (s, 3H, CH_3[d]), 3.32 (s, 3H, CH_3[e]), 6.15-7.30(m, 10H, arom.)[f].
6b	1.10 (t, 3H, -CH_2-CH_3[d], J=7 Hz), 1.18 (t, 3H, -CH_2-CH_3[e], J=7 Hz), 3.17 (q, 2H, -CH_2-CH_3[d], J=7 Hz), 3.75 (q, 2H, -CH_2-CH_3[e], J=7 Hz), 6.18-7.30 (m, 10H, arom.)[a].
6c	1.08 (t, 3H, -CH_2-CH_3[d], J=7 Hz), 1.17 (t, 3H, -CH_2-CH_3[e], J=7 Hz), 2.02 (s, 3H, C_6H_4-CH_3[d]), 2.20 (s, 3H, C_6H_4-CH_3[e]), 3.13 (q, 2H, -CH_2-CH_3[d], J=7 Hz), 3.73 (q, 2H, -CH_2-CH_3[e], J=7 Hz), 6.00-7.18 (m, 8H, arom.)[a].
6d	4.23 (s, 2H, C_6H_5-CH_2-[d]), 4.85 (s, 2H, C_6H_5-CH_2-[e]), 6.18-7.28 (m, 20H, arom.)[a].
6e	0.80-2.17 (m, 22H), 2.77 (s, 3H, N-CH_3[d]), 2.85 (s, 3H, N-CH_3[e])[a].
6f	3.12-3.55 (m, 8H, -CH_2-N-CH_2-), 3.62-3.95 (m, 8H, -CH_2-O-CH_2-)[a].
7a	3.22 (s, 6H, N-CH_3), 6.28-7.50 (m, 10H, arom.)[a].
7c	1.17 (t, 6H, CH_2-CH_3, J=7 Hz), 2.15 (s, 6H, -C_6H_4-CH_3), 3.63 (q, 4H, -CH_2-CH_3), 6.03-7.17 (m, 8H, arom.)[f].
7d	4.72 (s, 4H, C_6H_5-CH_2-), 6.25-7.42 (m, 20H, arom.)[a].
7f	3.17-3.48 (m, 8H, -CH_2-N-CH_2-), 3.68-4.02 (m, 8H, -CH_2-O-CH_2-)[a].

a: in $CDCl_3$; b: in DMSO-d_6; c: obscure signal because of the low solubility of compound; d: 3-N-substituent; e: 4-N-substituent; f: in CCl_4.

In connection with our recent work on oxidation of some 2,3-bis-hydroxyimino-1,2,3,4-tetrahydroquinoxalines with phenyliodine ditrifluoroacetate (5) to furoxano-[3,4-b]quinoxalines and their subsequent deoxygenation to the corresponding furazano-[3,4-b]quinoxalines[11] we present in this paper the preparation of diamino-glyoximes 4(a-f), their oxidation with 5 to the corresponding furoxans 6(a-f) and further the preparation of furazans 7(a,c,d,f) (Scheme 1), as well as a spectroscopic study of all these compounds.

Table III. ^{1}H-NMR spectra of Diamino-glyoximes RR′N-C(=NOH)C(=NOH)-NRR′, 4(f-l) and Furoxans RR′N-C—C-NRR′, 6(f-j), reported by Walstra et al[4].

Compound	R	R′	δ[ppm]
4f	$-CH_2-CH_2-O-CH_2-CH_2-$		3.21-3.57 (m, 8H, $-CH_2-O-CH_2-$), 3.73-3.95 (m, 8H, $-CH_2-N-CH_2-$), 4.68 (s, 2H, =N-OH)[a].
4g	CH_3	CH_3	2.89 (s, 12H, CH_3), 5.80 (br.s, 2H, =N-OH)[b].
4h	C_2H_5	C_2H_5	1.20 (t, 12H, CH_3), 3.22 (q, 8H, CH_2), 7.66 (s, 2H, =N-OH)[b].
4i	$CH(CH_3)_2$	$CH(CH_3)_2$	1.24 (d, 12H, CH_3), 1.36 (d, 12H, CH_3), 3.45-3.91 (m, 4H, CH), 4.68 (s, 2H, =N-OH)[c].
4j	$-(CH_2)_5-$		1.60 [s, 12H, $-(CH_2)_3-$], 3.19 (m, 8H, $-CH_2-N-CH_2-$), 4.70 (s, 2H, =N-OH)[c].
4k	H	C_2H_5	1.15 (t, 6H, CH_3), 3.17 (q, 4H, CH_2), 4.82 (br., 4H, N-H and =N-OH)[c].
4l	H	C_6H_5	6.77-7.17 (m, 10H, C_6H_5), 7.45 (br.,2H, =N-OH), 9.45 (br., 2H, N-H)[d].
6f	$-CH_2-CH_2-O-CH_2-CH_2-$		3.21-3.57 (m, 8H, $-CH_2-O-CH_2-$), 3.72-3.96 (m, 8H, $-CH_2-N-CH_2-$)[b].
6g	CH_3	CH_3	2.82 (s, 6H, CH_3), 2.97 (s, 6H, CH_3)[e].
6h	C_2H_5	C_2H_5	0.97-1.34 [m, (two triplets), 12H, CH_3], 3.02-3.69 [m, (two quartets), 8H, CH_2][b].
6i	$CH(CH_3)_2$	$CH(CH_3)_2$	1.13 (d, 12H, CH_3), 1.32 (d, 12H, CH_3), 3.50-3.94 (m, 2H, CH), 4.15-4.60 (m, 2H, CH)[b].
6j	$-(CH_2)_5-$		1.63 [br., 12H, $-(CH_2)_3-$], 3.09-3.44 (m, 8H, $-CH_2-N-CH_2-$)[b].

a: in D_2O; b: in $CDCl_3$; c: in CD_3OD; d: in $(CD_3)_2CO$; e: in CCl_4.

Results and Discussion

The reactions studied and the compounds prepared are depicted in Scheme I, while their analytical and spectral data are given in Tables I, II, IV. Compounds 4(a-f) were prepared by the reaction of the appropriate amine with dicyano-di-N-oxide (2) (Method A) or with dichloroglyoxime (3) (Method B). Products from both methods were identical to each other and the known 4(a-c)[6] 4(f)[4] to those reported in the literature.

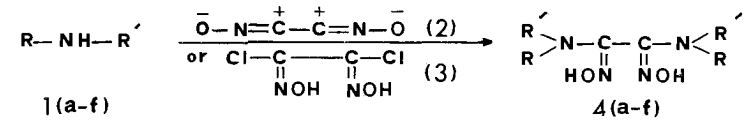

1(a-f) 4(a-f)

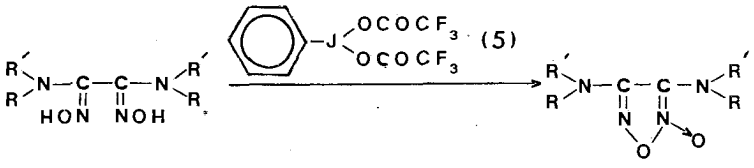

4(a-f) 6(a-f)

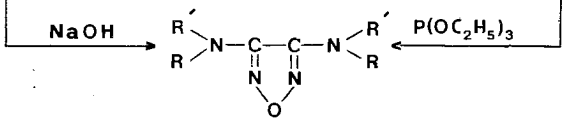

7(a,c,d,f)

1, 4, 6, 7 a: R=CH_3, R'=C_6H_5; b: R=C_2H_5, R'=C_6H_5; c: R=C_2H_5, R'=3-CH_3-C_6H_4;
d: R=C_6H_5-CH_2, R'=C_6H_5; e: R=CH_3, R'=cyclo-C_6H_{11};
f: R-R'=-CH_2-CH_2-O-CH_2-CH_2-

Scheme 1

Compounds 4(a-f) showed in their ^{1}H-NMR spectra in DMSO only one sharp singlet peak for both their hydroxyl protons (=N-OH) at δ=8.87-11.43 ppm (Table II). This observation is very informative on the stereochemistry of compounds in question, which generally may exist in anti- (8a), syn- (8b) or amphi - configuration (8c).

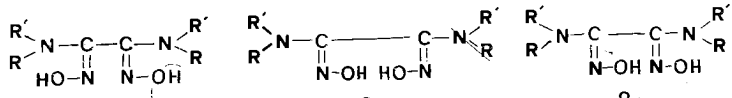

8a 8b 8c

Scheme 2

Kleinspehn et al.[12] found that most oximes exhibit in their ^{1}H-NMR spectra in DMSO a hydroxyl proton resonance signal whose chemical shift value is essentially concentration independed and thus characteristic of the particular syn- or anti-isomer. Similarly Tanaka et al.[13] reported that the anti- and syn- forms of benzil- and furil-dioxime give one sharp signal for both their hydroxyl protons in different

fields, while the non-symmetric amphi- forms give two singlets. These signals were not affected by mixing of isomers. Recently, Gozlan et al.[14] and Dignam et al.[15] prepared the (E)- and (Z)- isomers of some benzamidoximes and found that the hydroxyl proton of (Z)- isomers resonates in the ^{1}H-NMR spectra (DMSO) at a lower field than that of the corresponding (E)- isomers. Significant and normal differences were also observed for the other protons in each pair of all (E)-, (Z)- isomers. In addition to these data, it was also reported that in some benzamidoximes an equilibrium between the conformers 9a - 9b is established, as it was indicated in their ^{1}H-NMR spectra, where absorptions for the protons of both conformers were observed[16,17].

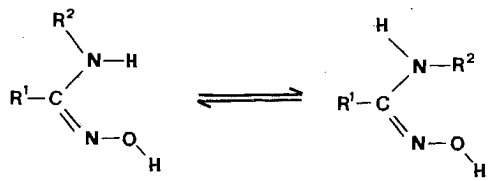

9a 9b

It is obvious from these data that the ^{1}H-NMR spectroscopy is very useful for the configurational and conformational study of amidoximes and generally of oximes, since the chemical shifts of their protons and especially of hydroxyl protons in DMSO are greatly affected by the enviromental differences between the structural isomers. In contrast to the reported extensive studies on simple amidoximes, diamino-glyoximes have not been studied systematically up today. Walstra et al.[4] studied the ^{1}H-NMR spectra of two isomeric bis- diisopropylamino-glyoxime diacetates at different temperatures (-20^0 to +65^0 C). They found that one of the isomers showed in all temperatures a multiplet, a singlet and a doublet signal for $(CH_3)_2C\underline{H}$, $-OCOC\underline{H}_3$ and $CH(C\underline{H}_3)_2$ protons respectively, while the other isomer gave for these protons at -20^0 to +20^0 C a multiplet, a broad singlet and a multiplet respectively, but the last multiplet collapsed at +65^0 C into a broad unseparated doublet. The authors considered that in the case of the isomer with the temperature depended ^{1}H-NMR spectrum the rotation about the central C-C bond is less sterically hindered and suggested for this isomer the anti-configuration and for the other one the amphi-configuration, with the N-substituents in trans conformation. Treatment of both isomeric diacetates with dimethylamine resulted to the same dioxime 4i (Table III) for which the authors proposed the amphi-configuration. They also prepared the diamino-glyoximes 4(f-l) and proposed for all of them the amphi-structure. Oxidation of 4(f-j) with potassium ferricyanide gave the corresponding furoxans 6(f-j). The reported ^{1}H-NMR spectra of compounds 4(f-l), 6(f-j) are given in Table III.

It is obvious from the data of Table III that, with exception of compound 4i, both R, both R′ and both N-OH groups of all diamino-glyoximes 4 are

Table IV. Mass spectra of compounds 4(d,e,f), 6(a-f) and 7(a,d,f).

Compound	m/e (relative intensity %)
4d	450(M^+, 2); 434(8); 433(24); 432(10); 414(2); 402(1); 341(13); 208(27); 183(26); 182(17); 181(22); 180(23); 106(15); 105(12); 91(100); 77(40).
4e	310(M^+, 16); 294(20); 293(100); 292(3); 278(4); 262(8); 211(12); 180(18); 155(6); 151(15); 138(6); 124(6); 113(12); 112(47); 83(35); 74(20); 70(38).
4f	258(M^+, 36); 242(18); 241(100); 226(3); 211(16); 210(19); 171(6); 156(18); 153(15); 141(13); 129(12); 125(52); 112(16); 111(16); 87(31); 86(72); 69(25); 57(58); 56(46); 55(33); 42(55); 40(45).
6a	296(M^+, 13); 280(2); 279(2); 266(10); 236(63); 221(15); 160(34); 132(68); 118(20); 117(10); 107(80); 106(100); 91(32); 77(73); 30(19).
6b	324(M^+, 12); 308(3); 294(19); 264(100); 235(30); 174(15); 159(10); 146(26); 132(17); 131(14); 121(22); 120(15); 119(13); 118(41); 106(52); 104(50); 91(17); 77(81);30(13).
6c	325(M^+, 1); 336(2); 322(2); 292(4); 272(7); 188(26); 173(11); 168(17); 167(13); 160(26); 154(24); 153(18); 141(17); 135(47); 134(15); 132(30); 120(100); 104(25); 91(44); 30(52).
6d	448(M^+, 9); 432(3); 431(3); 418(18); 388(64); 297(38); 236(26); 208(26); 194(23); 183(29); 182(21); 181(47); 180(45); 159(41); 144(39); 119(35); 91(100); 77(51); 30(12).
6e	308(M^+,5); 292(3); 278(12); 262(2); 250(60); 248(98); 235(70); 166(97); 139(18); 138(15); 128(86); 124(30); 113(45); 112(15); 84(100); 83(77); 70(73);42(97);30(97).
6f	256(M^+, 2); 240(2); 226(3); 196(100); 140(10); 138(8); 114(9); 113(9); 112(41); 110(10); 98(4); 87(12); 86(12); 85(9); 57(29); 56(25); 55(50); 54(40); 42(97);30(28).
7a	280(M^+, 51); 250(24); 149(24); 132(22); 118(51); 106(12); 91(40); 77(100); 51(40); 41(40).
7d	432(M^+, 13); 402(0.5); 341(25); 224(1); 208(7); 207(4); 194(3); 182(5); 181(8); 180(7); 91(100); 77(31); 65(34); 51(19).
7f	240(M^+, 100); 211(7); 210(47); 209(21); 183(5); 166(7); 125(7); 124(8); 113(10); 105(7); 98(8); 86(22); 69(14); 56(28); 54(34); 45(42); 42(24); 41(23).

magnetically equivalent giving in the ^{1}H-NMR spectra one absorption for the same protons. This is a strong evidence for a symmetric structure of compounds in question and is in disagreement with the suggested amphi-form for these compounds, since the corresponding furoxans 6(f-j) with the non-symmetric structure exhibited different chemical shifts for 3-N-, and 4-N-substituents. Compound 4i, like the corresponding furoxan 6i, gave two doublets for the methyl protons of the isopropylamino-substituents, in agreement with the proposed non-symmetric amphi-form, even though this differentiation in chemical shifts was not so clear for the methine (as in furoxan 6i) and hydroxyl protons.

Although the diamino-glyoximes can also exist in a conformation with the N-substituents in trans-position, it is apparent that a structural correlation between

the stereochemical forms of a symmetrically substituted dioxime and the corresponding furoxan and furazan can be considered, concerning the spatial arrangements of N-substituents and the -C=N-O groups. The amphi-form can be related to the furoxan-structure and the syn-form to the furazan-structure, while the symmetric anti-form of a dioxime can be related to the moiety of the corresponding furoxan bearing the N⟶O bond. The other moiety of the furoxan is very similar to the corresponding symmetric furazan. Table III reveals a significant similarity between the ^{1}H-NMR spectra of the amphi-dioxime 4i and the furoxan 6i.

Then we prepared the furoxans 6(a-f) and the furazans 7(a,c,d,f) (Scheme 1) and compared their ^{1}H-NMR spectra with those of the diamino-glyoximes 4(a-f) (Table II) as well as with those of compounds in Table III. We also studied the spectra of compounds 4(k,l) and of several other similar diamino-glyoximes previously prepared by us[6]. As it has been pointed above, the ^{1}H-NMR spectra in DMSO-d_6 of all studied diamino-glyoximes exhibited one absorption for both hydroxyl protons (N-OH), and generally revealed a symmetric molecular structure. The same symmetry, as it was expected, was also observed in the spectra of furazans, while the ^{1}H-NMR spectra of all furoxans gave the expected two absorptions for each pair of non-symmetric N-substituents, R, R′. Table II showes that, in agreement with the ^{1}H-NMR spectra of many other substituted furoxans[18], the protons of 3-N-alkyl substituents of the studied furoxans resonate at a higher field than the same protons of their 4-N-alkyl stbstituents and very close to that of both same N-alkyl substituents of the corresponding diamino-glyoximes. On the other hand, the protons of 4-N-alkyl substituents of these furoxans resonate at about the same field with that of N-substituents of the corresponding furazans and lower than that of both N-alkyl substituents of the corresponding diamino-glyoximes. On the base of these observations we consider that the ^{1}H-NMR spectra of all diamino-glyoximes 4(a-l) are in favour of the symmetric anti-configuration 8a (Scheme 2), with exception of bis-diisopropylamino-glyoxime 4i, where the reported ^{1}H-NMR spectrum agrees sufficiently with the proposed amphi-structure.

The suggested anti-configuration for compounds 4 is also in agreement with the proposal that the reaction of primary and secondary amine nucleophiles with nitrile-N-oxides in aqueous solution leads to the (Z)-isomers in which the nucleophile and the -OH group are adjacent[15]. The anti-configuration has also been suggested for some symmetric derivatives of oxalo-bis-thiohydroximic acid, prepared by reaction of dicyano-di-N-oxide with thiols[19]. The recorded mass spectra of new compounds 4(e,f,d) (Table IV) showed generally a similar fragmentation patern to that reported for compounds 4(a-c) and other diamino-glyoximes[9], giving $[M\text{-}O]^+$ $[M\text{-}OH]^+$ $[M\text{-}NO_2H_2]^+$, $[M\text{-}(RNHR')]^+$, $[RR'N\text{-}C{=}NOH]^+$, $[RR'N\text{-}C \equiv N]^+$, $[RNHR']^+$, $[R\text{-}N\text{-}R']^+$ as characteristic fragment ions.

Treatment of compounds 4(a-f) with one equivalent of phenyliodine ditrifluoroacetate (5) at room temperature, gave the corresponding furoxans 6(a-f) in good to moderate yields (88-48%) (Scheme 1, Table 1). The reactions were completed in less than 5 min, as it was monitored by TLC and the produced furoxans were generally separated from the reaction mixture by column

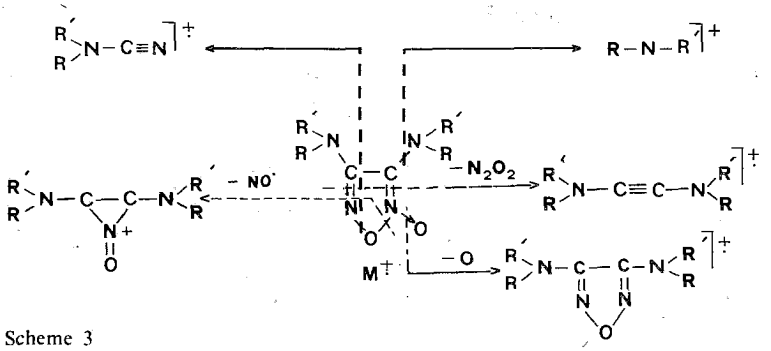

Scheme 3

chromatography. The structure of compounds 6(a-f) was confirmed by their spectral data (^{1}H-NMR, IR, MS) and microanalyses. Compounds 6(a-f) exhibited in the IR spectra the characteristic[20] bands in the region 1630-1300 cm^{-1} for C=N, O-N⟶O and N-O bonds (Table I). The mass spectra of these compounds gave the expected molecular ion (M^+) and most of the fragments reported for the fragmentation of other furoxan derivatives[21,22], as it is shown in Scheme 3. Besides these fragments the recorded mass spectra of compounds 6(a-f) gave also several other abudant ions which can be easily explained considering the participation of the alkyl and aryl groups in the fragmentation reactions as well as the expected eliminations of amine and nitrile fragments.

Then we tried to deoxygenate compounds 6(a-f) to the corresponding furazans by heating them with triethyl phosphite (Scheme 1). Although many furazans have been prepared in this way in excellent yields[18], our efforts resulted in the preparation of furazans 7(d,f) only, while traces of furazans 7(a,c) were isolated and identified from the other reactions. Generally small amounts of furoxans 6(a,b,c,e) were available and used in these reactions. It is possible that the deoxygenation procedure depends on the nature of the substituents, since in contrast to some 3-methyl-4-alkoxy (or alkylthio, or their sulfones)-furoxans which were deoxygenated to the corresponding furazans in higher than 90% yield, 3-methyl-4-pyrrolidino-furoxan gave the corresponding furazan in only 45% yield. Furazans 7(a,d,f) were also prepared by direct dehydration of diamino-glyoximes 4(a,d,f) (Scheme 1) and were identical to those prepared by deoxygenation of the furoxans. The structure of compounds 7(a,c,d,f) was also confirmed by their spectral data and microanalyses. The observed general fragmentation pathway in the mass spectra of furazans 7(a,d,f) is in good agreement with that proposed for furazan 7c[9], giving $[M\text{-}NO]^+$, $[RR'N\text{-}C \equiv N]^+$, $[RR'NC]^+$, $[R\text{-}N\text{-}R']^+$ as characteristic fragments.

Experimental Part

M.p.s' are given without correction and were determined with a Kofler hot-stage apparatus. ^{1}H-NMR spectra were obtained in different solvents with a Varian A-60A spectrometer with tetramethylsilane as internal standard. IR spectra were recorded on a Perkin-Elmer 297 spectrophotometer. The mass spectra were

obtained with a Hitachi Perkin-Elmer RMU-6L mass spectrometer; The ionization energy was maintained at 70 eV.

General Procedure for the preparation of diamino-glyoximes 4(a-f).

Method A. To a cold solution of the appropriate amine (0.02 mol) and dichloroglyoxime (0.01 mol) in chloroform (130 ml) a 2N solution of sodium carbonate (30 ml) was added dropwise under stirring. The organic layer was separated, dried with anhydrous sodium sulfate, concentrated in a rotary evaporator under reduced pressure to 50 ml and then was allowed to stand for 12 h at -15° C. Part of compounds 4d and 4f was precipitated and isolated while the rest of them as well as the other prepared dioximes 4 were separated from their reaction mixture by column chromatography on silica, eluting with chloroform.

Method B. Dichloroglyoxime (0.005 mol) and the appropriate amine (0.02 mol) were dissolved in tetrahydrofuran (10 ml) and the resulting solution was refluxed for 3 h. The precipitated amine hydrochloride (if any) was removed from the cooled reaction mixture, the solvent was evaporated under reduced pressure and the residue was dissolved in chloroform. The rest amine hydrochloride was extracted from the solution with water and the organic layer was boiled with Norite. After the Norite had been removed by filtration, petroleum ether was added to the filtrate until no more product precipitated and the mixture was allowed to stand at -15° C. The collected crude products were then recrystallized from the solvents given in Table I.

General Procedure for the preparation of furoxans 6(a-f).

To a magnetically stirred suspension of a diamino-glyoxime 4(a-f) (1 mmol) in dichloromethane (20 ml) a solution of phenyliodine ditrifluoroacetate (5, 1 mmol) in dichloromethane (20 ml) was added at 20° C. After 5 min all dioxime was dissolved and consumed, as monitored by TLC. The reaction mixture was treated with sodium bicarbonate solution, the organic layer was dried with anhydrous sodium sulfate and concentrated under reduced pressure in a rotary evaporator to a small volume. Furoxan 6f was precipitated quantitatively and isolated. Furoxans 6(a-e) were separated from the concentrated reaction mixture by column chromatography on silica eluting with chloroform and were further purified by recrystallisation (Table I).

General Procedure for the Preparation of Furazans 7.

Method A. Deoxygenation of furoxans 6(a-f) with triethyl phosphite:

A solution of furoxan 6(a-f) (0.5 mmol) in triethyl phosphite (5 ml, excess) was heated under reflux for 1 h and then was concentrated under reduced pressure in a rotary evaporator up to dry. The residue was dissolved in chloroform, washed with water and the organic layer dried with anhydrous sodium sulfate and concentrated to a small volume. Furazan 7f was precipitated and isolated from the concentrated

mixture. The other concentrated reaction mixtures were separated by preparative TLC on silica with chloroform. Furazan 7d was isolated in low yield. Furazans 7(a,c) were isolated in traces and identified by ^{1}H-NMR and mass spectroscopy. The expected furazans 7(b,e) were not detected in their reaction mixtures.

Method B. Dehydration of diamino-glyoximes 4(a,d,f).

Diamino-glyoxime 4(a,d,f) (1 mmol) was added to a solution of sodium hydroxide (40 mg, 1 mmol) in ethylene glycol (3.5 ml) and the resulting mixtures was heated at 140° C for 5 h. The solution was cooled to 25° C and poured into ice-water (10 ml) and was allowed to stand for 12 h. The precipitated furazan was collected by filtration and crystallized (Table I). The prepared furazans 7(a,d,f) were identical to those prepared by method A.

Περίληψη

Σύνθεση καί Μελέτη μερικῶν Συμμετρικῶν Διάμινο-υποκατεστημένων Γλυοξιμῶν, Φουροξανίων καί Φουραζανίων.

Ἀπό ἀντιδράσεις δευτεροταγῶν ἀμινῶν μέ δικυανο-δις-N-ὀξείδιο (2) ἤ μέ διχλωρογλυοξίμη (3) παρασκευάσθηκαν οἱ διαμινο-γλυοξίμες 4(a-f) (Σχῆμα 1) καί μελετήθηκε ἡ δομή τους. Οἱ ἐνώσεις 4(a-f) ἔδωσαν κατά τήν ὀξείδωσή τους μέ διτριφθοροακετοξυ-ιωδοβενζόλιο (5) σέ καλές ἀποδόσεις τά ἀντίστοιχα φουροξάνια 6(a-f) ἀπό τά ὁποῖα κατά τήν ἐπίδραση φωσφορώδη τριαιθυλεστέρα παρασκευάστηκαν τά φουραζάνια 7(a,c,d,f). Τά φουραζάνια 7(a,d,f) παρασκευάστηκαν ἐπίσης ἀπό τήν ἀφυδάτωση τῶν ἀντιστοίχων διαμινο-γλυοξιμῶν 4(a,d,f) μέ ἐπίδραση ὑδροξειδίου τοῦ νατρίου. Μελετήθηκαν τά φάσματα IR, MS καί ^{1}H-NMR ὅλων τῶν ἐνώσεων. Ἀπό τή συστηματική καί συγκριτική μελέτη τῶν φασμάτων ^{1}H-NMR τῶν ἐνώσεων 4(a-f), 6(a-f), 7(a,c,d,f) καθώς καί τῶν ἐνώσεων 4(f-l) καί 6(f-j) πού ἀναφέρονται στή βιβλιογραφία (Πίνακας III) προκύπτει ὅτι σέ ἀντίθεση μέ τήν προτεινόμενη στή βιβλιογραφία ἀμφί-δομή γιά τήν ἕνωση 4f καί γιά ἄλλες ἀνάλογες διαμινο-γλυοξίμες, οἱ ἐνώσεις 4(a-f) ἐμφανίζονται συμμετρικές καί προτείνεται γι' αὐτές ἡ ἀντί-δομή 8a (Σχῆμα 2).

References

1. Holleman, A.F.: *Chem. Ber.* **26**, 1403 (1893).
2. Coburn, M.D.: *J. Heterocyclic Chem.* **5**, 83 (1968).
3. Houben, J. & Kauffmann, H.: *Chem. Ber.* **46**, 2821 (1913).
4. Walstra, P., Trompen, W.P. & Hackmann, J. Th.: *Rec. Trav. Chim.* **87**, 452 (1968).
5. Grundmann, C.: *Angew. Chem.* **75**, 450 (1963).
6. Alexandrou, N.E. & Nicolaides, D.N.: Report of the Fourth Conference of the Greek Chemists, Athens 1970, p. 39; *Chem. Abstr.* **85**, 77826m (1976).
7. Grundmann, C., Mini, V. Dean, M.J. & Frommeld, H.D.: *Ann.* **687**, 191 (1965).

8. Alexandrou, N.E. & Nicolaides, D.N.: *J. Chem. Soc. (C)*, 2319 (1969).
9. Nicolaides, D.N.: *Sci. Annals, Fac. Phys. and Mathem., Univ. Thessaloniki*, **16**, 433 (1976); *Chem. Abstr.* **87**, 200328w (1977).
10. Behr, L.C. in: The Chemistry of Heterocyclic Compounds, Vol. 17, Weissberger, A., Ed., Interscience Publishers, New York, 1962, p. 283.
11. Nicolaides, D.N. & Gallos, J.K.: *Synthesis* 683 (1981).
12. Kleinspehn, G.G., Jung, J.A. & Studniarz, S.A.: *J. Org. Chem.* **32**, 460 (1967).
13. Tanaka, M., Shono, T. & Shinra, K.: *Anal. Chim. Acta* **46**, 125 (1969).
14. Gozlan, H., Michelot, R., Riche, C. & Rips, R.: *Tetrahedron* **33**, 2535 (1977).
15. Dignam, K.J., Hegarty, A.F. & Quain, P.L.: *J. Chem. Soc. Perkin Trans. II*, 1457 (1977).
16. Exner, O., Jehlicka, V., Dondoni, A. & Boicelli, A.C.: *J. Chem. Soc. Perkin Trans. II*, 567 (1974).
17. Dondoni, A., Lunazzi, L., Giorgianni, P. & Macciantelli, D.: *J. Org. Chem.* **40**, 2979 (1975).
18. Gasco, A. et al.: *J. Heterocyclic Chem.* **9**, 577 (1972); *J. Heterocyclic Chem.* **9**, 837 (1972); *J. Heterocyclic Chem.* **10**, 587 (1973).
19. Nicolaides, D.N. & Kouimtzis, Th. A.: *Chimika Chronika, New Series* **3**, 63 (1974).
20. Boyer, J.H., Toggweiler, U. & Stonner, G.A.: *J. Am. Chem. Soc.* **79**, 1748 (1957).
21. Ungnade, H.E. & Loughran, E.D.: *J. Heterocyclic Chem.* **1**, 61 (1964).
22. Boulton, A.J., Hadjimihalakis, P., Katritzky, A.R. & Hamid, A.M.: *J. Chem. Soc. (C)*, 1901 (1969).

GUIDE TO AUTHORS

Scope and Editorial Policies. — This International edition invites original contributions on research in all branches of Science related to chemistry, including biology, physics etc. at the molecular, submolecular and nuclear level. Negative results will only be accepted when they can be considered to advance our knowledge. In the selection by the editors of manuscripts for publication, emphasis is placed on the quality and originality of the work. The following quotation from the *General Notes on the Preparation of Scientific Papers* (Cambridge University Press, 1950) expresses precisely a highly important criterion for the acceptance of a paper and should always kept in mind during the preparation of manuscripts: "Most journals prefer papers written for the moderate specialist, that is to say, an author should write, not for the half-dozen people in the world specially interested in his line of work, but for the hundred or so who may be interested in some aspect of his work if the paper is well written".

Accepted languages are: Greek, English, French, German and Italian. Authors need not be members of the Greek Chemists Association.

Manuscripts are classified as (normal-length) *papers, short papers or notes, preliminary communications or letters, and reviews. A short paper* is a concise but complete description of a small, rounded-off investigation or of a side part from the main line of investigation, which will not be included in a later paper. It is not a portion of work, that can be more suitably incorporated in a normal-length paper, after the investigation has progressed further. Presentation of results in smaller papers or notes leads to undesirable fragmentation, especially in the case of continuing studies, and is contrary to most journals policies.

As *Notes* are characterized short papers on limited facets of an investigation e.g. describing a usefull modifications of an experimental technique or method, reporting additional data and eventually, more precise values for measurements already existing in the literature, and so on.

A *Preliminary Communication* is a brief report of work, which will be included in a later normal-length paper. Criteria for its publication are first, when it is considered that the science would be advanced if results were made available as soon as possible to others working on the same subject and second, for the protection of priority for the author. Every endeavour is made in order to publish preliminary communications as soon as possible and it would help the editors if the author, in a covering letter, were to give his reasons for believing that publication is urgent. Although extensive references to the earlier literature are not usually needed, the most recent papers on the same subject should be referred to, and sufficient experimental details should be given so that those familiar with the subject can immediately repeat the experiments. In general, preliminary communications should be more than an abstract or a summary.

As *Letters* are characterized any other types of communications, previously included in the terms "letter to editor" or "communication to editor", but not fulfilling the criteria mentioned above for a preliminary communication or a note, or dealing with scientific criticism of pulished work in this (or other) journals.

Reviews should be fully comprehensive on a narrow field of specialized research, expected to be interesting for a broad number of scientists; they are invited papers, otherwise submitted after contacting the editors.

Organization of Manuscripts. — Authors should submit *three copies* of the manuscript in double-spaced typing on the one side of pages of uniform size, with a margin 5-cm wide on the left; this applies also to summaries, references and notes, legends to figures etc.

Every manuscript should begin with a *Cover Page* and attached to it on a separate sheet, the *Aknowledgments* and notice of grant support (if appropriate).

The cover page should contain the title, the name(s) of author(s) (first-name in full, middle, surname), the name and adrress of laboratory of research, the footnotes to the title and/or to an author's name (both made with asterisks), and the name and address of the galley proofs' recipient. It should also contain a Running Title, not exceeding 40 letters.

The purpose of this arrangement is to facilitate the reviewing procedure, which is based on a protective anonymity between reviewers and authors, chosen in order to meet the requirements of a highly objective selection of papers to be published in this journal, and to increase the validity of criticisms. Cover page and aknowledgements are not sent to reviewers and accordingly, sentences in first person accompanied by literature references to earlier papers of the author(s) should be completely avoided in the text. In spite, authors are encouraged to suggest possible reviewers for their papers.

The next pages of the manuscript should be numbered in one consecutive series by the following sequence:

Page 1. — *Title* followed by a *summary* in the language of the text. The title should consist of carefully selected and properly presented key words which clearly identify the subjects considered in the paper. The *summary* should be as brief as possible but intelligible in itself, without reference to the paper, and containing sufficient information to serve as an *abstract.*

Every *summary* should end with up to ten *key words*, necessary to direct the attention of abstracting services and readers to subjects in the article that are not referred to in the title.

Page 2. — *Abbreviations* and *Terminology,* ie. a list of all abbreviations and unusual terms used in the paper; it may include the systematic name of any compound, mentioned in the text by a shorter "trivial" or "common" name.

Page 3 and subsequent. — The text divided into sections and, if necessary, subsections. The first section of a normal-length paper is always an *Introduction.* stating the reasons for performing the work, with brief reference to previous work on the subject; the back-ground discussion should be restricted to pertinent material, avoiding an extensive review of prior work; and documentation of the literature should be selective rather than exhaustive, particularly if reviews can be cited.

The arrangement of the text after the introduction is left to the author(s). The order *Materials, Methods, Results* and *Discussion,* with headings, subheadings and sideheadings chosen by the author(s), is usually the most satisfactory. However, in lengthy papers (usually, of synthetic work) the manuscript may be organized so that the principal findings and conclusions are concisely presented in an initial section (Theoretical Part), with supporting data, experimental details, and supplementary discussion in a separate section (Experimental Part).

The pages of the text should not contain tables and figures as well as footnotes. The proper positions of tables and figures should be indicated by an arrow in the margin. The explanatory footnotes, will appear together with the literature citations at the end of the paper, in the section References and Notes (see below). Therefore, they should be numbered in one consecutive series by order of mention in the text, using reference numbers in the form of superscripts (not in parentheses), placed after any mark of punctuation.

Subsequent Pages.— After the text pages separate sheets should be used for the following: a) english summary; b) greek summary; c) references and notes; d) tables; and e) legends to figures attached to the corresponding figures or illustrations.

The *english summary,* headed by an english translation of the title, is needed only when the text is not written in english; it should be a translation of the summary of page 1.

The *greek summary,* headed by a greek translation of the title, is needed only in foreign papers. In contrast to the rule, this summary should be extensive and may refer to literature citations and to tables or figures of the paper, in order to give a brief but factual account of the contents and conclusions of the paper, and of its relevance; for this purpose, it may exceed half printed page. In its place, foreign authors may submit an extensive summary in english, which will be gladly translated into greek by care of the editors.

References and Notes, as already mentioned, should be brought together at the end of the paper in one consecutive series by order of citation in the text (not in alphabetical order). Authors should check whether every reference in the text appears in the list and *vice versa.* References to papers "in press" imply that the paper has been accepted for publication and, therefore, the name of the journal should be given. References to a "personal communication" (never "private") will be accepted only when the author submits written permission of the worker concerned. References should be listed according to the following style:

For journal articles:[1] Last name(s) of author(s) and initials: "Title of article" (desirable, but left to author's decision), *Name of journal* (abbreviated according to Chemical Abstracts, 1961, or to Biological Abstracts, 1968, and their supplements), *Volume number,* First page of article, Year in parentheses.

Example: 1 Smith, J.B. and Jones, A.B.: "Synthesis of ethyl alcohol", *J. Am. Chem. Soc.* 47, 115 (1945).

For books and monographs:[2] Author's names as above: *Title of book,* (Number of edition), Page, Publisher, City, Year of edition.

Example: 2 Smith, J.B.: *Organic Chemistry,* (2d edition), p. 57, Wiley, London (1945).

For multi-author volumes (Articles in books):[3] Authors' names as above: "Title of article" in... Name of editor(s): *Name of book,* Volume number and, if appropriate, Part number, page(s), Publisher, City, Year of edition.

Example: 3 Smith, J.B.: "Synthesis of ethyl alcohol" in Jones, A.B.: *Organic Chemistry,* Vol. 5. Part A, p. 57 (or pp. 46-62), Elsevier, Amsterdam, 1953.

Tables should be typed on separate sheets numbered with Roman numerals, and provided with a descriptive title, making clear the kind of results presented in the table and the experimental technique(s) used. A legend describing the way the particular experiment(s) was carried out, should be given below the title. (It is usually preferable to give such details here instead of in the text). The units in which the results are expressed may be given either in the legend, or in the columns' headings. In general, the title together with the legend and the column headings should make a table intelligible without reference to the text. Vetrical lines are not used to separate columns. Lines or columns largely empty should be avoided; details referring to one or two isolated items (e.g. an abnormal feature of a single experiments) should be given as footnotes to the table, indicated by superscript lowercase letters or asterisks. Considerable thought should be given to the layout of tables (and figures) so that the significance of the results can be most readily and quickly grasped by the reader. It is surprising sometimes how much easier is to understand the results presented in a table if it is turned through 90°.

Legends to figures should not be written on the figures but should be typewritten, each on a separate sheet attached to the corresponding figure. The legend should begin with the number of figure in Arabic numerals, and provided with a descriptive title and experimental details, as for tables.

One set of figures should be in a form suitable for reproduction, and about twice the size of final reproduction. Whenever possible, a line drawing rather than a photograph is preferred. Diagrams for reproduction should be drawn on smooth tracing paper in black water-proof ink, *with lettering and numbers* sufficiently large to be legible after reduction to print size. Photographs should be glossy and as rich in contrast as possible. Coloured illustrations are reproduced at the author's expence. The second and third copies of the typescript should be supplied with photostatic copies of the original figures or illustrations.

Manuscripts for short papers and preliminary communications should be organized on the same principles. Besides some minor modifications in their published form (see recent issue for style), they differ from a normal-length paper in that the headings and subheadings in the text, as well as the summary preceeding the text are ommitted. In these cases, the first paragraph of the text may serve the purpose of an abstract, summing up very briefly the scope and the main findings and conclusions of the investigation. However, for reasons already mentioned, the text is always followed by an english summary (unheaded in english papers) and, in all foreign papers, by a greek extensive summary.

Page Charge and Reprints. A page charge (500 drachmas or 15 U.S. dollars per printed page) is assessed to cover in part the cost of publication, *on assumption of payment from author's supporting funds or institution.* Payment is expected but is not a condition for publication: papers are accepted or rejected only on the basis of merit, and the decision to publish a paper is made before the charge is assessed.

A reprint rate schedule will be distributed to authors with galley proofs. Payment of page charge provides 100 reprints free of charge and lower cost for additional reprints. Authors should define the title and address of institution, to which page charge — if accepted — and reprint cost should be invoiced.

Galley Proofs. Manuscript and proofs will be forwarded to the author before publication. They should be carefully corrected and verified against the manuscript. Excessive alterations in the text will not be accepted at this stage. New material may be permitted only as a "note added in proof", at the end of References and Notes. The corrected *and initialed* galley proofs, together with the reprint order form should be returned within 3 days from receipt.